9-17-1968

A Study Of Thermoacoustic Oscillations At Elevated Static Pressures

Michael Einar Berger

MANUSCRIPT THESES

Unpublished theses submitted for the Master's and Doctor's degrees and deposited in the University of New Mexico Library are open for inspection, but are to be used only with due regard to the rights of the authors. Bibliographical references may be noted, but passages may be copied only with the permission of the authors, and proper credit must be given in subsequent written or published work. Extensive copying or publication of the thesis in whole or in part requires also the consent of the Dean of the Graduate School of the University of New Mexico.

This thesis by Michael Einar Berger has been used by the following persons, whose signatures attest their acceptance of the above restrictions.

A Library which borrows this thesis for use by its patrons is expected to secure the signature of each user.

NAME AND ADDRESS	DATE

This thesis, directed and approved by the candidate's committee, has been accepted by the Graduate Committee of The University of New Mexico in partial fulfillment of the requirements for the degree of

Master of Science in Mechanical Engineering

A STUDY OF THERMOACOUSTIC OSCILLATIONS AT ELEVATED STATIC PRESSURES

Title

Michael Einar Berger

Candidate

Mechanical Engineering

Department

Arthur V. Houghton

Dean

Sept 17, 1968

Date

Committee

K. T. Feldman

Chairman

Maurice W. Wildin

Alexander

W. E. Baker

A STUDY OF THERMOACOUSTIC OSCILLATIONS AT ELEVATED STATIC PRESSURES

BY

MIKE E. BERGER

B.S., University of New Mexico, 1967

THESIS

Submitted in Partial Fulfillment of the
Requirements for the Degree of
Master of Science in Mechanical Engineering
in the Graduate School of
The University of New Mexico
Albuquerque, New Mexico
June, 1969

ACKNOWLEDGEMENTS

The author wishes to express his sincere thanks to Dr. Karl Thomas Feldman, Jr., Associate Professor of Mechanical Engineering, for his guidance and assistance throughout this investigation and the author's entire master's program. The topic of this investigation and its application to the thesis was suggested by Dr. Feldman.

The author has also benefited from discussions on dimensional analysis with Dr. Charles G. Richards of the Department of Mechanical Engineering.

Special thanks is due to Mr. Don Pierce who meticulously constructed the experimental system and assisted in the taking of data and its reduction.

The author is grateful for the skill and attention of Mrs. Clarice Chavarria and Mrs. Harriet Evans and others of the University of New Mexico Bureau of Engineering Research who prepared this manuscript.

This research investigation was greatly helped by the constant support of the author's family and particularly his wife, Pat.

A STUDY OF THERMOACOUSTIC OSCILLATIONS AT ELEVATED STATIC PRESSURES

BY

Mike E. Berger

ABSTRACT OF THESIS

Submitted in Partial Fulfillment of the
Requirements for the Degree of
Master of Science in Mechanical Engineering
in the Graduate School of
The University of New Mexico
Albuquerque, New Mexico
June, 1969

ABSTRACT

An experimental investigation was conducted to determine the effect of high static pressure on a closed thermoacoustic sound generator.

The theory for thermoacoustic oscillations is reviewed and analyzed for the case of elevated static pressure. Design equations for high internal pressure oscillators are developed from the principles of dimensional analysis, and a general design equation is proposed.

A closed double-end thermoacoustic oscillator was designed to withstand high temperatures and pressures and was used in the experimental investigation. Both air and helium were used as the working gases.

The results of both the theoretical and experimental investigations show that acoustic sound-pressure level increases with static pressure as long as sufficient thermal power is supplied. The thermoacoustic and mechanical efficiencies were studied as functions of internal pressure. Thermoacoustic efficiency abruptly increases and then gradually decreases with increasing static pressure. Mechanical efficiency monotonically increases with increasing static pressure.

Criteria for the inception of thermoacoustic oscillations are developed. It is shown that the power required to initiate an oscillation is an exponential function of pressure. In addition, it is determined that at pressures above a certain

minimum, the static mechanical efficiency becomes constant for the inception of oscillations. A criterion for the maintenance of a thermoacoustic oscillation, once it has been initiated, is also developed. It is shown that the power required to sustain an oscillation is a linear function of pressure. A table of design data for thermoacoustic oscillations at elevated static pressures is presented.

CONTENTS

LIST OF FIGURES

LIST OF TABLES

ABBREVIATIONS AND SYMBOLS

I. English Letters

A	inside cross-sectional area of pipe
a	acoustic velocity
b_1	arbitrary constant
b_2	arbitrary constant
C	molar specific heat
c_p	specific heat at constant pressure
c_v	specific heat at constant volume
d	inside diameter of pipe
L	length
m	mass
N	non-dimensional number
n	number of variables
p	pressure
Q	heat transfer
q	heat transfer per unit mass
R	gas constant
r	rank of dimensional matrix
r^2	correlation coefficient
s	number of independent non-dimensional numbers
T	temperature
t	time
V	volume
w	heat transfer per unit area
x	distance coordinate
Y	dependent variable

II. Greek Letters

γ	ratio of specific heats c_p/c_v
ε	arbitrary constant
η	efficiency
ρ	density
ω	frequency

III. Subscripts

a	gas A, atmospheric
b	gas B
M	mechanical
MS	static mechanical
m	mixture
o	static, steady state
r	reference
ta	thermoacoustic

IV. Abbreviations

SPL	sound-pressure level
∇^2	Laplacian operator
$\cdot$	denotes derivative with respect to time

CHAPTER I

THE PROBLEM AND DEFINITIONS OF TERMS USED

Thermoacoustic oscillations are self-induced pressure oscillations caused by a steady heating of a gas column. This study was concerned with the type of thermoacoustic known as the Sondhauss oscillation, and the terms Sondhauss oscillations and thermoacoustic oscillations are used interchangeably.

Problem

The purpose of this study was to theoretically and experimentally investigate the behavior of thermoacoustic oscillations at elevated static pressures, to correlate the theoretical and experimental results, and specify a design equation that will predict acoustic sound-pressure levels for a given system at elevated pressures.

Importance of the study

It has been proposed that the Sondhauss oscillator be used to drive an underwater sound source.[1] For this application, it was necessary to investigate the thermoacoustic oscillations at elevated static pressures, since it is desirable to have the pressure inside the oscillator equal to the pressure of the surrounding water.

---

[1] K. T. Feldman, Jr., Application to the Office of Naval Research for funds to support research entitled "Investigation of a Thermoacoustic Oscillator as an Underwater Sound Source," Mechanical Engineering Department, University of New Mexico, Albuquerque, New Mexico, February 1967 (in the files of the department).

Other applications where information concerning the behavior of thermoacoustic oscillations at elevated internal pressures could be pertinent are the utilization of the Sondhauss oscillator as a driving mechanism for an alternating-current magnetohydrodynamic generator[2,3,4] and as a driving mechanism for an eccentric crank engine. A high, internal pressure Sondhauss oscillator could also be used an an environmental testing chamber for subjecting equipment to extreme acoustic intensities.[5]

Another discipline where knowledge of high, internal-pressure thermoacoustic oscillations would be valuable is in the avoidance of the inception of oscillations in cryogenic systems.[6]

---

[2] R. L. Carter, M. White, and A. M. Steele, (Atomics International Division of North American Aviation, Inc.), private communication to K. T. Feldman, Jr., September 24, 1962.

[3] R. L. Carter and K. T. Feldman, Jr., "An Acoustically Resonant Stirling Engine," (Associated Midwest Universities - Argonne National Laboratory Conference on Direct Energy Conversion, Argonne, Illinois), November 4-5, 1963, ANL-6802, pp. 166-169.

[4] R. L. Carter, K. T. Feldman, Jr., and C. N. McKinnon, Jr., "Applicability of Thermoacoustic Phenomena to Magnetohydrodynamic Conversion Systems," Engineering Experiment Station Reprint No. 64, The University of Missouri, Columbia, Missouri, July 1964, p. 1.

[5] R. L. Henderson, (Environmental Test Group, Sandia Corporation, Albuquerque, New Mexico), private communication to K. T. Feldman, Jr., June 1965.

[6] R. S. Thurston, J. D. Rogers, and V. J. Skoglund, "Pressure Oscillations Induced by Forced Convection Heating of Dense Hydrogen," Proceedings of Cryogenic Engineering Conference, Paper H-4, 1966.

Definitions of terms used

Thermoacoustic oscillation -- The term thermoacoustic oscillation refers to any type of heat-generated acoustical oscillation occurring in a gas.

Sondhauss oscillation -- The term Sondhauss oscillation refers to gas oscillations occurring when heat is added by internal or external means to a gas-filled pipe having at least one closed end and having no net flow of gas through the pipe. Several different geometries and orientations of Sondhauss oscillators are possible. These are described in Footnote 7.

Acoustic sound-pressure level -- The term sound-pressure level, in decibels (db), is defined as 20 times the logarithm to the base 10 of the ratio of the pressure of the sound wave to a reference pressure. The reference pressure is 2×10^{-4} dynes/cm^2 (microbars), which is equal to 2.900×10^{-5} psi.[8] Unless otherwise stated, the sound pressure is the effective, root-mean-square sound pressure. A table of sound-pressure level (db) as a function of sound pressure (psi) is included in Appendix A.

Static pressure -- The term static pressure refers to the average pressure level inside the Sondhauss oscillator.

---

[7] K. T. Feldman, Jr., "Review of the Literature on Sondhauss Thermoacoustic Phenomena," Journal of Sound and Vibration, (1968) VII(1), pp. 71-82.

[8] L. E. Kinsler and A. R. Frey, Fundamentals of Acoustics, (second edition; New York: John Wiley and Sons, Inc., 1962), p. 125.

The term internal pressure is used as a synonym for the static pressure. Both gage and absolute pressures are used as units for static pressure.

Absolute pressure -- Absolute pressure is gage pressure plus atmospheric pressure. An atmospheric pressure of 12.3 psia is consistently used throughout the thesis.

Oscillatory pressure -- Oscillatory pressure is defined as the peak-to-peak amplitude of thermoacoustic pressure waves. Over-pressure is used as a synonym for oscillatory pressure. The sound-pressure level (SPL) is calculated according to the previously defined equation, using the root-mean-square of the oscillatory pressure.

Organization of the remainder of the thesis

In Chapter II, the literature on thermoacoustic phenomena pertinent to the problem will be reviewed and discussed. In Chapter III, the mechanism causing Sondhauss oscillations will be reviewed and the pertinent theory will be presented. The basis for a design equation derived from dimensional analysis will be given.

The experimental investigation of Sondhauss oscillations at elevated static pressures is described in Chapter IV. In Chapter V, the results of the theoretical and experimental analyses will be presented. In Chapter VI, the conclusions of the study will be discussed, along with recommendations for further investigation.

CHAPTER II

REVIEW OF THE LITERATURE ON THERMOACOUSTIC PHENOMENA RELEVANT TO THE PRESENT STUDY

In this chapter the work germane to the study of thermoacoustic oscillations at elevated static pressures is presented. The references are reviewed in chronological order to show the historical development of thermoacoustical work. In general, the literature is divided into two sections, that dealing with Rijke oscillations and that dealing with Sondhauss oscillations. An extensive review of the Rijke oscillations appears in Footnote 9. Only Sondhauss oscillations will be considered in this study.

In 1850, Sondhauss first experimentally studied the heat-generated sound often observed by glass blowers when blowing a bulb on the end of a narrow tube.[10] Such a "Sondhauss tube" was open at one end and terminated in a bulb at the other end. Sondhauss observed that a steady gas flame applied to the closed bulb end caused the air in the entire tube to oscillate and produce a clear sound which was characteristic of the dimensions of the tube.

---

[9] K. T. Feldman, Jr., "Review of the Literature on Rijke Thermoacoustic Phenomena," Journal of Sound and Vibration, (1968) VII(1), pp. 83-89.

[10] C. Sondhauss, "Uber die Schallschwingungen der Luft in erhitzten Glasrohren und in gedeckten Pfeifen von ungleicher Weite," Poggendorff Annalen der Physik und Chemie, 79:1-34, February 1850.

Lord Rayleigh, in 1878, included several discussions of thermoacoustical phenomena in his classic works on sound.[11] He verified and expanded the work previously done by Sondhauss. The Rayleigh criterion for the production of any type of thermoacoustical oscillation was:

> If heat be given to the air at the moment of greatest condensation or be taken from it at the moment of greatest rarefaction, the vibration is encouraged.[12]

This criterion has generally been accepted as the correct explanation of how thermoacoustic oscillations are maintained.[13]

Cryogenic researchers were next to report on thermoacoustic oscillations. Taconis,[14] and Clement and Gaffney[15] experimentally attempted to determine optimum conditions for spontaneous thermal oscillations.

Another cryogenic researcher, Kramers, was apparently the first to theoretically analyze the Sondhauss oscillation.[16]

---

[11] Lord Rayleigh, Theory of Sound, (New York: Dover Publications, 1945), II, pp. 224-234.

[12] Lord Rayleigh, "The Explanation of Certain Acoustical Phenomena," Nature, 18:319, July 1878.

[13] K. T. Feldman, Jr., "A Study of Heat Generated Pressure Oscillations in a Closed End Pipe," Ph.D. dissertation, University of Missouri, also available as Report ME-18, Bureau of Engineering Research, University of New Mexico, November 1965, p. 34.

[14] K. W. Taconis, et al., "Vapor-Liquid Equilibrium of Solutions of He^3 in He^4," Physica, 15:738, September 1949.

[15] J. R. Clement and J. Gaffney, "Thermal Oscillations in Low-Temperature Apparatus," Advances in Cryogenic Engineering, Vol. I, (Proceedings of 1954 Cryogenic Engineering Conference, Boulder, Colorado, September 1954, paper H-7), pp. 302-306.

[16] H. A. Kramers, "Vibrations of a Gas Column," Physica, 15:971-983, December 1949.

His method, which was limited in success, utilized the linearized fluid dynamic equations of mass, momentum, and energy. Trilling followed with an analysis similar to Kramer's.[17] He presented the concept of the heat-generated pressure wave acting like a piston.

Chu, in a series of four articles, presented the first detailed theoretical analyses of heat-generated pressure waves. He did not present any experimental verification. In the first paper,[18] for a moderate rate of heat release, he developed the heat-generated wave equation which describes the pressure field as

$$\frac{\partial^2}{\partial t^2}\left[\frac{p}{\gamma p_o}\right] - a_o^2 \nabla^2 \left[\frac{p}{\gamma p_o}\right] = \frac{\partial}{\partial t}\left[\frac{\dot{q}}{c_p T_o}\right] \qquad (1)$$

which is a modified wave equation with the heat addition term acting as a driving function. In the equation, p is the over-pressure, p_o is the average steady state pressure, a_o is the steady state acoustic velocity, γ is the ratio of specific heats, t is time, ∇^2 is the Laplacian operator, c_p is the specific heat at constant pressure, and $\dot{q}$ is the rate of heat release per unit mass. The moderate amount of heat released was defined as

---

[17] L. Trilling, "On Thermally Induced Sound Fields," The Journal of the Acoustical Society of America, 27:425-431, May 1955.

[18] B. T. Chu, "Pressure Waves Generated by Addition of Heat in a Gaseous Medium," National Advisory Committee for Aeronautics, Technical Note 3411, June 1955.

$$\frac{\dot{q}L}{c_p T_o a_o} << 1 \qquad (2)$$

where L is the length of the heating zone.

For low rates of heat release, the solution to Equation (1) is

$$\frac{p}{\gamma p_o} = \left(\frac{\gamma-1}{2\gamma}\right)\frac{\dot{w}}{a_o p_o} \quad , \qquad (3)$$

where $\dot{w}$ is the rate of heat release per unit cross-sectional area of the pressure field. Chu showed that Equation (3) describes a pressure field which is identical to that produced by two pistons moving away from each other with the same velocity. This fact is known as "Chu's reduction theorem".[19]

For higher rates of heat release,

$$\frac{\dot{q}L}{c_p T_o a_o} \approx 1 \quad , \qquad (4)$$

Chu showed that shock waves are generated and the solution to Equation (1) is

$$\frac{\dot{w}}{a_o p_o} = \frac{\frac{2}{\gamma-1}\frac{p_1}{p_o}\left[\frac{p_1}{p_o} - 1\right]}{\left[\frac{\gamma+1}{\gamma}\frac{p_1}{p_o} + \frac{\gamma-1}{2\gamma}\right]^{1/2}} \quad , \qquad (5)$$

where p_1 is just behind the shock.[20]

---

[19] Feldman, op. cit., p. 17.

[20] Chu, op. cit., p. 26.

In the second paper,[21] Chu discussed the stability of the heat-generated wave equation and proposed as a simplified wave equation for plane, one-dimensional pressure fields

$$\frac{1}{a^2}\frac{\partial^2 p}{\partial t^2} - \frac{\partial^2 p}{\partial x^2} = \varepsilon(p_o^2 - p^2)\frac{\partial p}{\partial t} \quad , \tag{6}$$

where a is the local sonic velocity and ε is a positive quantity. Equation (6) was subsequently solved by Feldman on the analog computer.[22] Chu also described the Rayleigh criterion physically by making use of an "engine analogy". This essentially amounted to applying the reduction theorem to a heat driven gas oscillation in a pipe. Chu's other two papers were not pertinent to this investigation.

In 1962, Carter, White, and Steele experimentally investigated the Sondhauss phenomena.[23] They constructed a double-ended closed tube and apparently were the first to investigate the effect of elevated static pressures on thermoacoustic oscillations. Their tests showed that the amplitude of the oscillations increased steadily with system pressure up to two atmospheres, but their results were only qualitative.

In 1963, Carter and Feldman,[24] and in 1964, Carter, Feldman, and McKinnon, discussed the Sondhauss oscillator in the

---

[21] B. T. Chu, "Stability of Systems Containing a Heat Source--The Rayleigh Criterion," National Advisory Committee for Aeronautics, Research Memorandum 56D27, June 1956.

[22] Feldman, op. cit., pp. 142-171.

[23] Carter, White, and Steele, loc. cit.

[24] Carter and Feldman, loc. cit.

[25] Carter, Feldman, and McKinnon, loc. cit.

light of its similarity of a regenerative Stirling engine. For a Sondhauss oscillator shown in Figure 1, they pointed out that the closed end acted as an acoustic compliance, or, in terms of a mechanical analogy, as a spring. The bundle of pyrex glass tubes, across which a temperature gradient is maintained, acted as an acoustic impedance, and the column of gas in the open end acted as a distributed acoustic inertance, or as a distributed mass. They found that the amplitude of oscillations increased when water vapor was present in the heated air.

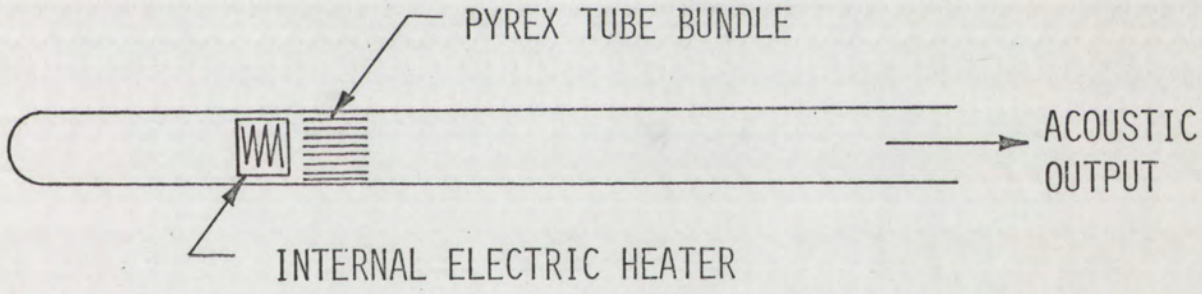

Figure 1. Line drawing of an internally heated Sondhauss thermoacoustic oscillator

Feldman, in 1965, presented the first comprehensive study, both theoretical and experimental, of heat-generated pressure oscillations in a closed-end pipe.[26] As previously mentioned,

[26]Feldman, op. cit.

he solved Chu's wave equation (Equation 6) on the analog computer. Feldman explained the functions of the various parts of the Sondhauss oscillator and explained the mechanisms for causing and maintaining thermoacoustic oscillations. These are elaborated upon and discussed in detail in the section on the mechanisms of thermoacoustic oscillations in Chapter III. He combined all the previous work on thermoacoustic oscillations and interrelated it. His experimental and theoretical results compared within 5 percent error. Feldman initiated studies of the optimum design for Sondhauss oscillators. He recommended the investigation of thermoacoustic phenomena at elevated static pressures which was the basis for this study.

In 1966, Feldman and Hirsch reviewed the previous work of Feldman and experimentally investigated the analogy of the Stirling engine.[27] This involved the measurement of the acoustic wave velocity, the measurement of the phase angle between acoustic pressure and velocity, and the comparison of the pressure-volume diagram of the Sondhauss oscillator to that of the Stirling engine.

Thurston, in 1966, studied thermoacoustic oscillations using parahydrogen (two-phase hydrogen) as the working fluid.[28]

---

[27] K. T. Feldman, Jr., and H. Hirsch, "Final Report on the Mechanism Causing Heat Driven Pressure Oscillations in a Gas," Technical Report ME-22, Bureau of Engineering Research University of New Mexico, June 1966.

[28] R. S. Thurston, "Thermal-Acoustic Oscillations Induced by Forced Convection Heating of Dense Hydrogen," Ph.D. dissertation, University of New Mexico also available as LA-3543, Los Alamos Scientific Laboratory of the University of California, Los Alamos, New Mexico, August 26, 1966.

His system, unlike those previously mentioned utilized the evaporation of liquid hydrogen flowing from a plenum at various speeds. He developed a criterion for the inception of oscillations for parahydrogen as a function of static pressure but did not investigate steady oscillations at elevated static pressures.

In 1967, Feldman presented an optimization guide for designing Sondhauss oscillators.[29] This information is discussed and utilized in Chapter IV.

---

[29] K. T. Feldman, Jr., "The Mechanism Causing Heat Driven Pressure Oscillations in a Gas-Thermoacoustic Generator Design," Technical Report ME-29, Bureau of Engineering Research, University of New Mexico, September 1967.

CHAPTER III

PHYSICAL AND THEORETICAL ANALYSIS OF THERMOACOUSTIC OSCILLATIONS

In this chapter, the mechanisms causing and sustaining thermoacoustic oscillations will be reviewed. The functions of the various parts of a Sondhauss oscillator will be presented. Based on this and previous theory, a discussion of the behavior of thermoacoustic oscillations at elevated static pressures is presented. A design-prediction equation will be derived from dimensional analysis.

The mechanisms causing thermoacoustic oscillations

The following physical analysis and descriptions of the mechanisms causing and sustaining thermoacoustic oscillations were proposed by Feldman and are based on a variety of experiments with the Sondhauss type of thermoacoustic oscillator.[30]

A thermoacoustic oscillation may be produced when a steady or fluctuating heat addition occurs in a gas-filled cavity. For the thermoacoustic oscillation to grow, energy must be added so that there is a net increase in the total energy of the system after each cycle of oscillation. The Rayleigh criterion stated that in order to encourage oscillations when heat is added in a gaseous system, the heat must be added at the moment of greatest compression and must

---

[30] Feldman, "A Study of Heat Generated Pressure Oscillations in a Closed End Pipe," op. cit., pp. 43-68.

be removed at the moment of greatest expansion. In such a case, the basic driving mechanism is simple thermal expansion; when heat is added to a specified volume of gas, the gas normally expands producing a pressure wave. Thus the Rayleigh criterion explains how a thermoacoustic oscillation grows and is maintained, but it does not explain how the oscillation is started.

Many times, when heat is added to a resonant cavity, a thermoacoustic oscillation is not initiated. Therefore, it is desirable to have a knowledge of the requirements necessary for the inception of oscillations. It will be shown later that this information is very important in the study of thermoacoustic oscillations at elevated pressures.

The first requirement to initiate a thermoacoustic oscillation is to have a minimum rate of heat addition, $\dot{Q}_{min}$, into a cavity which is sufficient to drive the oscillation and to supply the inherent system losses. Consider a resonant cavity into which there is a steady heat addition rate, $\dot{Q}_{min}$. Initially the system is cold and nearly all the heat input is required to heat the system. After a lapse of time a thermal equilibrium state is reached which is indicated by a leveling off of the system's temperature. From this time on, the continued addition of heat not only supplies the system losses but tends to cause the system to become slightly superheated and unstable. This instability causes the system to release energy by some mode other than by normal heat transfer.

Thus, in this condition the system is ready to maintain a thermoacoustic oscillation as an additional mode of energy release, if one can be initiated.

The second requirement necessary to encourage a thermoacoustic oscillation is to have the heated cavity shaped so that a resonant gas oscillation can occur. Experimentally, it has been determined that a length-to-diameter ratio (L/d) near 12-15 is an optimum design condition.[31]

The third requirement is to locate the heat source at a point in the pipe where both the gas velocity and the pressure are of the same sign and of similar amplitude. This is necessary because the heat transfer driving the oscillations is proportional to the acoustic velocity (so the velocity must be large at the heat source for high heat transfer) and gives rise to pressure oscillations (so it must be possible for the pressure also to become large at the heat source).

When these three requirements have been met, the system is capable of sustaining a thermoacoustic oscillation. However, a fourth condition must be provided to start the oscillation, since the system cannot actually initiate the oscillation by itself even though it may be unstable. This fourth condition can be either of two distinct mechanisms by which the oscillation can be initiated, one mechanism for high rates of heat addition, $\dot{Q} >> \dot{Q}_{min}$, where $\dot{Q}$ is the rate of

---

[31] Feldman, "The Mechanism Causing Heat Driven Pressure Oscillations in a Gas--Thermoacoustic Generator Design," op. cit., p. 15.

energy addition, and one for low rates of heat addition near Q_{min}.

For low rates of heat addition, it has been determined that an external disturbance such as an induced pressure pulse is required to initiate the disturbance. For high rates of heat addition, of the order of $qL/c_pT_oa_o \approx 1$, thermal expansion pressure waves are the starting mechanism. This mechanism is described in detail by Trilling[32] and Feldman.[33]

The final requirement for the inception of thermoacoustic oscillations is that the response of the heat source to the initial disturbance be such that the disturbance is amplified as well as providing for a net increase of the total energy of the system after each cycle of oscillation. If the energy release fluctuates at a rate controlled by an external agency and is independent of the internal oscillation, the system will oscillate only when energy is released at certain characteristic frequencies. Such a phenomenon is usually described as resonance. A second type of heat source response occurs if the energy release depends upon the fluctuation inside the system. This is the case when the heat release is proportional to the pressure fluctuation. Thus, even if all the other requirements for the initiation of a thermoacoustic oscillation have been met, the buildup or damping of the

---

[32] Trilling, op. cit., p. 1.

[33] Feldman, "A Study of Heat Generated Pressure Oscillations in a Closed End Pipe," op. cit., pp. 49-50.

thermoacoustic system is still governed by the response of the heat source to the gas oscillations.

The functions of the parts of a Sondhauss oscillator

As previously mentioned, the function of the closed end of a Sondhauss oscillator can best be described as that of a mechanical spring. The function of the gas column is to provide a medium in which thermoacoustic oscillations can occur. It is analogous to a distributed mass in a mechanical system. The function of the heat source was explained in the previous section. It provides a limited method for controlling the oscillations.

The function of the tube bundle or constriction is somewhat more complicated. First, it makes a small contribution as a regenerator similar to the regenerator of a Stirling engine. That is, it absorbs heat during the expansion and cooling strokes, and it gives up heat during the return compression and heating strokes. Second, the tube bundle or constriction acts as a porous low-friction insulator; it thermally insulates the heated region from the cooled region while allowing the oscillating gas to pass freely from one region to the other.

As previously mentioned, the third essential function of the tube bundle or constriction is to act as an acoustic impedance. It causes a phase shift between the pressure and the specific volume (or pressure and velocity per unit area) per cycle. A phase shift is essential to the generation of the thermoacoustic oscillations.

Feldman also demonstrated that if two Sondhauss tubes are coupled mouth-to-mouth, a more efficient double-ended thermoacoustic oscillator is made. He also showed that the generated pressure waves tend to reinforce each other in a push-pull function. This fact is demonstrated in Figure 2. In the figure, it is seen that when one end is at a high pressure, the other end is at low pressure and vice versa. The difference in the amplitudes of the pressure waves in the photograph is due to the different sensitivities of the pressure transducers. The amplitudes of the two pressure waves are actually the same.

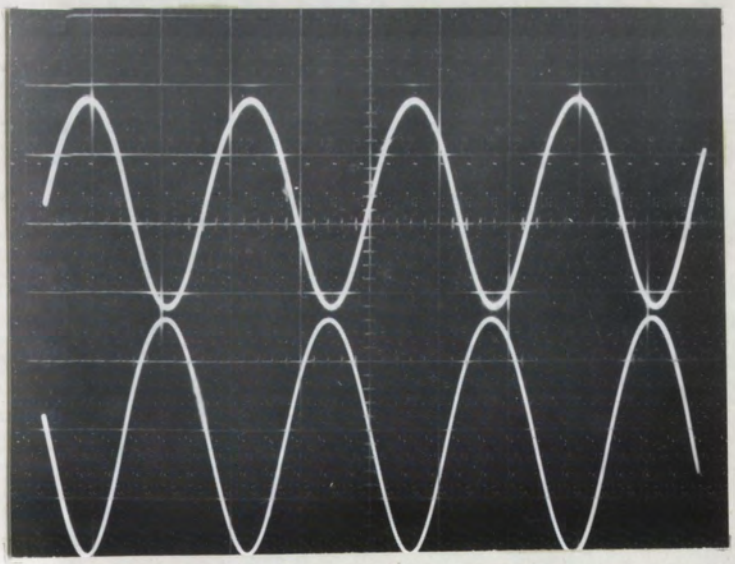

Figure 2. Oscilloscope photograph showing push-pull mechanism of a double-end thermoacoustic oscillator

The theory of Sondhauss oscillations at elevated pressures

The purpose of this section is to qualitatively investigate the behavior of previous theories at elevated static pressures and not to prove a given theory. Since no theory has been developed explicitly for the Sondhauss oscillation, the theories considered here are those derived for pressure generation due to a heat release in a gas. These theories are applied to and then analyzed for the special case of thermoacoustic oscillations.

The previous physical analysis was based on the equation of state for an ideal gas with constant specific heats. However, at high temperatures, the specific heats of most real gases are not constant. In the Sondhauss oscillator, the temperatures often reach 1000-1200°F. Therefore, when high heat release rates occur in a thermoacoustic system, high temperatures result and the effect of the variation of specific heats with temperature must be considered in addition to the Rayleigh criterion.

Feingold has shown that for conditions where specific heat varies with temperature, the mixing of two quantities of the same gas at the same original pressure but different original temperatures will cause a rise in pressure of the mixture.[34] This was expressed by an equation derived from basic thermodynamic relationships,

---

[34] A. Feingold, "Mixing of Gases at the Same Original Temperatures," (paper presented at the Missouri Academy of Sciences, University of Missouri, Columbia, Missouri, April 18, 1964), pp. 2-3.

$$\frac{p_m}{p_o} = 1 + \frac{QR}{p_o V_m}\left(\frac{1}{C_a} - \frac{1}{C_b}\right) \quad , \tag{7}$$

where p_m is the pressure of the gases after mixing, p_o is the original pressure which is the same for both gases, Q is the heat transfer from the hot gas to the cold gas as a result of mixing, R is the universal gas constant, V_m is the total volume of the gas mixture, C_a and C_b are the molar specific heats of gases A and B. Equation (7) indicates p_m equals p_o only if C_a equals C_b. If $C_b > C_a$ there will be a pressure rise due to mixing; this occurs when $T_b > T_a$.

Therefore, for very large temperature gradients between the hot region and the cold region in the thermoacoustic oscillator, the variation of specific heats with temperature causes added pressure changes which encourage oscillations.

It has been shown that for a thermoacoustic oscillator operating between the ranges of 1000°F and 100°F with air as the working fluid, Equation (7) predicts that the pressure ratio would be $p_m/p_o = 1.0072$.[35] It was concluded that the driving of oscillations by mixing expansions contributed very little to the maintainance of oscillations. This is true when p_o is on the order of 1 atmosphere. However, when p_o is increased to the order of several atmospheres, the effect of mixing expansions becomes more important. For this study, Equation (7) becomes

$$p_m = 1.0082\, p_o \quad . \tag{8}$$

---

[35] Feldman, op. cit., p. 67.

The reason Equation (8) differs from that arrived at by Feldman is in the arbitrariness of defining Q, which depends upon the mass transferred from the hot region to the cold region. The amount of mass can only be estimated.

Therefore, it can be concluded that although thermal expansion (the Rayleigh criterion) is the main driving mechanism for sustaining thermoacoustic oscillations, the contribution of mixing expansion becomes more significant at elevated static pressures, thereby increasing the acoustical output.

Since thermal expansion has been determined to be the more important contributor in thermoacoustic oscillations, the theory of thermal expansion will be dwelt upon in more detail.

Feldman found that the solution to Chu's wave equation (Equation 3) described thermoacoustic oscillations at atmospheric pressure within 4 per cent error.[36] Simplifying, Equation (3) becomes

$$p = \frac{\gamma-1}{2} \frac{\dot{w}}{a_o} \quad . \tag{9}$$

Inspection of the above equation shows that an increase of the static pressure has no effect on the generated over-pressure. However, if it is assumed that the over-pressure is a linear addition (superposition) of the over-pressures due to mixing and thermal expansion, the result is

---

[36] Feldman, op. cit., p. 178.

$$p = \frac{\gamma-1}{2} \frac{\dot{w}}{a_o} + \frac{QR}{V_m} \left(\frac{1}{C_a} - \frac{1}{C_b} \right) \tag{10}$$

In equation (10), p is the total over-pressure generated by mixing and thermal expansion. The sound-pressure level determined by Equation (10) as a function of static pressure is plotted in Figure 3 for a constant energy rate of 700 watts. Inspection of Figure 3 shows that the acoustic output increases with an increase in static pressure. Equation (10) and Figure 3 are valid only for low rates of heat release ($\dot{q}L/c_p T_o a_o << 1$).

For higher rates of heat release ($\dot{q}L/c_p T_o a_o \approx 1$), Chu showed that the result to Equation (1) is[37]

$$\frac{\dot{w}}{a_o p_o} = \frac{\frac{2}{\gamma-1} \frac{p_1}{p_o} \left[\frac{p_1}{p_o} - 1 \right]}{\left[\frac{\gamma+1}{\gamma} \frac{p_1}{p_o} + \frac{\gamma-1}{2\gamma} \right]^{1/2}} \tag{5}$$

Equation (5) is a quartic equation and therefore difficult to solve. Chu noted that the solution to Equation (5) for air is[38]

$$\frac{p_1}{p_o} = 0.325 \left(\frac{\dot{w}}{a_o p_o} \right)^{2/3} \tag{11}$$

A least squares curve fit was used to check Equation (11). Data for the fit was generated by substituting values of p_1/p_o

---

[37] Chu, "Pressure Waves Generated by Addition of Heat in a Gaseous Medium," op. cit., p. 26.

[38] Ibid.

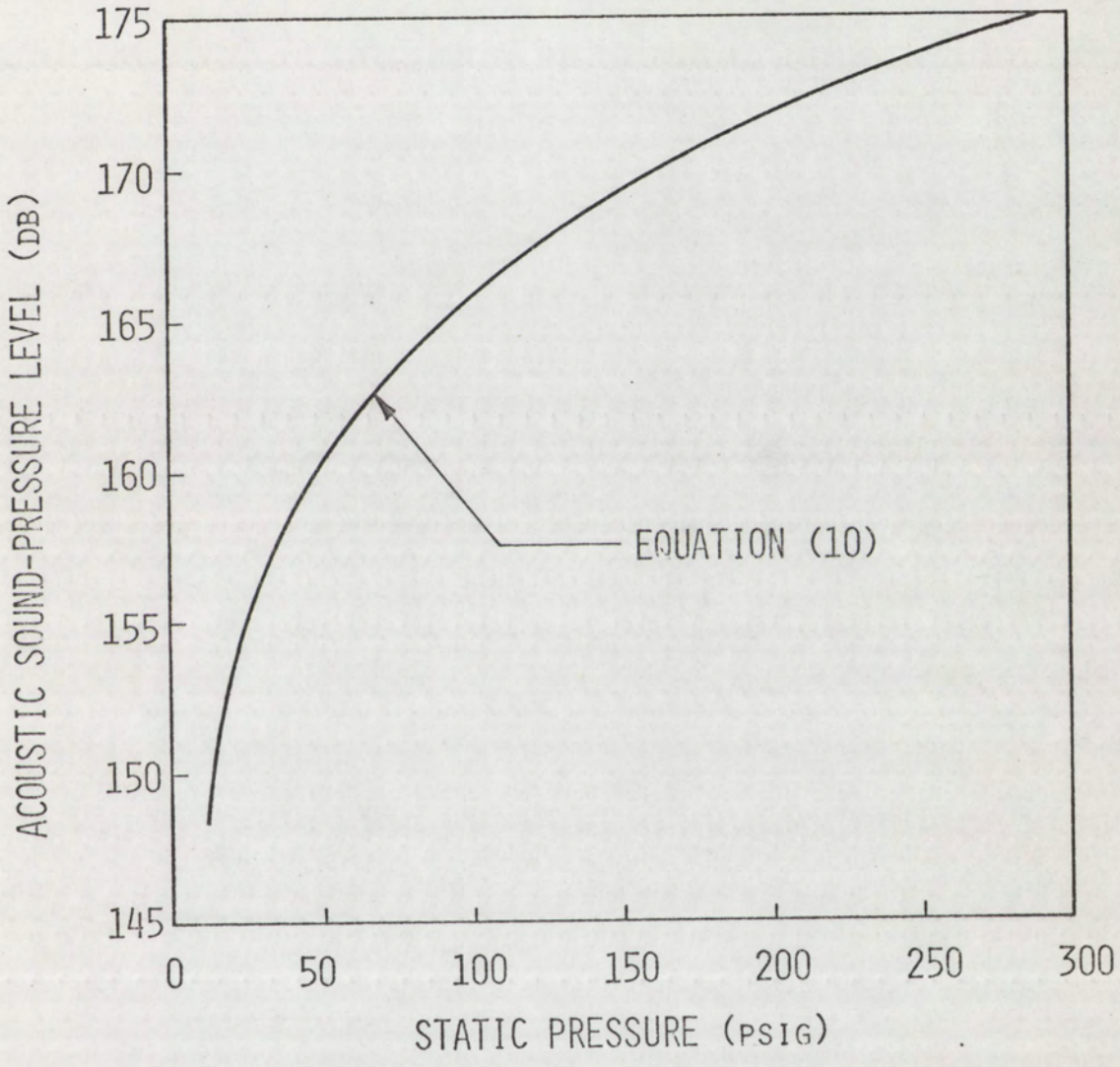

Figure 3. Sound-pressure level as a function of static pressure as given by Equation (10) The working gas is air

into Equation (5) to obtain values for $\dot{w}/a_o p_o$. One point, $p_1/p_o=2$, deviates somewhat from the trend of the curve drawn through the other points. If this point is neglected, Equation (11) is given as the best fit; if $p_1/p_o=2$ is included in the calculations, the equation determined by the curve fit is

$$\frac{p_1}{p_o} = 0.551 \left(\frac{\dot{w}}{a_o p_o}\right)^{.586} \tag{11a}$$

In the same manner, if helium is considered to be the working fluid, the solution to Equation (5) is

$$\frac{p_1}{p_o} = 0.917 \left(\frac{\dot{w}}{a_o p_o}\right)^{.545} \tag{12}$$

The sound-pressure levels as a function of static pressure given by Equations (11), (11a), and (12) are plotted in Figure 4 for a constant rate of heat addition of 700 watts. The over-pressure due to mixing was considered negligible for high rates of heat release. Inspection of Equations (11), (11a), and (12) show that the heat-generated pressure p_1 increases with static pressure to the one-third or .414 power for air, and to the .455 power for helium.

The results shown in Figures 3 and 4 will be compared with the experimental results in Chapter V. However, the significant concept of this section is that the theory indicates that an increase in static pressure of a thermoacoustic system yields an increase in acoustic output.

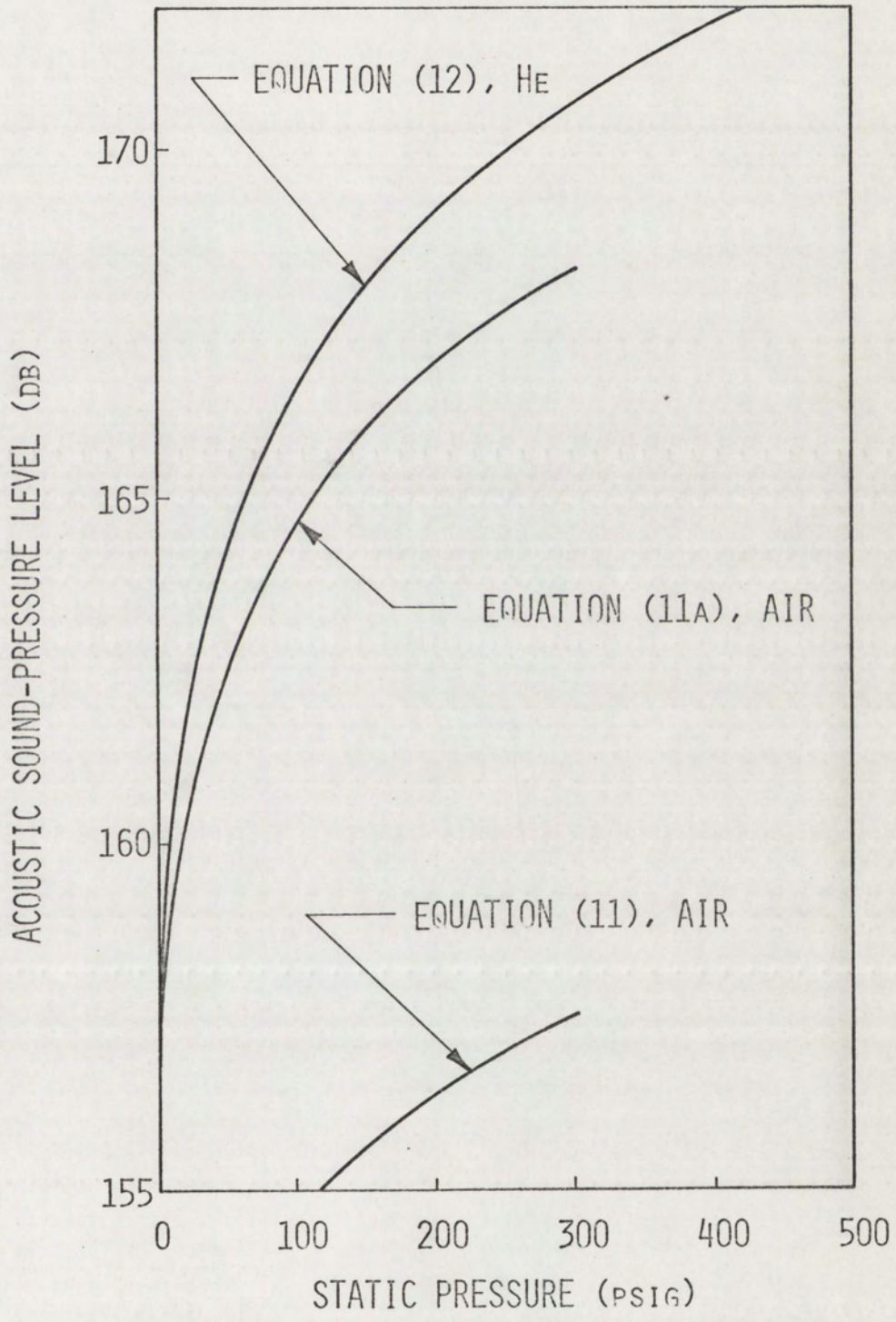

Figure 4. Sound-pressure level as a function of static pressure as given by Equations (11), (11a), and (12)

Dimensional analysis

The purpose of this section is to derive a prediction criterion from dimensional analysis, which, when coupled with experimental data will give design information.

The pertinent variables and their dimensions in the MLtT (mass-length-time-temperature) system for a gas-filled thermo-acoustic system are:

overpressure	$p, \{p\}$	$= ML^{-1}t^{-2}$
static pressure	$p_o, \{p_o\}$	$= ML^{-1}t^{-2}$
length	$L, \{L\}$	$= L$
length coordinate	$x, \{x\}$	$= L$
diameter	$d, \{d\}$	$= L$
power addition	$\dot{Q}, \{\dot{Q}\}$	$= ML^2t^{-3}$
gas density	$\rho, \{\rho\}$	$= ML^{-3}$
temperature	$T, \{T\}$	$= T$
specific heat	$c_p, \{c_p\}$	$= L^2t^{-2}T^{-1}$
gas constant	$R, \{R\}$	$= L^2t^{-2}T^{-1}$
specific heat ratio	$\gamma, \{\gamma\}$	$= 1$
sonic velocity	$a, \{a\}$	$= Lt^{-1}$
frequency	$\omega, \{\omega\}$	$= t^{-1}$

(13)

The significant variables for Equation (13) are pressure p, length x, power $\dot{Q}$, density ρ, temperature T, gas constant R, specific heat ratio γ, sonic velocity a, and frequency ω. Since R and c_p have the same dimensions, either variable can be chosen to represent the other.

The Buckingham Pi Theorem states that

$$s = n-r \tag{14}$$

where s is the number of non-dimensional numbers that can be found from the significant variables, n is the number of significant variables, and r is the number of basic dimensions needed to describe the variables.[39] For the thermoacoustic system, n=9, r=4, therefore s=9-4=5 non-dimensional numbers. Using the method of Skoglund,[40] the non-dimensional numbers N_i are

$$N_1 = \frac{pax^2}{Q} \tag{15}$$

$$N_2 = \frac{p}{\rho RT} \tag{16}$$

$$N_3 = \gamma \tag{17}$$

$$N_4 = \frac{a^2}{RT} \tag{18}$$

$$N_5 = \frac{x\omega}{a} \tag{19}$$

A check of the matrix formed by listing the exponent of a variable as it appears in a non-dimensional number where the rows of the matrix are the non-dimensional numbers and the columns are the variables, shows the numbers in Equations (15)-(19) to be independent. Combining N_3 and N_4 results in

---

[39] I. H. Shames, Mechanics of Fluids, (New York: McGraw-Hill Book Company, Inc., 1962) p. 191.

[40] V. J. Skoglund, Similitude: Applications and Theory, (Scranton: International Textbook Company, 1967) pp. 38-49.

a new number,

$$N_6 = N_3^{-1}N_4 = \frac{a^2}{\gamma RT} \tag{20}$$

In a similar manner

$$N_7 = N_1^{2/3}N_4^{-1/3}N_2^{1/3} = \frac{px^{4/3}}{\rho^{1/3}\dot{Q}^{2/3}} \tag{21}$$

Another check of the exponential matrix using N_7 to replace N_1 and N_6 to replace N_4 shows the set of non-dimensional numbers to still be independent. However, N_7 and N_1 will be used, depending on which is more advantageous, but they cannot be used together.

It is sometimes useful to set a non-dimensional number equal to a constant.[41] Applying this to the previous numbers,

$$N_2 = \frac{p_o}{\rho_o RT_o} = 1 \tag{22}$$

$$N_6 = \frac{a_o^2}{\gamma RT_o} = 1 \tag{23}$$

$$N_5 = \frac{\omega L}{a_o} = 1/4 \tag{24}$$

In equations (22)-(24) the subscript o denotes that the significant variables have been chosen to be those at the steady state static pressure. Inspection of the above equations

---

[41] Ibid., p. 20.

reveals that Equation (22) is the equation of state for an ideal gas, Equation (23) is the definition of sonic velocity for an ideal gas, and Equation (24) is the familiar "organ-pipe frequency" equation.[42]

A prediction equation is obtained by setting N_7 equal to a constant,

$$\frac{p x^{4/3}}{\rho_o^{1/3} \dot{Q}^{2/3}} = \text{constant} \tag{25}$$

If the constant in Equation (25) is chosen to be some reference level denoted by the subscript r, then the equation becomes

$$\frac{p x^{4/3}}{\rho_o^{1/3} \dot{Q}^{2/3}} = \frac{p_r x_r^{4/3}}{\rho_{or}^{1/3} \dot{Q}_r^{2/3}} \tag{26}$$

Combining Equation (26) with Equation (22) to eliminate and solving for the over-pressure p,

$$p = p_r \left(\frac{\dot{Q}}{\dot{Q}_r}\right)^{2/3} \left(\frac{x_r}{x}\right)^{4/3} \left(\frac{p_o R_{or} T_{or}}{p_{or} R_o T_o}\right)^{1/3} \tag{27}$$

For this study, $R_{or}=R_o$ and $T_{or}=T_o$. Therefore, Equation (27) becomes

---

[42] L. L. Beranek, Acoustics, (New York: McGraw-Hill Book Company, Inc., 1954), p. 286.

$$p = p_r\left(\frac{\dot{Q}}{\dot{Q}_r}\right)^{2/3}\left(\frac{x}{x_r}\right)^{4/3}\left(\frac{p_o}{p_{or}}\right)^{1/3} \qquad (28)$$

If a single operating point of a thermoacoustic system is known, Equation (28) can be used to predict the acoustic over-pressure at other operating points of the system. The retention of the variable x in Equation (28) allows the prediction of the acoustic oscillatory pressure at different locations inside the oscillator.

Two special cases of Equation (28) which are of interest are $x=x_r$ and $\dot{Q}=\dot{Q}_r$. For these special cases, Equation (28) becomes

$$p = p_r\left(\frac{\dot{Q}}{\dot{Q}_r}\right)^{2/3}\left(\frac{p_o}{p_{or}}\right)^{1/3} \qquad (29)$$

and

$$p = p_r\left(\frac{p_o}{p_{or}}\right)^{1/3} , \qquad (30)$$

respectively. Equation (29) predicts the acoustic over-pressure if static pressure and power input are considered to be the only significant variables, and Equation (30) predicts the over-pressure if static pressure is considered to be the only significant variable.

Equations (28), (29), and (30) will be correlated with experimental results in Chapter V. The limitation of Equations (28)-(30) is that they are restricted to a given

thermoacoustic system for which at least a single operating condition is known. It is interesting to note that Equation (11) in the previous section indicates that over-pressure increases with static pressure to the one-third power, as do Equations (28)-(30), derived by dimensional analysis.

An important non-dimensional number is the thermoacoustic efficiency, η_{ta}.[43] It is defined by

$$\eta_{ta} = \frac{Ap^2}{2\rho_o a_o \dot{Q}} \quad , \tag{31}$$

where A is the cross-sectional area normal to the pressure wave. The thermoacoustic efficiency can be obtained by combining N_1, N_2, and N_4. Physically, the thermoacoustic efficiency is the average rate of flow of acoustic energy through a unit area normal to the direction of wave propagation (acoustic intensity), divided by the thermal power input. Kinsler and Frey give the acoustic intensity of a plane wave as $\frac{p^2}{2\rho_o a_o}$.[44]

Another non-dimensional number used in this study is the mechanical "efficiency". It is defined as

$$\eta_M = \frac{p_o A a_o}{\dot{Q}} \tag{32}$$

It is obtained by making p_o the significant pressure in N_1 and replacing x^2 by the cross-sectional area A. It is termed

---

[43] Feldman, op. cit., p. 94.

[44] Kinsler and Frey, op. cit., p. 121.

an "efficiency" because the numerator represents an acoustic power (pressure times area times velocity) and the denominator $\dot{Q}$ is the thermal power input. Although it does not represent the efficiency of the thermoacoustic system, the mechanical efficiency will be useful in the correlation of results in Chapter V.

In summary, the dimensional analysis yields three prediction equations

$$p = p_r\left(\frac{\dot{Q}}{\dot{Q}_r}\right)^{2/3}\left(\frac{x_r}{x}\right)^{4/3}\left(\frac{p_o}{p_{or}}\right)^{1/3} \tag{28}$$

$$p = p_r\left(\frac{\dot{Q}}{\dot{Q}_r}\right)^{2/3}\left(\frac{p_o}{p_{or}}\right)^{1/3} \tag{29}$$

$$p = p_r\left(\frac{p_o}{p_{or}}\right)^{1/3} \tag{30}$$

subject to the limitations discussed earlier, and two non-dimensional numbers useful in the correlation of data:

thermoacoustic efficiency,

$$\eta_{ta} = \frac{Ap^2}{2\rho_o a_o \dot{Q}} \tag{31}$$

and

mechanical efficiency,

$$\eta_M = \frac{p_o A a_o}{\dot{Q}} \quad . \tag{32}$$

CHAPTER IV

EXPERIMENTAL ANALYSIS OF THERMOACOUSTIC OSCILLATIONS AT ELEVATED STATIC PRESSURES

In this chapter, the system which was designed to experimentally determine the behavior of thermoacoustic oscillations at elevated pressures is described. The procedures used in calibrating the measurement system and the techniques used in obtaining the experimental data are discussed.

The experimental system

The pipe

Figure 5 is a schematic drawing of the system used for the experimental study. A completely closed, double-end Sondhauss thermoacoustic oscillator was chosen because it permits control of the internal gas pressure and because of its greater efficiency.[45]

The pipe had a 1/8-inch thick wall, was of 3-3/8-inch ID stainless steel of AISI Type 308, form rolled and seam welded along one side, with flanges of the same material welded to each end to permit the joining of the pipe sections. Instrumentation ports were welded to the pipe and then drilled and tapped with a 1/4-inch NPT. The pipe was in three sections; two were 16 inches long and the third was 48 inches long. The pipe was joined, with the long section in the middle between the two

---

[45] Feldman, "The Mechanism Causing Heat Driven Pressure Oscillations in a Gas-Thermoacoustic Generator Design," op. cit., p. 26.

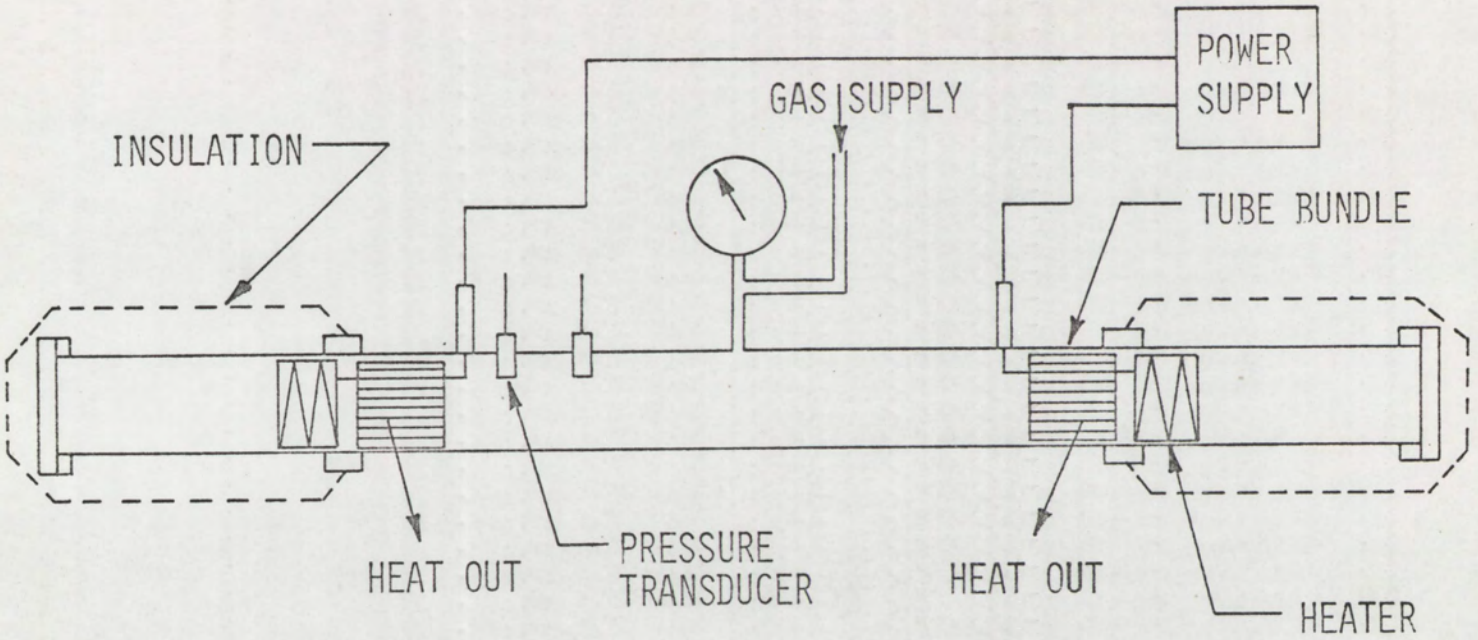

Figure 5. Schematic line drawing of double-end Sondhauss oscillator

shorter sections. The tube bundles and heater elements were placed at the pipe junctions, making their placement ratio $x/L=0.390$, which is within the optimum range, $0.33 \leq x/L \leq 0.40$.[46] The butt plates were 1-inch-thick steel, AISI type 4043. The assembly is shown in Figure 6.

By using design data and equations from Marks, the maximum operating pressure limit of the pipe was calculated to be 800 psi at 1000°F.[47] This limit includes a safety factor of 2.

The pipe and end plates were held together with four 3/4-inch 10-NC-2A high-strength bolts. The same kind of bolts were used for joining the pipe sections. Each bolt was tightened to 160 foot-pounds torque.

To insure leakproof junctions and to provide insulation between the sections, high-temperature gaskets were used in sealing the sections of the pipe and the end plates. These gaskets were made from 1/16-inch-thick Garlock gasket material, number 002568, manufactured by Garlock Gasket Company. The gaskets were coated with silicone vacuum grease for better seals.

The assembled pipe was safety checked by filling it with water, submerging it in water, and pressurizing the system to 600 psig by the addition of air. Water was used because it would not expand like a gas if the pipe ruptured. After the

---

[46] Ibid., p. 17.

[47] T. Baumeister, Ed., Marks' Standard Handbook for Mechanical Engineers, (7th ed., New York: McGraw-Hill Book Company, 1967), pp. 5-14--5-47, 6-39--6-45.

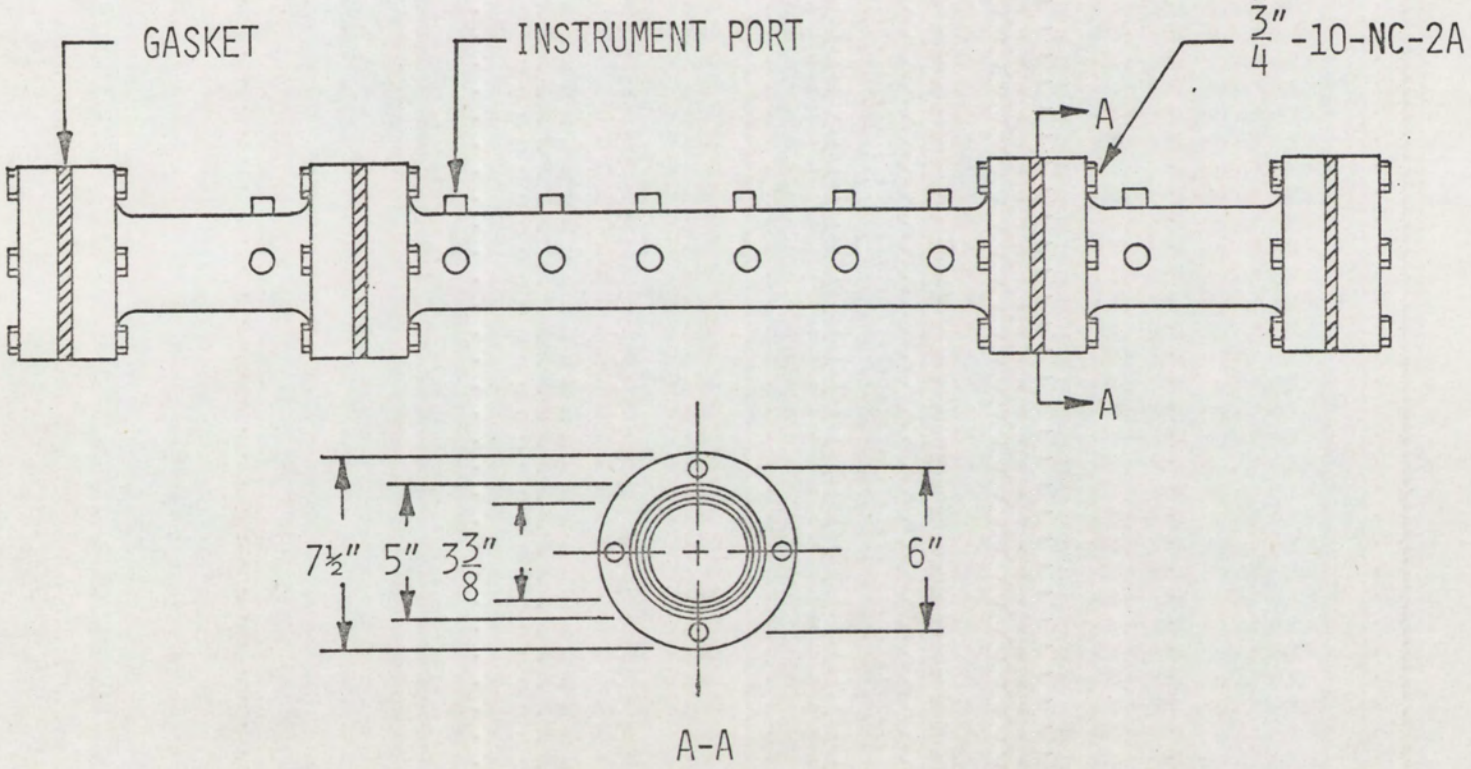

Figure 6. Pipe assembly used for the thermo-acoustic oscillator in this study

safety check, the pipe was emptied and pressurized again with air to check for air leaks.

Heater elements

The heater elements were made by threading chromel ribbon through a cylinder made to fit the tube. The chromel-C ribbon was 1/4-inch wide and 0.005-inch thick and was manufactured by the Hoskins Manufacturing Company, Detroit, Michigan. The heater support cylinder was machined from Lava, Grade A, which chemically is a hydrous aluminum silicate, manufactured by the American Lava Corporation (subsidiary of 3M Co.), Chattanooga, Tennessee. The dimensions of the heater element are shown in Figure 7. After machining, the lava was placed in a furnace and heated for two days until 2000°F was reached. The furnace was turned off and the lava was allowed to cool naturally in the furnace for about one day until it was at a temperature of 200°F. The firing made the lava extremely durable and hard. It was removed and wound with the chromel ribbon. The resistance of each heated element was about 2.3 ohms. A photograph of a heater element is shown in Figure 8, along with a tube bundle.

Before insertion of the heater elements into the pipe, they were wrapped with a single layer of 1/16-inch asbestos cloth to provide exterior electrical insulation. They were then connected to electrical leads with small metal screws and the short sections of pipe were slipped over the elements.

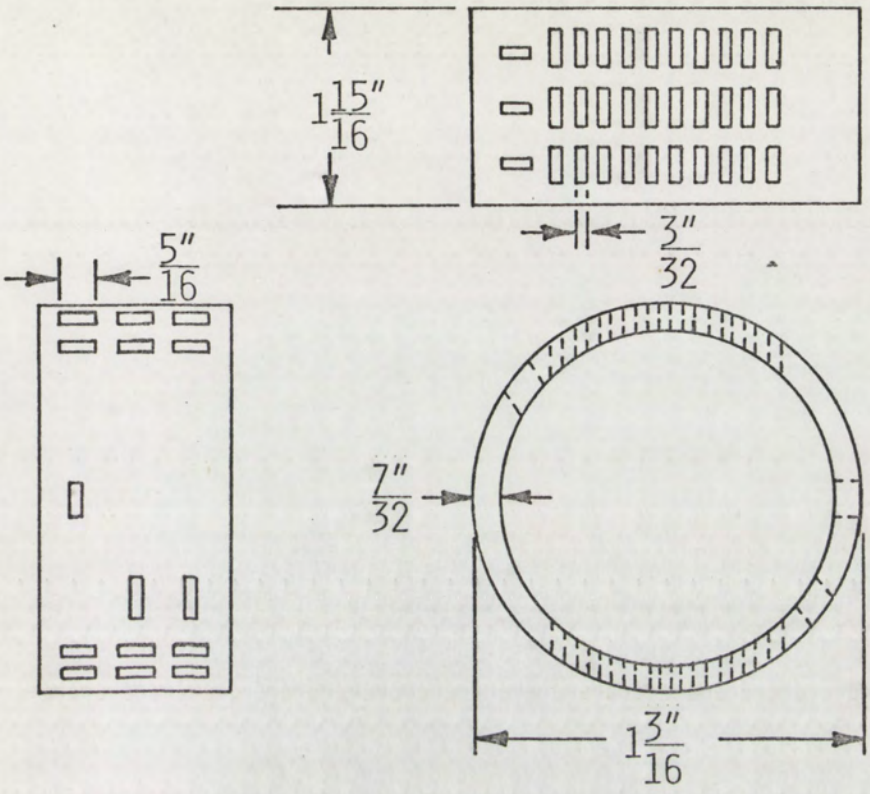

Figure 7. Line drawing of a heater element

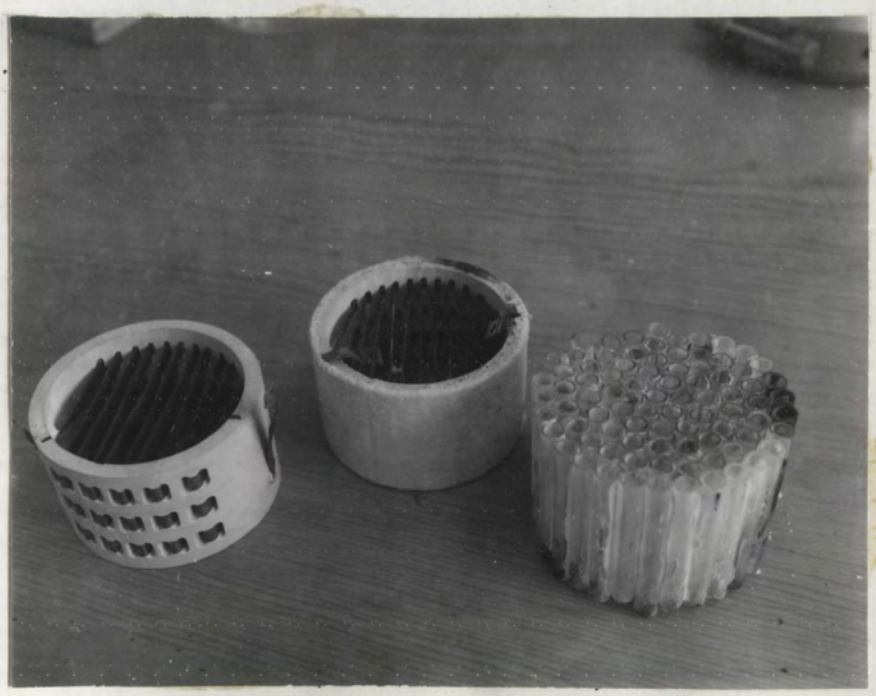

Figure 8. Photograph of a heater element and tube bundle

The electrical leads were 3/32-inch brass rods, 9-3/4 inches long. Each end of the rod was flattened, and one end was drilled and the other was drilled and tapped. The drilled end was connected to an electrode and the drilled and tapped end was connected to the heater element. This method of connection is shown in the photograph in Figure 9.

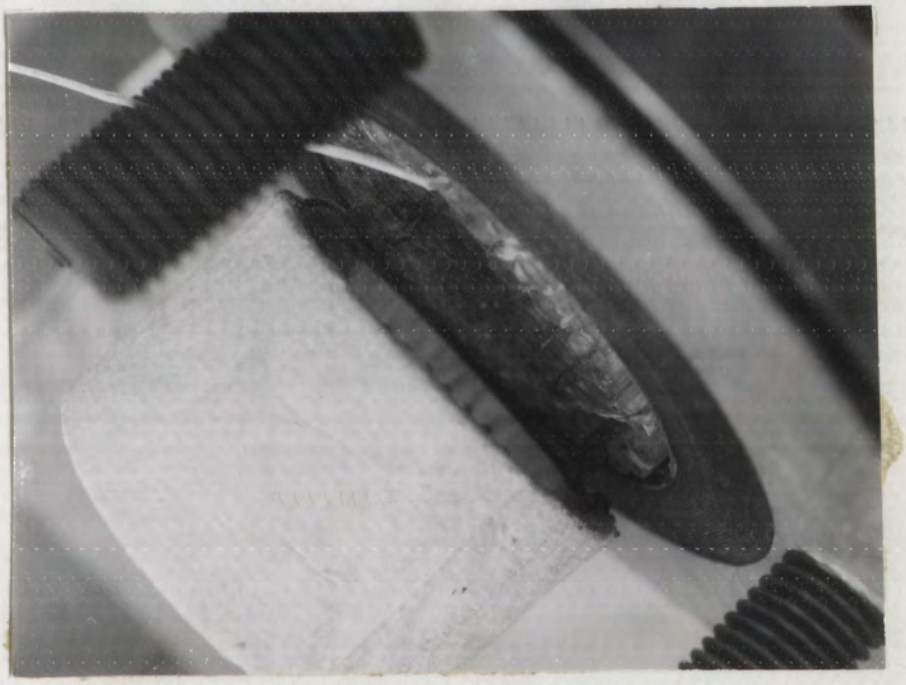

Figure 9. Photograph showing the method of connection of the heater element to power leads

The tube bundle

The glass tubes used in making the tube bundles had an L/d ratio of 12.7, which is in the optimum recommended range.[48] They were made of pyrex glass tubing of 6-mm OD and 7.62 cm

[48]Feldman, op. cit., p. 19.

long. The tube bundles were assembled with heat resistant Sauereisen No. 1 paste cement, manufactured by Sauereisen Cements Company, Pittsburgh, Pennsylvania. They were made so that the maximum number of tubes could make up the bundle and still fit into the 3-3/8-inch cavity of the pipe. A tube bundle is shown in Figure 7 with a heater element.

Electrodes

Initially, the system was designed so that the electrodes would enter the pipe in the heated section. This would have saved running long leads through the tube bundles to the heater elements. However, no electrodes could be found that could withstand the high temperatures involved.

After two failures to place the electrodes in the heated section, the final location, 10 inches in from either end, in the cool middle section of pipe, was chosen. The electrodes used were fabricated from four of the electrodes that had previously failed. These glands were Nan O Seal Electrode Glands, Series A-A1211-SS stainless steel glands with stainless steel electrodes, manufactured by Nanmac Corporation, Needham Heights, Massachusetts. A drawing of the modified glands, along with significant dimensions, is shown in Figure 10.

The epoxy used by Nanmac Corporation was burned out of the glands with a torch. The glands and electrodes were then cleaned and filled with GA-2 epoxy, manufactured by Budd Instrument Division, Phoenixville, Pennsylvania. A homogeneous filling of epoxy was insured by pulling a vacuum on one end

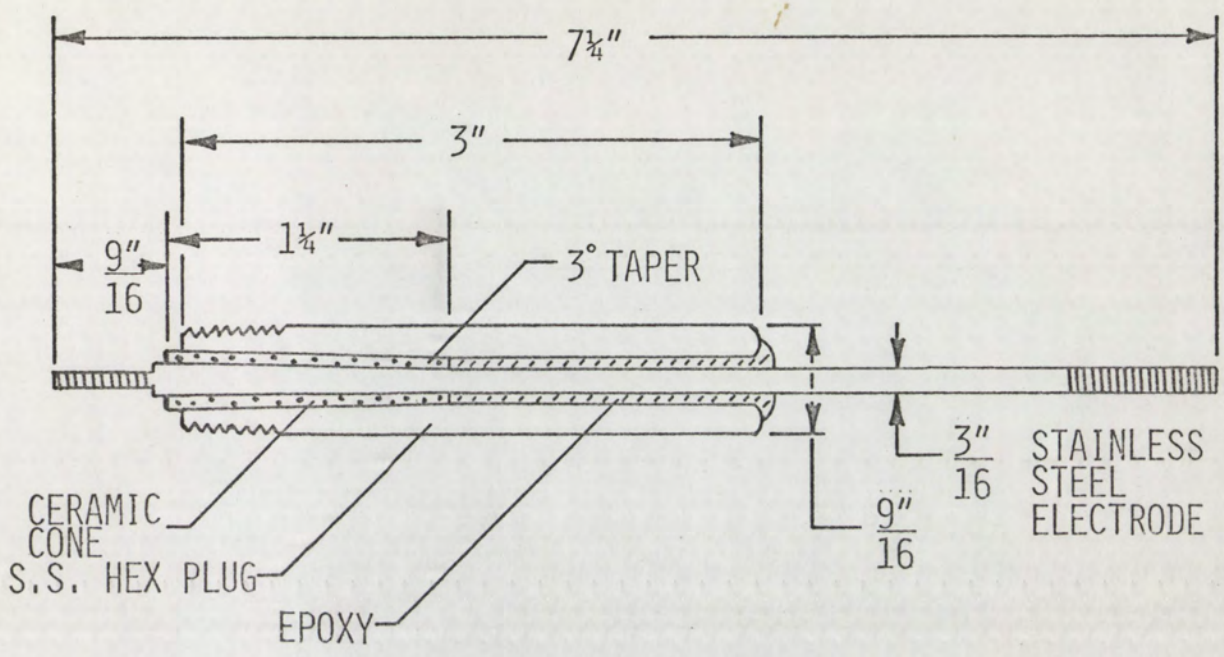

Figure 10. Line drawing of the modified electrode glands used in the experimental study

Figure 11. Photograph of the electrode and thermocouple glands used in this analysis

of the gland, and "working" the epoxy during the pouring. A photograph of an electrode gland, along with a thermocouple gland (to be explained later), is shown in Figure 11.

Cooling system

Cooling for the thermoacoustic oscillator was provided by water circulation through external baths surrounding the pipe. The baths were fabricated from 1/4- and 1/8-inch aluminum plate. The dimensions of the baths are shown in Figure 12. To create a steep temperature gradient in the gas, it was desirable to have the cooling section as close to the hot section as possible. The water baths encompassed about three-fourths of the tube bundles region.

The water circulation was provided by a small pump. The flow rate was maintained constant at 1/4 gallon per minute per bath. The pump was immersed in a large reservoir of approximately 12 gallons, in which a 25-pound block of ice was continuously maintained. Although no precise measurement of the amount of heat removal by the water baths was made, it was estimated that they removed a maximum of 29 Btu/min (0.51 kw) at 1500 watts power input and 200 psig pressure.

Insulation

In order to minimize heat losses, the heated sections were insulated. The first covering of insulation was two layers of 1/64-inch paper asbestos which was dampened with water and molded onto the pipe and end plates. Upon hardening, this provided a solid homogeneous insulator. This was

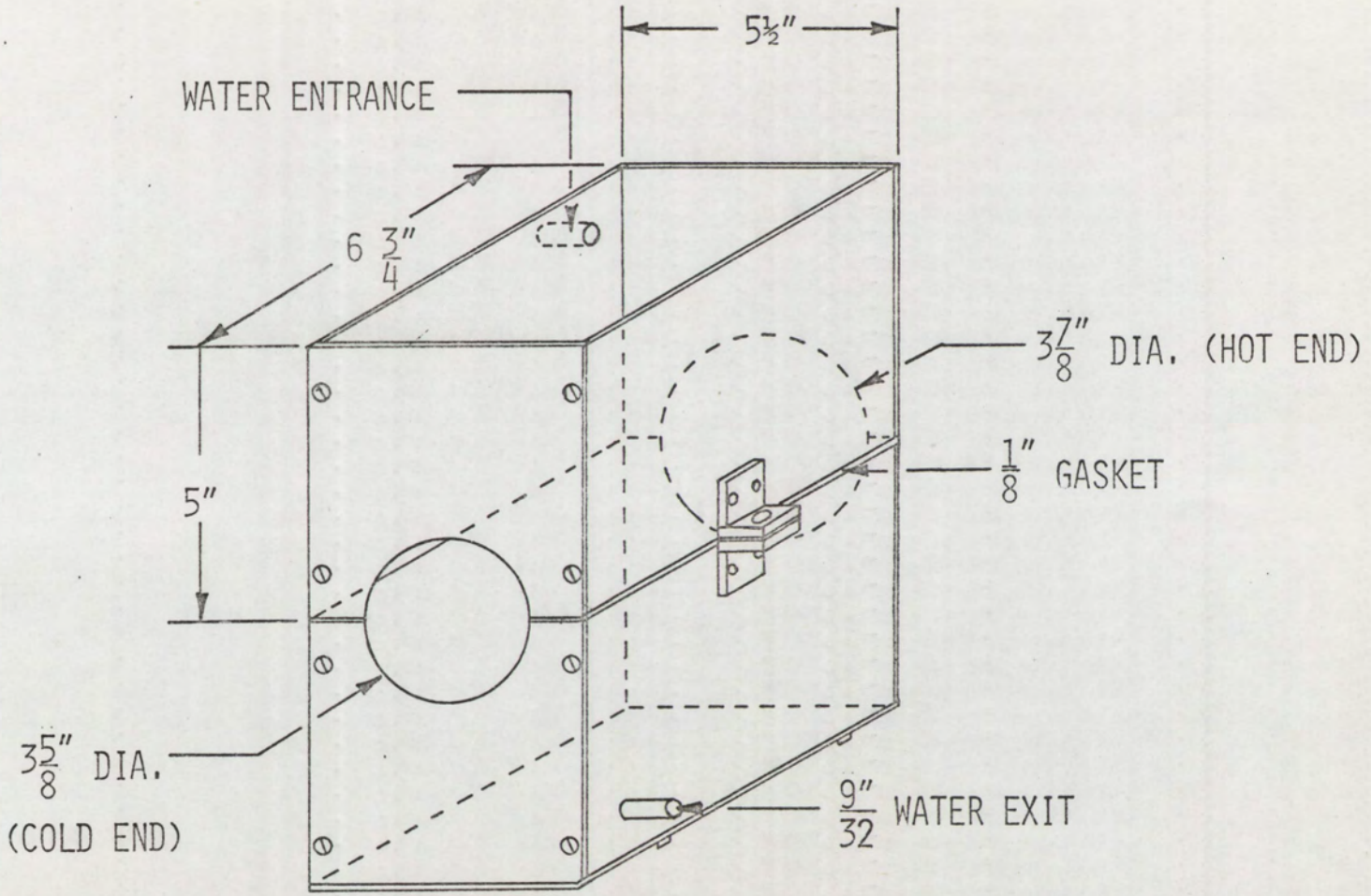

Figure 12. Drawing of the cooling baths used in the analysis

covered with two layers of 1-inch-thick fiberglass insulation.which was surrounded with a layer of aluminum foil. The foil was covered with two more layers of fiberglass insulation, followed by a final layer of aluminum foil.

No attempt was made to measure heat losses from the hot ends of the heated pipe or, as previously stated, heat absorbed by the water baths. Therefore, the specified rate of heat input does not indicate the amount of thermal power actually transferred to the oscillating air but simply the thermal power available to the system.

Power supply

Power for the thermoacoustic oscillator was supplied by two variable transformers. One was a Volt Pac, manufactured by General Electric Company, Fort Wayne, Indiana, that had a 120 volt input with a 0-120/140 volt output and could handle up to 50 amps. The other was manufactured by General Radio Company, Cambridge, Massachusetts; it had a 120-volt input with a 0-135-volt output and could handle up to 45 amps.

The power input to each element was measured by a wattmeter. One was a low-power-factor wattmeter manufactured by Sensitive Research Instrument Company, Mount Vernon, New York, rated at 30 amps and with a 2500-watt range. It was accurate within ±5 watts. The other wattmeter was a Simpson Model 880, manufactured by Simpson Electric Company, Chicago, Illinois, which was capable to handling up to 30 amps and had a 2000-watt range. It was accurate to ±7-1/2 watts.

Gas supply

Bottled air and grade A helium were the working gases used in the thermoacoustic oscillator. Air was used, since it is the most common of all gases. The use of air also allowed comparison of the results of this investigation with those of previous studies. Helium was chosen because of its high specific heat and low mass, which should cause high thermoacoustic intensities. Because it is inert, helium also prevented oxidation of the electrodes and heater elements, prolonging the life of the system. Pertinent constants for air and helium are tabulated in the Appendix.

The gases were charged and discharged from the pipe by means of two valves, Dragon Model 816 soft-seat valve, 6000 psi, manufactured by Dragon Valves Inc., Norwalk, California. The valves were located on both sides of a piping cross, one end of which was connected to the pipe and the other end was attached to a Bourdon gage for static pressure measurement. The Bourdon gage was manufactured by U.S. Gage Company, New York, New York, and had a full-scale reading of 800 psig.

In addition, another gage was mounted on the outside of one of the valves for vacuum measurement. It was attached to a piping tee so that a vacuum pump could also be connected to the system. This gage was a Marsh Safecase Gage, Type 200-C, manufactured by Marsh Instrument Company, Skokie, Illinois, and had a full-scale range of 30 inches of mercury.

Pressure measurement instrumentation

The pressure tranducers chosen for the experimental measurement of oscillatory pressure were Susquehanna Model ST-2 piezoelectric gages manufactured by Susquehanna Instruments, Bel Air, Maryland.

Piezoelectric transducers were chosen because of their very high natural frequencies, low damping, and close similarity to the elements used in acoustic microphones.[49] The ST-2 was chosen because it was readily available and easily adapted to the system.

The specifications on the two tranducers chosen for the experimental analysis are as follows:

Sensor	Lead zirconate
Range	0.1-500 psi (lower limit corresponds to 150 db)
Sensitivity #262	22 picocoulombs/psi
#263	27.3 picocoulombs/psi
Capacitance	150 picofarads
Maximum Temperature	300°F
Linearity	±2% full scale
Natural Frequency	250 kilocycles
Resistance	40×10^9 ohms

Transducer No. 263 was located at x/L=0.366 and No. 262 was located at x/L=0.417.

---

[49] E. O. Doebelin, Measurement Systems: Application and Design, (New York: McGraw-Hill Book Company, 1966), p. 387.

Since piezoelectric transducers are sensitive to temperature fluctuations, an attempt to thermally isolate them was made by mounting the gages in adapters attached to the pipe. A cross-sectional view of the adapter, along with dimensions, is given in Figure 13. A glass capillary tube was used in the adapter to serve two purposes; first it prevented the cavity in the adapter from becoming a resonant cavity thereby distorting the pressure signal, and second, it acted as a thermal insulator between the gas and the tranducer while still allowing measurement of the pressure pulse. Figures 14 and 15 are photographs of the ST-2 gages.

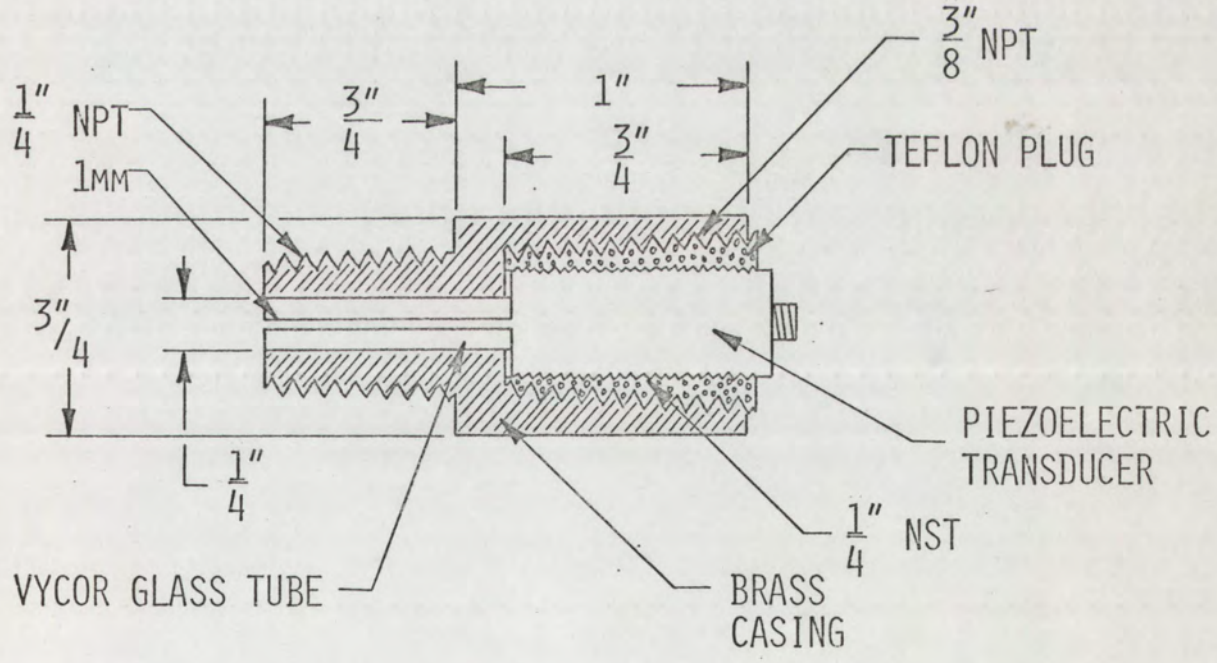

Figure 13. Line drawing of a piezoelectric pressure adapter

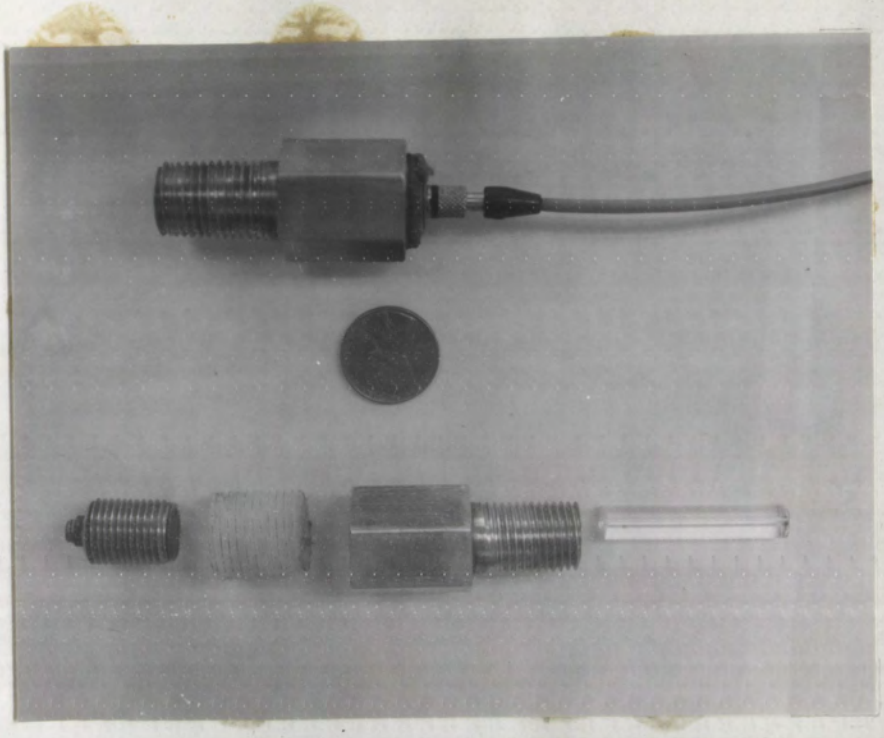

Figure 14. Photograph of piezoelectric pressure tranducers and adapters

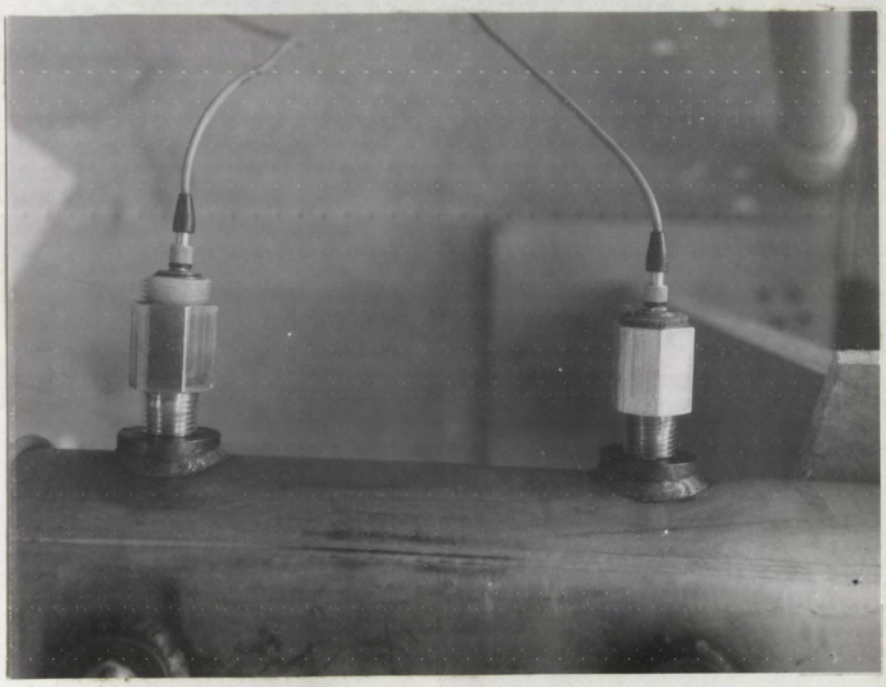

Figure 15. Photograph of the mounting of pressure tranducers and adapters

Since the piezoelectric transducer produces a high-impedance charge signal, a charge amplifier was required to convert this signal to a low-impedance voltage which could be displayed on an oscilloscope.[50] A charge amplifier was selected over the cathode follower because of its versatility and known gain.[51] A charge amplifier (or a cathode follower) was ideal for the analysis because it readily transmitted the AC signal of the oscillatory pressure. The charge amplifier used was a Kistler Model 566S3A, manufactured by Kistler Instrument Corporation, Clarence, New York. Microdot cables 8-feet long were used in the connection of the ST-2 gages to the charge amplifier.

The low-impedance voltage produced by the charge amplifier was displayed on a Type 502 dual-beam oscilloscope manufactured by Tektronix, Inc., Portland, Oregon. Since only one charge amplifier was available, the cables from the ST-2 transducers were interchanged at the charge amplifier for the taking of data.

Temperature measurement instrumentation

The temperature measurements taken during the experimental analyses were intended to qualitatively relate the temperature at one location to that of another location. Therefore, the

---

[50] Kistler Instrument Corporation, "Operating and Service Instructions for Kistler Quartz Transducers," Clarence, New York, p. 4.

[51] E. N. Kaufman, "Charge Amplifier Versus Source Follower," Instruments and Control Systems, Vol. 39, April 1966, p. 129.

number given for a temperature is that indicated by the measuring system; errors in the measurement due to radiation and conduction were not taken into account. The most important function of the temperature measurement was the determination of steady-state operating conditions.

Chromel-alumel thermocouples were chosen for the temperature measurements because of their linearity and high output in the anticipated range of measurement, their versatility, and ready availability.[52,53,54] The range of the chromel-alumel thermocouple is -200°-1300°F with an error of ±4°F (32° to 660°F) and 0.75 per cent (660°-1300°F).[55,56] Although the error for the chromel-alumel thermocouple is larger than that of other thermocouples, it had little effect on the temperature measurement, since the analysis was qualitative and the exact temperatures were not important. The chromel-alumel thermocouples used were ISA Type K, 28-gage, manufactured by Leeds and Northrup Company, Philadelphia, Pennsylvania. Each lead had an asbestos insulation with an overall fiberglass insulation. Ten thermocouples were located throughout the system, as shown in Figure 16. The numbers are the identification numbers used throughout the analysis.

---

[52] W. H. Kirk, "Thermocouple Primer," Instruments and Control Systems, Vol. 41, March 1968, pp. 77-82.

[53] R. A. Hartz, "Temperature Transducers: A Guide for Selection," Machine Design, September 15, 1966, pp. 188-192.

[54] R. F. Loeffler, "Thermocouples, Resistance Temperature Detectors, Thermistors--Which?", Instruments and Control Systems, Vol. 40, May 1967, pp. 89-93.

[55] Hartz, loc. cit.

[56] Doebelin, op. cit., p. 523.

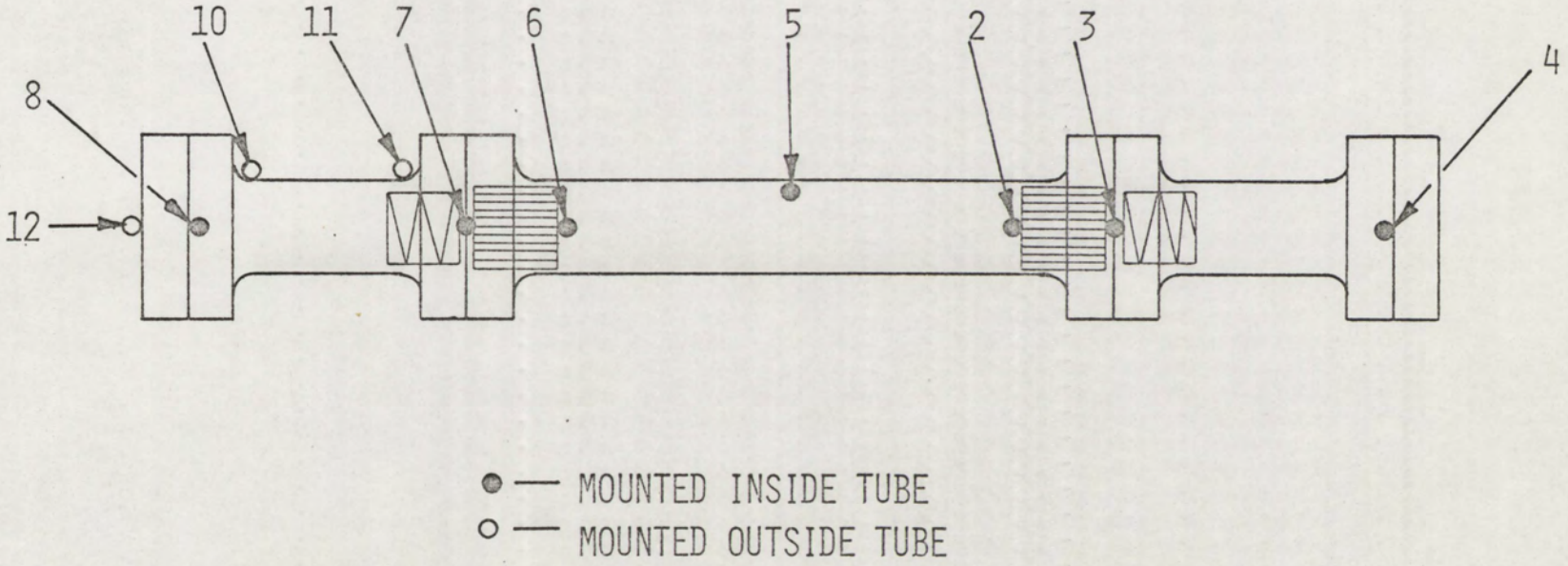

Figure 16. Drawing showing the locations of the thermocouples

The thermocouple leads were fed into the pipe through thermocouple glands fabricated in the laboratory. The glands consisted of a 1/4-inch NPT to 1/4-inch-diameter copper tubing flareless adapter connected to a 4-inch length of copper tubing. Each thermocouple lead was stripped of insulation in a 1-inch section, then coated with a thin layer of Sauereisen No. 1 cement. This was to prevent gas leakage through the insulation. The lead was inserted through the copper tubing and attached to the connecter. The connecter and tubing were then filled with plastic steel epoxy, Type B, manufactured by Dercon Corporation, Danvers, Massachusetts. While the epoxy was still wet, the copper tubing was slightly crimped in two places for better adhesion. When dry, the thermocouple glands were safety checked at 600 psig. Three glands were made in this manner; one gland had one thermocouple lead through it and two glands had three leads. Figure 17 is a cross-section of a thermocouple gland. A photograph also appears in Figure 11.

The thermocouples were mounted with Technical "B" copper thermocouple cement, manufactured by W. V-B. Ames Company, Fremont, Ohio.

Since a large number of thermocouples were used, a room-temperature reference junction was used.[57] Figure 18 is a photograph of the reference junction used in the analysis. The base is a 1/2x7x14-inch plexiglass plate with small, 1-inch

---

[57]Kirk, loc. cit.

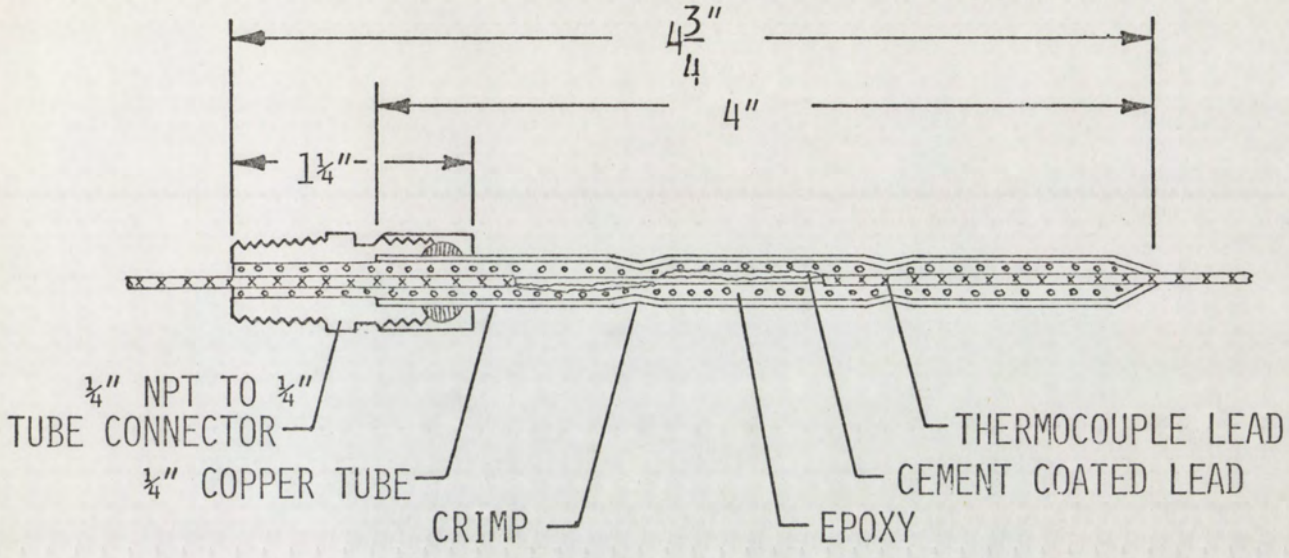

Figure 17. Cross-sectional view of a thermocouple gland

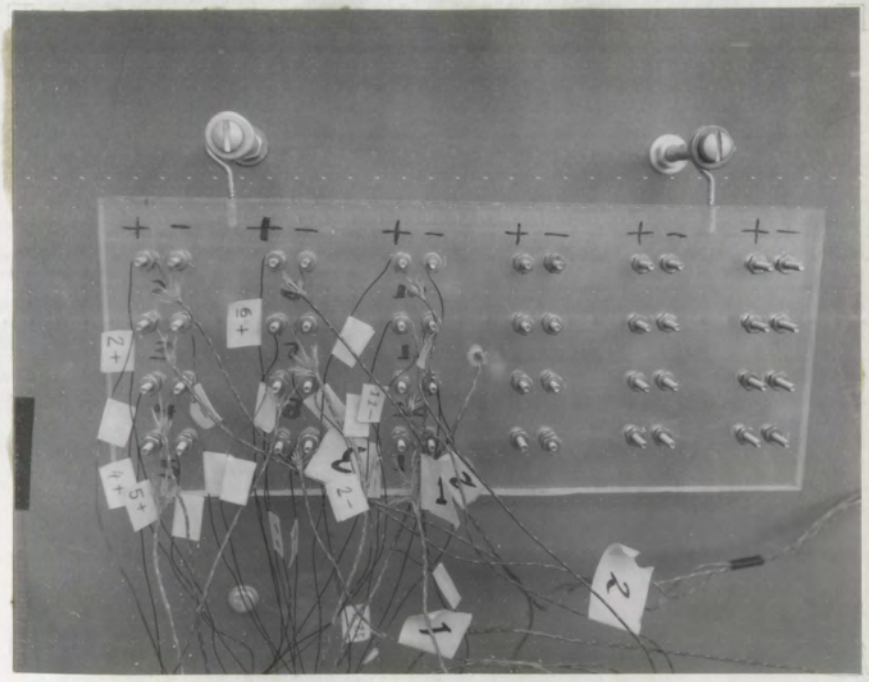

Figure 18. Photograph of the room-temperature reference junction

brass screws mounted in it for the connections. The temperature of the reference junction was monitored by a chromel-alumel thermocouple imbedded halfway in the plexiglass plate. This thermocouple utilized an ice-bath reference junction. All thermocouple leads were connected to 28-gage copper wires at the reference junctions.[58] The copper leads were then connected to the temperature recorder.

The temperature recorder was a Marksman 24-point multichannel recorder, manufactured by West Instrument Corporation, Schiller Park, Illinois. Jumper wires were used to convert the recorder to 12 channels, since 12 thermocouples were being used. The sample rate was set at one measurement per 15 seconds and the chart speed was 3 inches per hour. The span was set at 50 millivolts full range with a center zero.

The temperature measurements are tabulated in Chapter V.

A schematic of the experimental system appears in Figure 19. Figure 20 is a photograph of the actual system used in this analysis.

Calibration procedures

All instruments and transducers except the thermocouples were calibrated before and after the experimental data was taken. The thermocouples were not calibrated after the experimental analyses since the high temperatures made most of them extremely brittle and the majority were destroyed upon removal.

---

[58] T. G. Beckwith and N. L. Buck, Mechanical Measurements, (Reading, Mass.: Addison-Wesley Publishing Company, Inc., 1964), pp. 405-418.

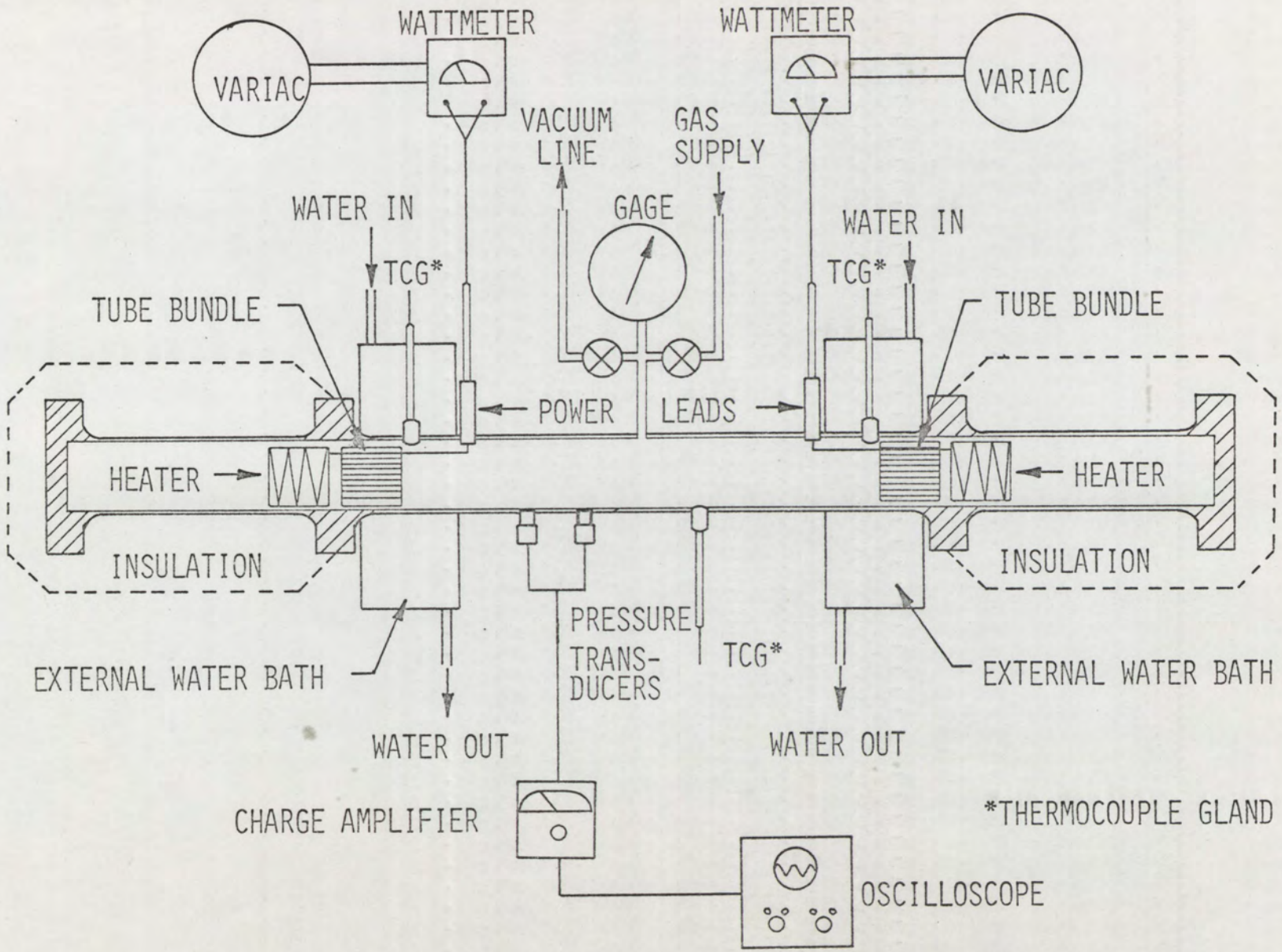

Figure 19. Schematic of the entire experimental system

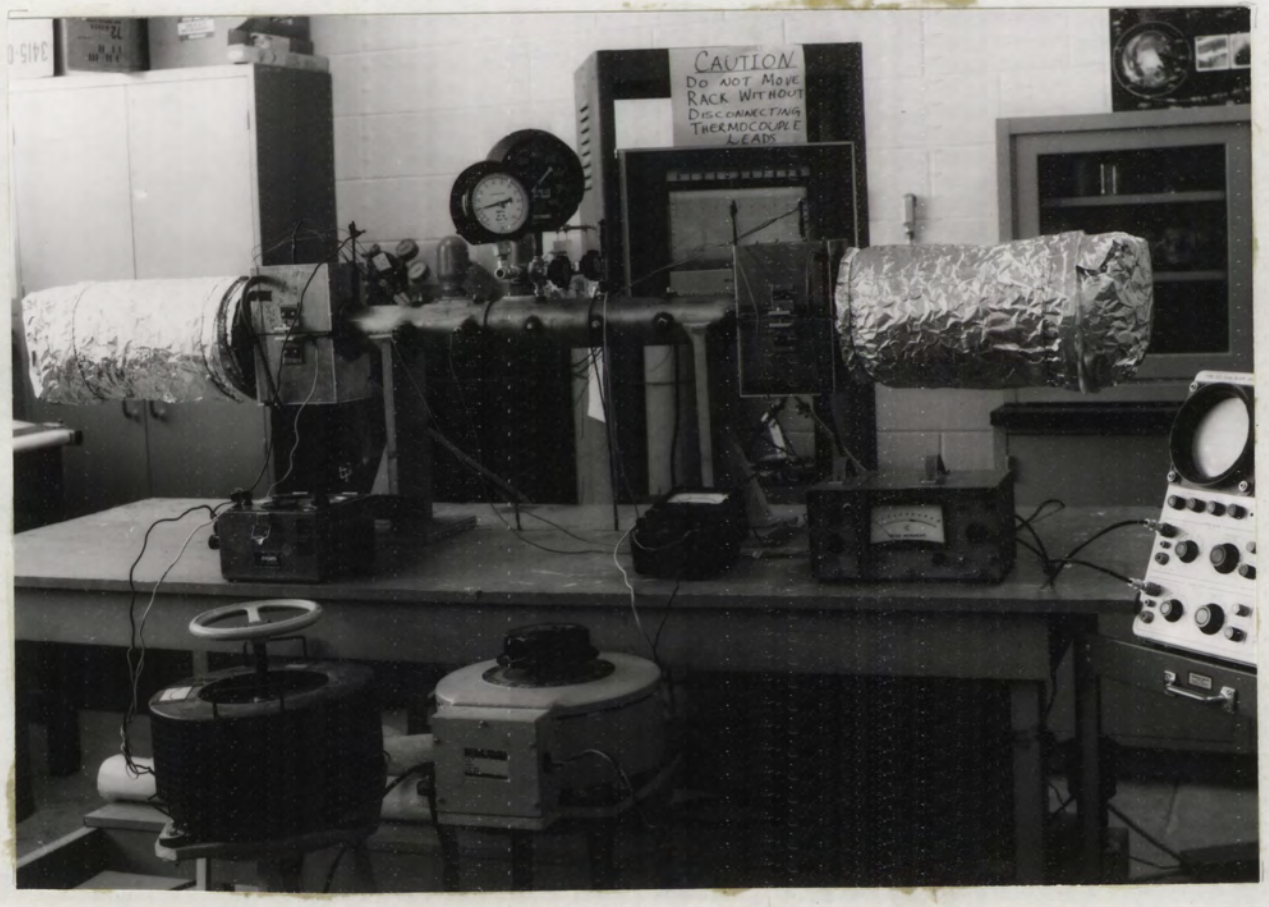

Figure 20. Photograph of the actual experimental system used in this analysis

The temperature recorder was calibrated by connecting it to a Leeds and Northrup millivolt potentiometer, Model 8686, and measuring the output of the accurate potentiometer cell. Adjustments were made according to the West Instrument Model FM series instruction manual. All channels of the recorder were checked to insure that they were functioning properly.

The oscilloscope was calibrated with the self-contained amplitude calibrator.

The Bourdon gage was calibrated on a dead-weight tester and was found to be accurate within 1 psig over the full range. Since the vacuum gage was used only for the indication of maximum vacuum in changing gases, it was not calibrated.

The ST-2 pressure transducers were calibrated against a Model 1551-C sound-level meter manufactured by General Radio Company, West Concord, Massachusetts. The pressure transducers were mounted on the oscillator, as previously noted. The microphone from the sound-level meter was mounted in an adapter which was fixed to the pipe at the same distance from the end as the ST-2 transducers. The adapter was similar to that used in previous studies.[59,60] A drawing of the adapter appears in Figure 21. The microphone was connected to the sound-level

---

[59] Feldman, "A Study of Heat Generated Pressure Oscillations in a Closed End Pipe," op. cit., p. 83.

[60] Feldman and Hirsch, "Final Report on the Mechanism Causing Heat Driven Pressure Oscillations in a Gas," op. cit., p. 18.

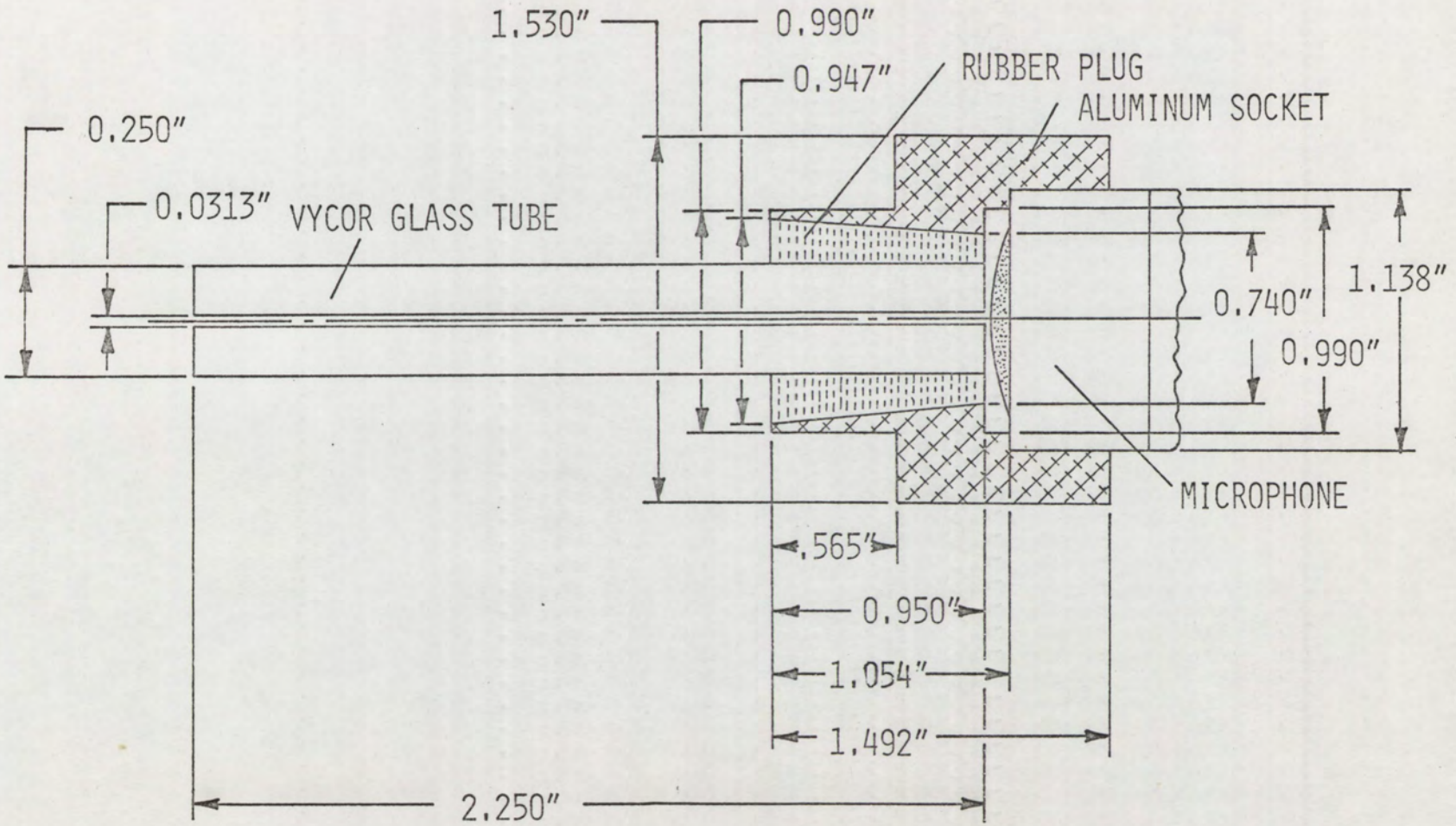

Figure 21. Cross-section view of the microphone adapter

meter with a 3 foot long cable which attenuated the signal by 1 db.[61] The instruments were calibrated within ±0.7 db.

The sound-level meter and the Kistler electrostatic charge amplifier were both calibrated and adjusted according to their respective manufacturer's instructions.

Each thermocouple was checked to insure that it was functioning properly before it was placed in the oscillator. The check was made by placing the thermocouple in a boiling water bath and comparing its output with that of a mercury-glass thermometer in the bath. A thermocouple was considered accurate if it was within ±1°F of the thermometer.

Experimental procedures

The experimental investigations were divided into three parts: 1) the variation of the thermoacoustic sound pressure level at elevated static pressures, 2) the conditions for inception of oscillations, and 3) the requirements for maintaining oscillations. Air and helium were used as working gases.

Main analysis: acoustic over-pressure as a function of static pressure

All data were taken at steady-state conditions. Steady-state was defined as the condition of thermal equilibrium; that is, when the system's temperatures reached constant values and when the acoustic over-pressure reached a steady value.

---

[61] A. P. G. Peterson and E. E. Gross, Jr., Handbook of Noise Measurements, 5th ed., (West Concord, Mass.: General Radio Company, 1963), p. 67.

A period of 4 hours was required for the system to reach its initial steady condition. This involved 2 hours of operation at atmospheric pressure, and 1-1/2 hours of operation at 100 psig. Because of the larger mass in the system at 100 psig, this pressurized condition was used during start-up. The larger mass accounted for better heat conduction and hence a shorter time for the system's temperatures to reach their steady values. One-half hour was required to feed the working gas into the tube until 100 psig was reached. The long time period was required to introduce the gas, because a sudden pressure increase would mix the hot and cold gases, terminating the oscillation. After the system reached its initial steady condition, only 1/2 hour was required to reach steady-state after a change in operating conditions.

The first data was taken at 100 psig and 700 watts. The power was then decreased to 600 watts and finally to 500 watts. Data was taken at each of the three power levels. The power was then increased to 700 watts and the static pressure was changed. It was determined early in the analysis that the pressure changes had to be made slowly (about 2 psig per minute) and that 700 watts was the best power level for static pressure changes. The internal pressure was varied in the following manner.

After data was taken at 100 psig, the pressure was increased in 50-psig intervals to the critical operating point for the working gas. The critical operating point was defined

as the maximum power and temperature above which thermoacoustic oscillations could not be sustained. Data was taken at the 50-psig intervals, varying the power as previously mentioned. The pressure was then decreased, duplicating the data points down to 100 psig. The pressure was finally decreased to 0 psig in 25-psig increments, with data being taken at these intervals. The data is presented in Chapter V.

Because of the long time periods required for static pressure variations and for steady operating conditions to be reached, the system was operated continuously until all data was taken for the working gas. This involved 10 hours of operation for air and 15 hours of continuous operation for helium.

For the introduction of helium into the system, a vacuum was imposed to remove most of the air. When a steady vacuum was reached, the system was sealed off. Then helium was introduced to a pressure of 50 psig. This was then bled out and a vacuum was again drawn on the system. After the system was sealed off, helium was added up to atmospheric pressure. The start-up procedure was then initiated.

During the analysis, two important facts were discovered. One was that the static pressure addition had to be made slowly and at high power levels, as previously mentioned, or the oscillation would cease. However, there was a critical pressure for every power level, above which the oscillation ceased, no matter how carefully the pressure was added. The other fact was that at higher static pressure levels, an oscillation could

not be initiated, because of the extremely large power required. This was observed even though a thermoacoustic oscillation could be maintained at the higher pressure condition if it was reached in slow, progressive steps. These two facts prompted the following two analyses.

Inception of oscillations

The same start-up procedure used in the main analysis was used for the inception of oscillations analysis. When the system was at the initial steady condition, the oscillation was suspended by cutting off the power, and the system was taken down to 0 psig. The power was then slowly increased until an oscillation started. Again the power was shut off and a given pressure was added to the system. The power was slowly increased until the oscillation started. The procedure was followed, up to 40 psig for air, and to 100 psig for helium. After these pressures were reached, no oscillation could be initiated with the power available.

Maintenance of oscillations

The procedure used for determining the minimum power required to sustain an oscillation at a given pressure once it had been started was the reverse of the inception of oscillations analysis. A thermoacoustic oscillation was initiated at 0 psig and the system was pressurized to a certain value. After steady-state conditions had been reached, the power was slowly decreased until the oscillation ceased. The procedure

(except start-up) had to be repeated for each pressure point used in the analysis. Both air and helium were tested in the investigation.

CHAPTER V

EXPERIMENTAL AND THEORETICAL RESULTS

In the first part of this chapter experimental results are presented. In the second part, the theoretical and experimental results of the study of high internal-pressure thermoacoustic oscillations are compared. Whenever possible, the results will be correlated with those of previous investigations.

Since the sound-pressure level (SPL) is a logarithmic function, errors in the pressure correlations given in terms of SPL are misleading. Therefore, errors in the pressure comparisons will be given in terms of the SPL and the actual equivalent pressure.

Experimental results

All data for the experimental results were taken from oscilloscope photographs such as that shown in Figure 22. The data were reduced, and all calculations were made on a digital computer. In this figure, the upper trace is the pressure wave at x/L=0.366 and the lower trace is at x/L=0.417. The photograph shows that the pressure wave at x/L=0.417 lags that of x/L=0.366, which is to be expected.[62]

At low pressures, especially with helium as the working gas, the phenomenon known as "beating" occurred.[63] Figure 23 is a slow sweep photograph of beating oscillations in helium.

---

[62] Feldman, op. cit., p. 137.

[63] Ibid., p. 89.

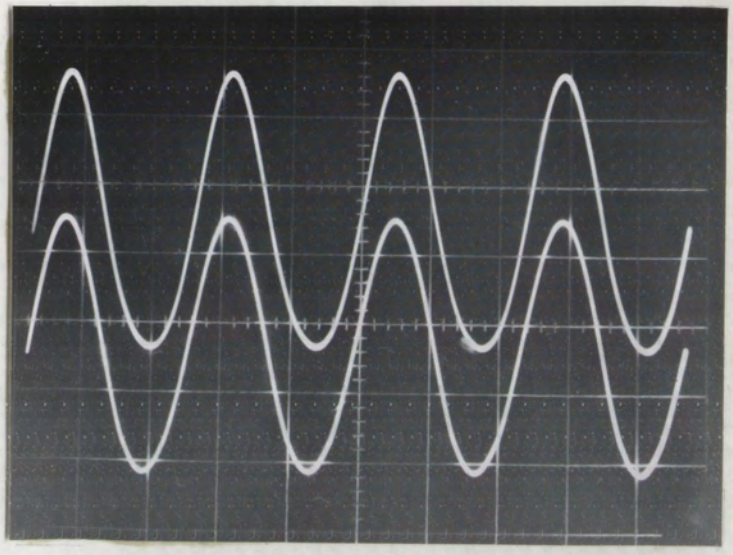

Figure 22. Typical oscilloscope photograph of thermoacoustic pressure wave

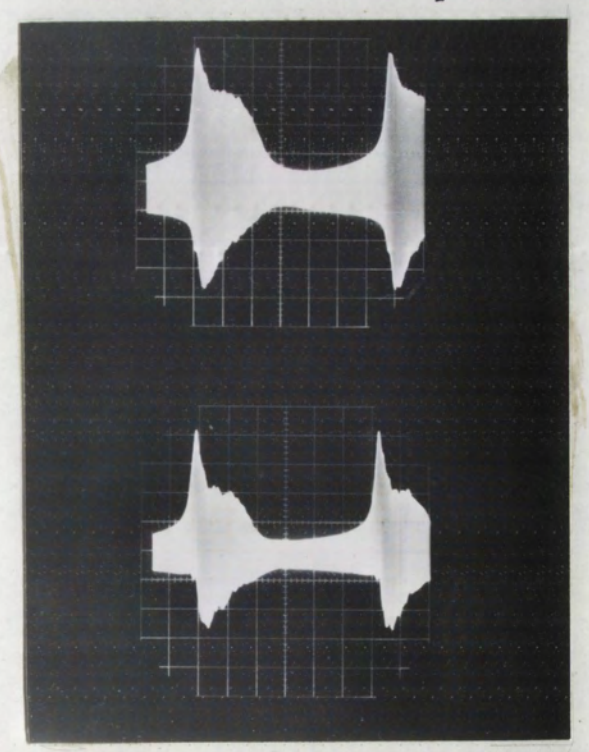

Figure 23. Slow sweep photograph showing the beating phenomena

The power input was 700 watts. The time lapse between the two major peaks was 8 seconds. The upper trace is the pressure generated at x/L=0.366 and the lower trace corresponds to x/L=0.417. The two traces were not taken simultaneously. When beating occurs in a thermoacoustic system, the acoustic pressure repetitively surges and decays as shown in Figure 23, although it retains a constant frequency of oscillation. It is similar to the beating phenomenon occurring in 2-degree-of-freedom mechanical systems. In fact, beating in a thermoacoustic system might be explained in terms of a mechanical analogy as follows.

Beating always occurred in the thermoacoustic oscillator when a small mass of gas (about 0.014 lb or less) was in the oscillator. Therefore, in terms of the analogy, the distributed mass (mass of the main body of gas) becomes small enough so that the mass of the spring (closed end) becomes significant. When the mass of the spring becomes significant, the system acts as a 2-degree-of-freedom system, and beating occurs.

Beating is significant in thermoacoustic systems because the maximum thermoacoustic efficiency during beating was almost 33 percent. As shown later in the chapter, this is 8 times the thermoacoustic efficiency obtained with "regular" thermoacoustic oscillations.

The results of the temperature measurements for the experimental analyses are tabulated in Table 1 for air and Table 2 for helium. Table 3 defines the locations of station numbers

Table 1. Results of the temperature measurements for air

STATION												
$\dot{Q}$	p_o	1	2	3*	4	5	6	7	8	9	10	11	12
500	0	82	641		440	86	624	989	752	73	707	820	643
600	0	82	707		486	86	654	1040	775	73	726	871	649
700	0	82	752		530	86	703	1076	791	68	733	901	658
500	25	82	427		469	84	422	947	775	66	741	824	664
600	25	82	473		493	84	453	1023	809	68	767	877	672
700	25	82	510		515	84	468	1078	831	73	780	915	677
500	50	82	379		453	84	379	905	793	66	761	803	695
600	50	82	400		480	84	386	947	805	66	767	707	684
700	50	82	429		513	84	424	1008	837	71	791	892	679
500	75	82	370		462	84	337	888	809	66	778	818	707
600	75	82	411		502	86	363	968	852	73	814	881	720
700	75	82	427		530	88	386	1000	871	71	829	915	724
500	100	77	321		247	82	278	809	731	71	690	778	567
600	100	77	368		262	82	314	884	752	71	703	824	552
700	100	77	395		285	82	350	943	807	77	752	871	606
600	150	77	332		285	86	283	896	848	71	782	854	649
700	150	77	377		285	86	305	911	846	71	786	879	632
700	200	82	361		357	99	283	977	909	84	850	930	697

*malfunction

Table 2. Results of the temperature measurements for helium

STATION												
$\dot{Q}$	p_o	1	2	3*	4	5	6	7	8	9	10	11	12
500	0	71	422	837	68	86	422	884	664	77	674	862	615
600	0	77	497	856	75	77	497	937	673	77	673	896	617
700	0	77	563	880	75	77	519	966	688	77	688	915	625
500	25	73	296	786	64	86	260	869	707	71	701	820	630
600	25	73	341	782	64	86	323	913	737	71	718	890	636
700	25	73	370	848	64	86	362	934	746	71	722	913	636
500	50	77	256	731	71	86	218	854	718	77	712	814	641
600	50	77	287	786	66	86	245	901	743	73	725	862	645
700	50	77	303	803	64	82	271	936	754	73	722	884	647
500	75	77	230	695	59	82	199	848	712	68	692	797	649
600	75	77	260	741	59	86	218	892	746	71	741	844	658
700	75	77	292	773	62	86	238	915	756	71	743	873	660
500	100	77	217	682	66	84	188	830	643	71	656	778	528
600	100	77	236	697	66	84	204	862	649	71	662	807	508
700	100	77	263	731	66	84	218	896	658	71	662	848	486
500	150	77	195	664	59	82	132	824	682	66	656	791	591
600	150	77	225	684	59	82	143	831	697	66	669	820	582
700	150	77	240	703	64	82	154	858	697	71	671	848	554
500	200	77	184	679	64	82	171	807	714	68	731	807	641
600	200	77	218	692	64	82	184	862	739	68	752	842	641
700	200	77	245	718	66	82	197	871	746	77	767	871	632
500	250	77	165	684	62	82	171	797	729	66	743	812	660
600	250	77	201	701	59	82	173	850	748	66	767	850	660
700	250	77	232	710	59	82	175	862	761	66	778	873	656
500	300	77	153	712	59	82	180	826	735	66	761	824	624
600	300	77	182	703	59	82	171	829	756	66	773	852	628
700	300	77	214	714	62	82	173	877	767	66	788	884	626
600	350	77	173	735	62	84	180	848	765	73	784	856	634
700	350	77	195	724	66	84	182	850	778	71	797	888	632
600	400	77	169	763	64	82	190	848	763	68	786	869	632
700	400	77	190	731	64	82	178	852	773	68	795	884	632
700	450	77	178	786	64	82	184	856	767	73	795	884	626

Table 3. Definitions of the station number locations

Station No.	Location
1	Reference junction
2	Right end tube bundle
3	Right end heater element
4 air	Right back end plate, inside
4 helium	Water bath entrance
5	Middle pipe temperature, inside
6	Left end tube bundle
7	Left end heater element
8	Left back end plate, inside
9	Water bath exit
10	Left end flange, outside pipe
11	Left heater element, outside pipe
12	Left end plate, outside pipe

used in the data. Station number locations are also shown in Figure 16. Inspection of Tables 1 and 2 show that the operating temperatures for helium are lower than those for air. In addition, the temperature differences between the heater elements and the tube bundles are greater for helium than for air.

As previously mentioned, corrections for errors due to thermal radiation and conduction were not made in the temperature measurements. This, in part, accounts for the discrepancies in the temperatures of the two ends of the oscillator. Location variations of thermocouples also caused deviations in the temperature measurement. In all calculations, the middle temperature (station 5) was used as the reference for calculating system properties.

Thermoacoustic sound-pressure levels measured at two locations in the system are plotted in Figures 24-27 for variations in static gage pressure. In all four figures, the sound-pressure level increases monotonically with static pressure up to the final data point for each power level. It will be seen later that at these final data points, the system was unstable and, if left long enough, the thermoacoustic oscillations would have ceased. That is, the system was unable to sustain steady-state thermoacoustic oscillations at these power and pressure levels. Inspection of Figures 24, 25, 26, and 27 shows that when the system is stable, there is a definite increase in thermoacoustic sound pressure level with increasing static pressure.

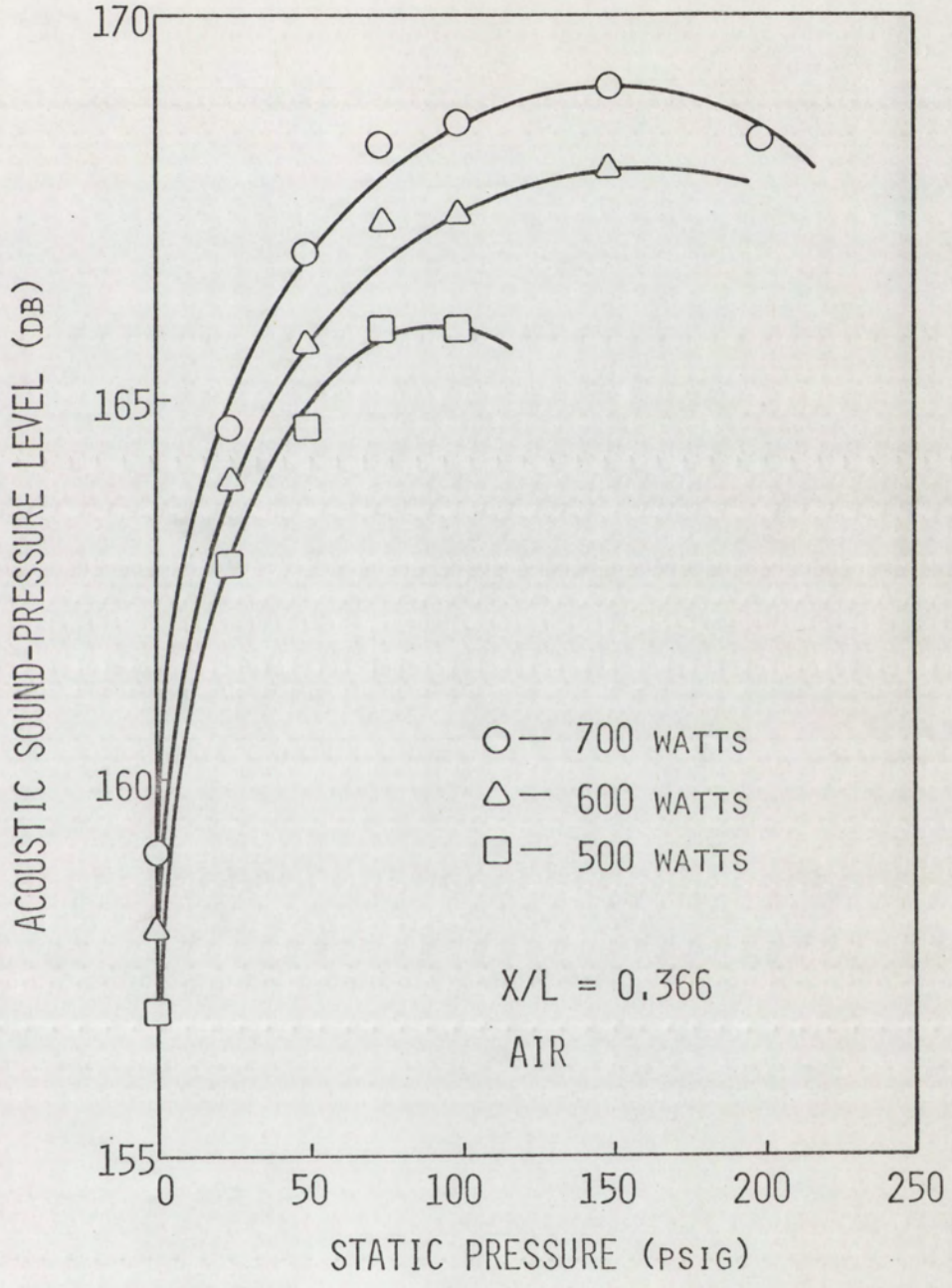

Figure 24. Experimental sound-pressure level as a function of static pressure for air. x/L=0.366

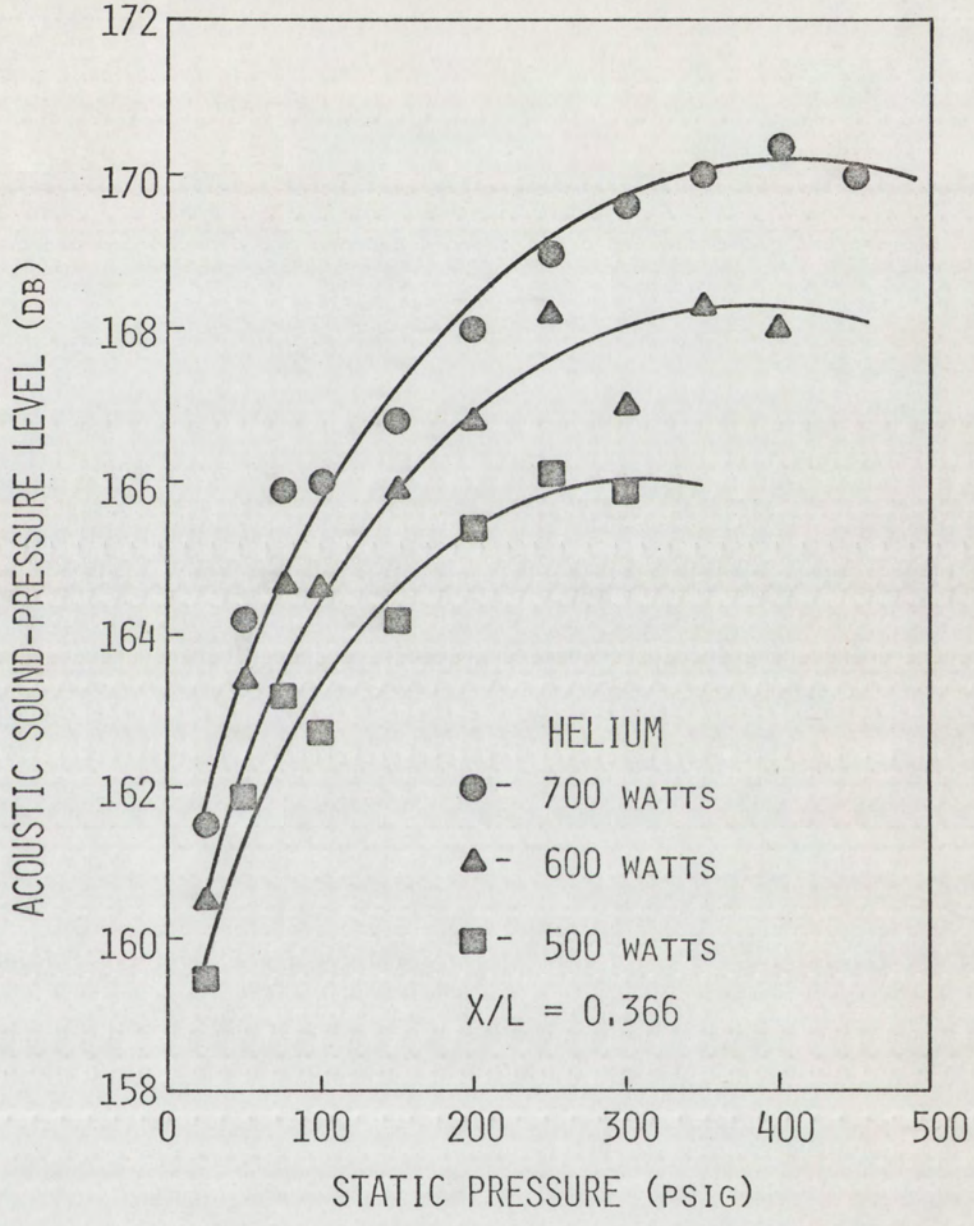

Figure 25. Experimental sound-pressure level as a function of static pressure for helium. x/L=0.366

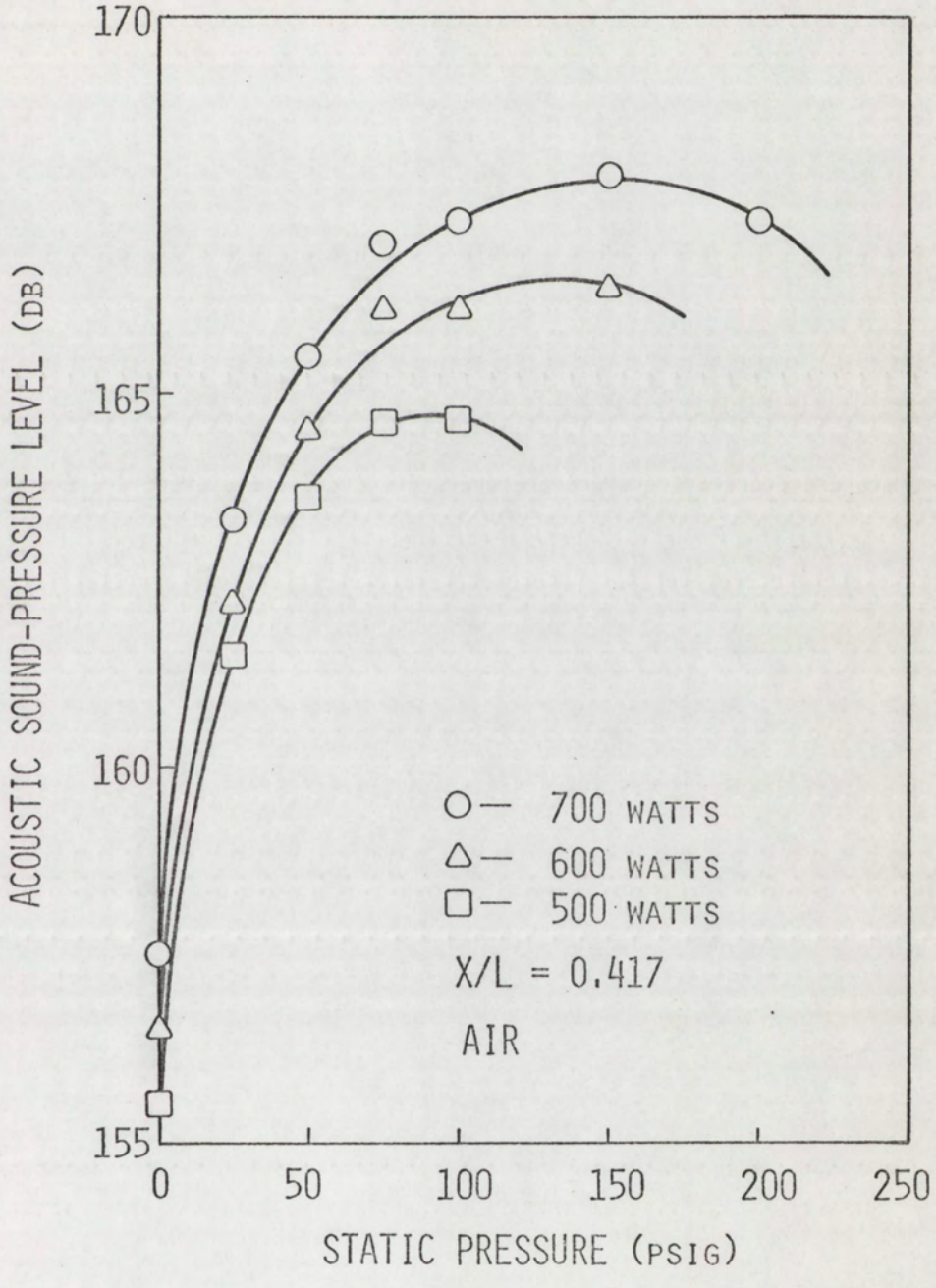

Figure 26. Experimental sound-pressure level as a function of static pressure for air. x/L=0.417

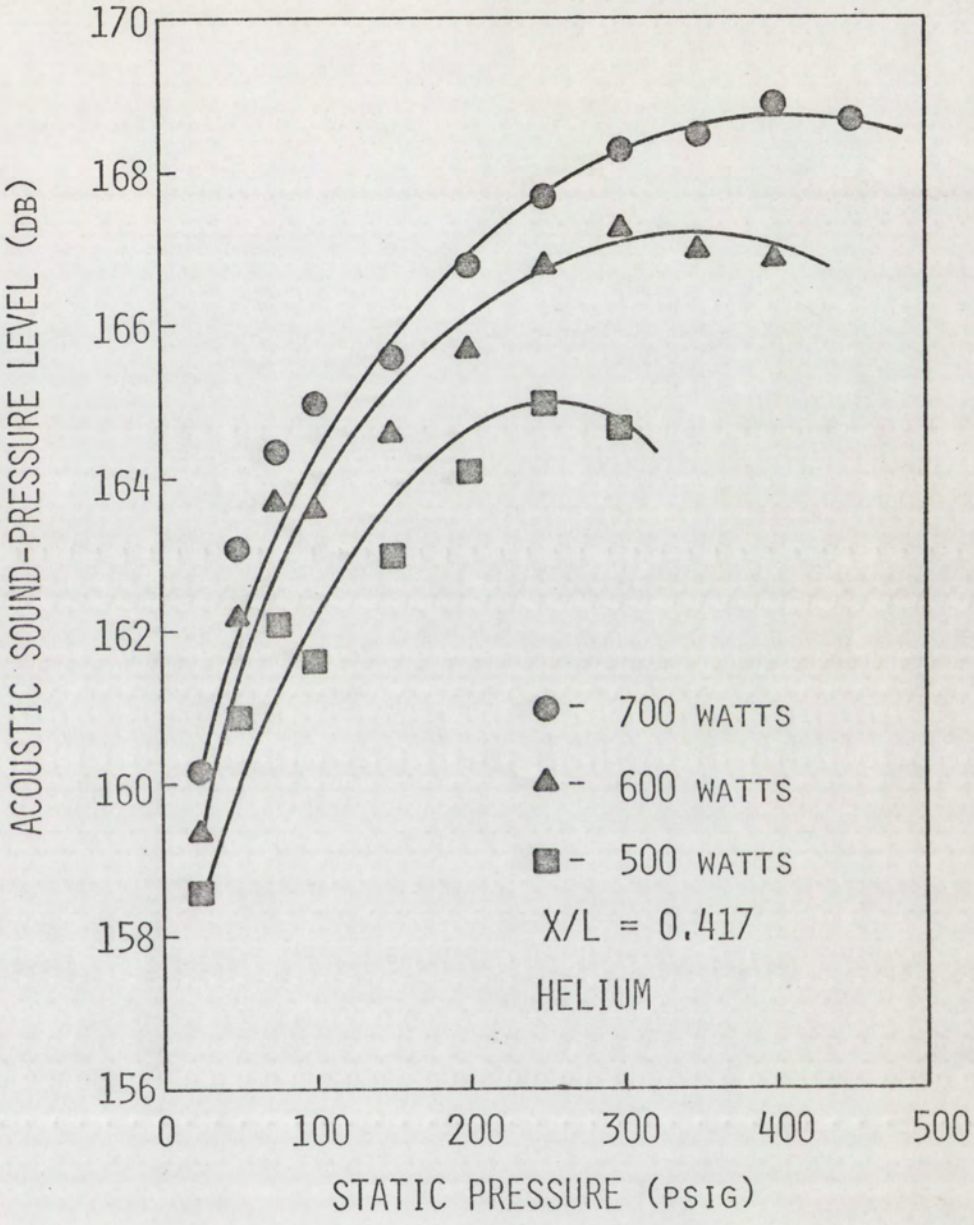

Figure 27. Experimental sound-pressure level as a function of static pressure for helium. x/L=0.417

Figures 28 and 29 show thermoacoustic efficiency $\eta_{ta} = Ap^2/2\rho_o a_o \dot{Q}$ as a function of static pressure ratio (p_o/p_a, atmospheres). The value of p used in calculating the thermoacoustic efficiency was the root-mean-square of the actual acoustic over-pressure. This value of p was used so that the data could be compared with similar thermoacoustic efficiencies of previous studies measured at 1 atmosphere static pressure.

In the figures, a distinction was not made between power levels, but only between locations. This was done since η_{ta} involves a power term but not an "x" or coordinate term. Therefore, the data was normalized with respect to power but not to location. The curves in Figures 28 and 29 were drawn as nearly as possible through the averages of each set of points. The figures show that there is an abrupt increase in thermoacoustic efficiency with increasing static pressure, followed by a gradual decrease in efficiency with increasing static pressure. It is interesting to note that the maximum thermoacoustic efficiency occurs in the region of 5 to 6 atmospheres for both air and helium.

The thermoacoustic efficiency at x/L=0.366 is greater than that at x/L=0.417. This agrees with the results of previous studies.[64] The thermoacoustic efficiency at 1 atmosphere pressure and 500 watts power input at x/L=0.366 for air was η_{ta} = 0.0315, compared to η_{ta}=0.0034 for previous studies.[65] This

---

[64] Ibid., p. 117.

[65] Ibid., p. 116.

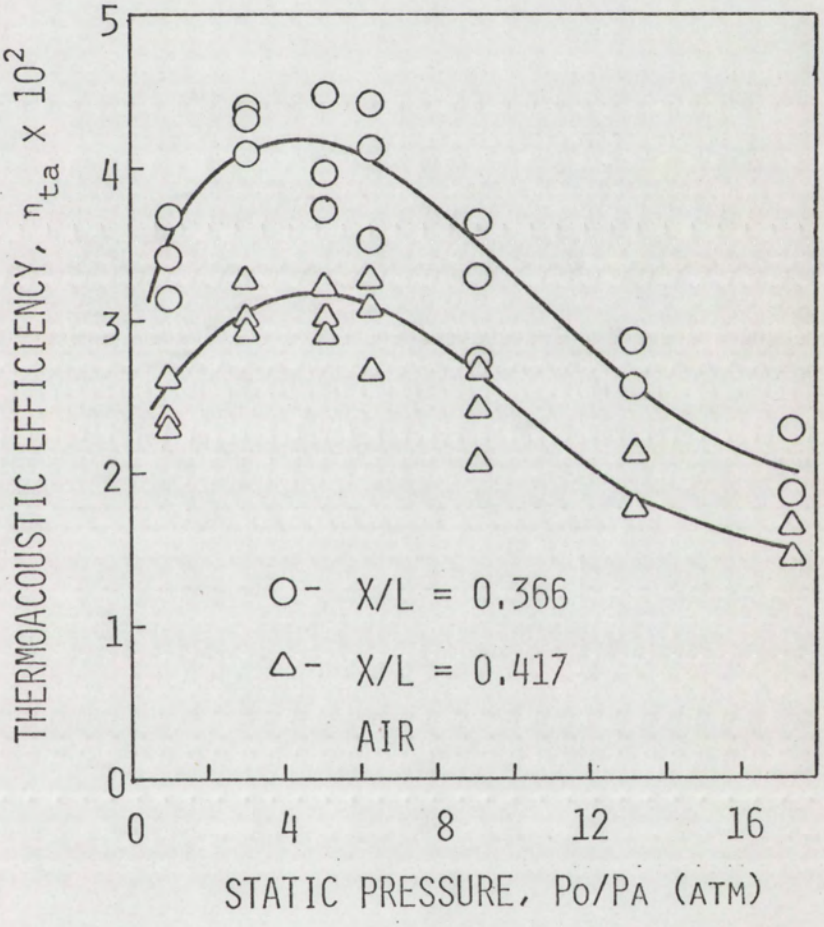

Figure 28. Thermoacoustic efficiency as a function of static pressure for air

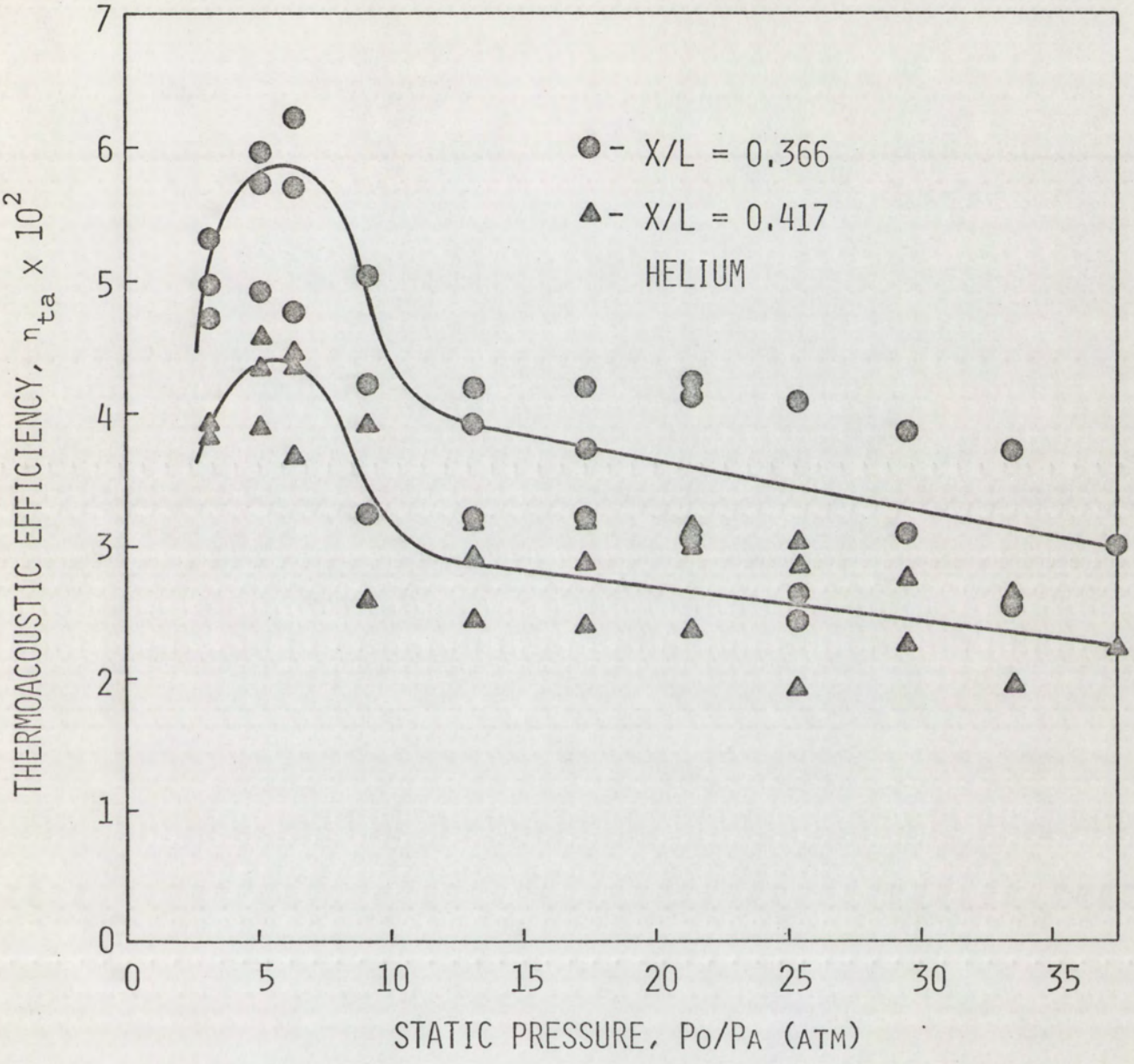

Figure 29. Thermoacoustic efficiency as a function of static pressure for helium

difference in order of magnitude was typical of all the measurements. The differences were attributed to the fact that the current thermoacoustic system is an optimized system which was the result of two years of optimization.

Figures 30 and 31 show the variation of mechanical efficiency $\eta_M = pAa_o/\dot{Q}$ with increasing static pressure in atmospheres. Again, the data was normalized with respect to power input but not to location. The pressure p used in these calculations was the actual over-pressure generated by the system. From the figures, it can be seen that mechanical efficiency increases with static pressure as long as the system is capable of sustaining a steady-state oscillation.

Inception and maintenance results

Figure 32 shows the results of the measurements made to determine the minimum power required to initiate thermoacoustic oscillations for a given static pressure. Inspection of the figure shows that the power required is exponentially proportional to the static pressure. A least squares curve fit of the data gives

$$\dot{Q} = 175\, e^{1.58(p_o/p_a)} \quad \text{for air} \tag{33}$$

and

$$\dot{Q} = 196\, e^{.604(p_o/p_a)} \quad \text{for helium.} \tag{34}$$

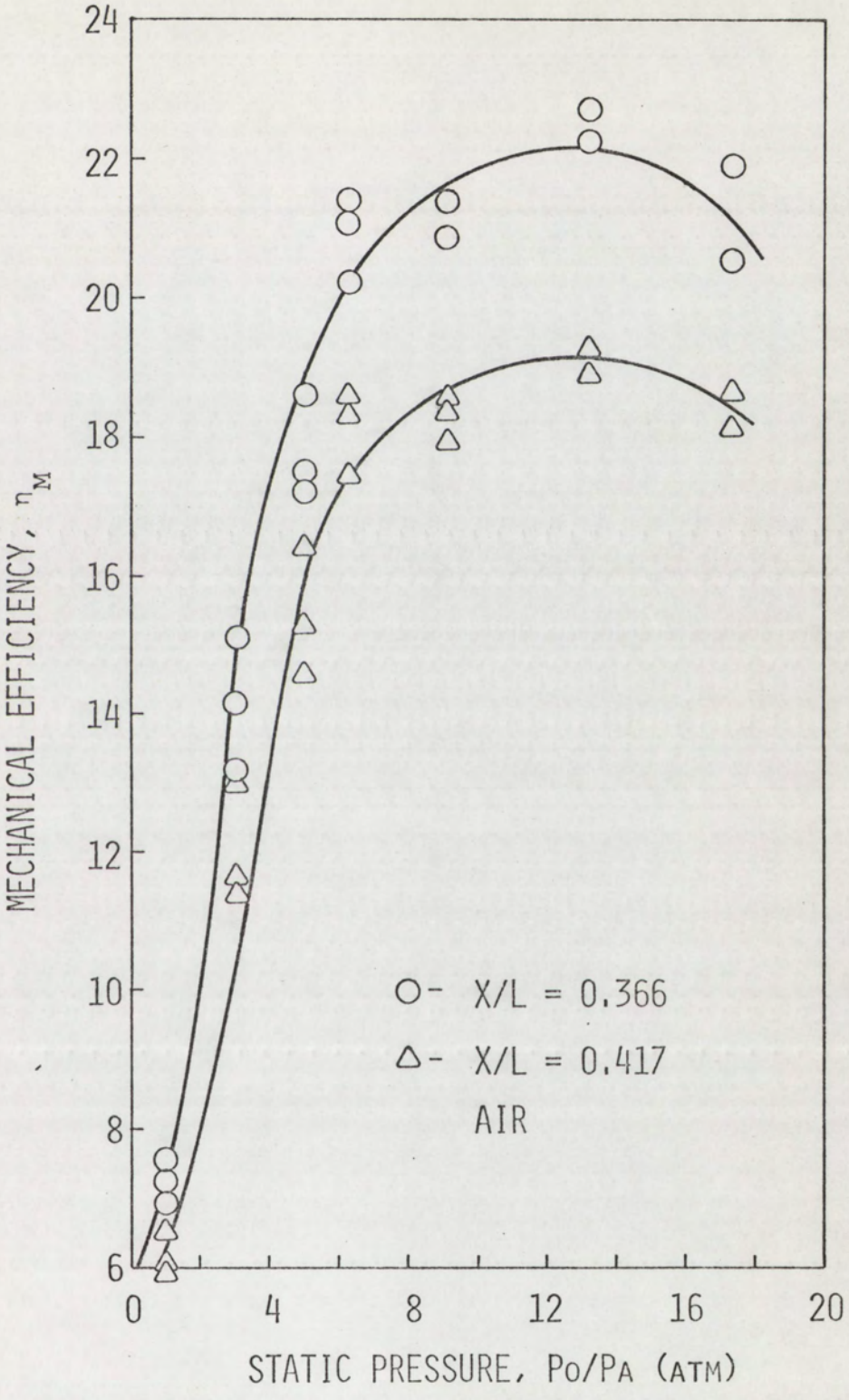

Figure 30. Mechanical efficiency as a function of static pressure for air

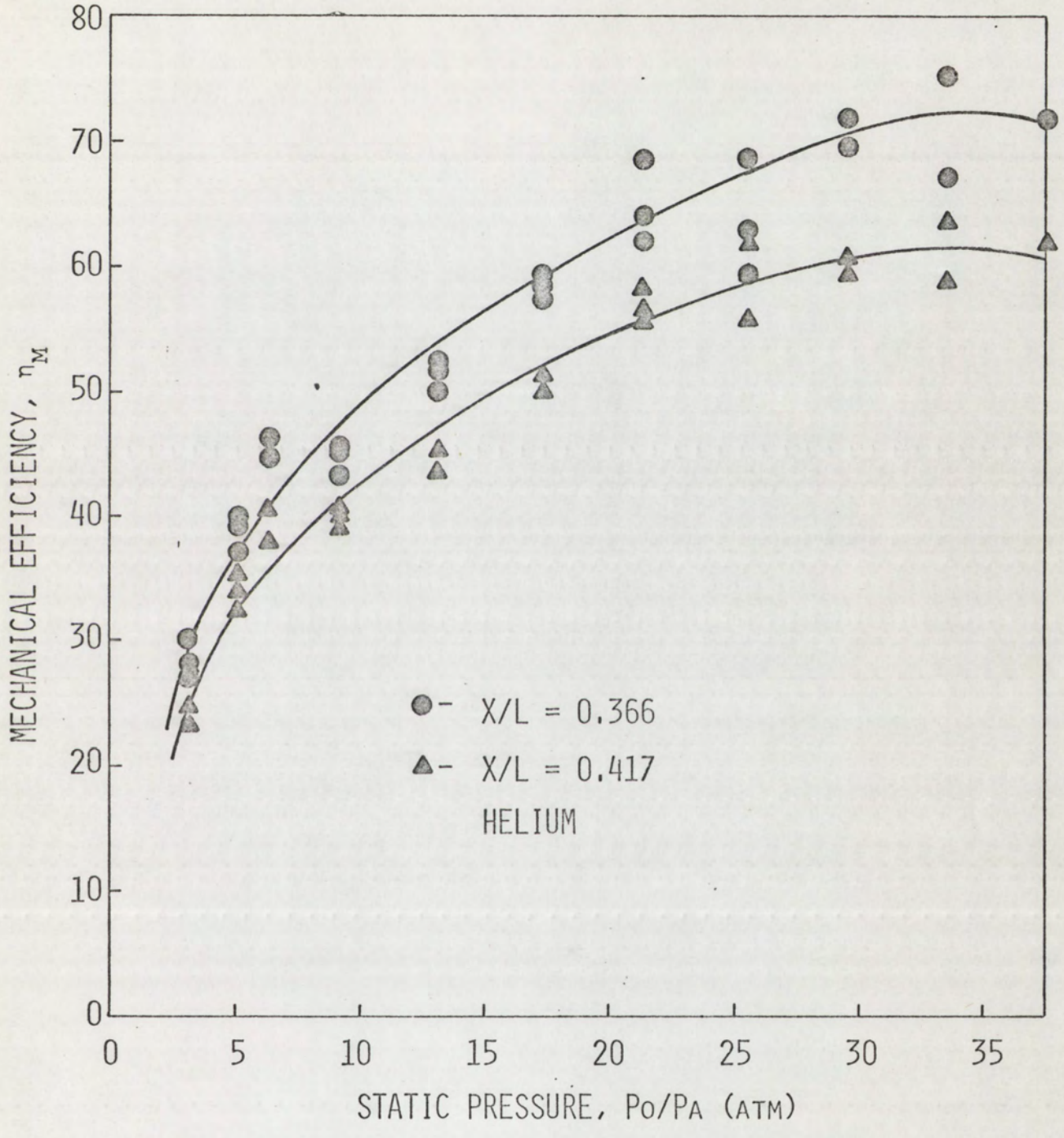

Figure 31. Mechanical efficiency as a function of static pressure for helium

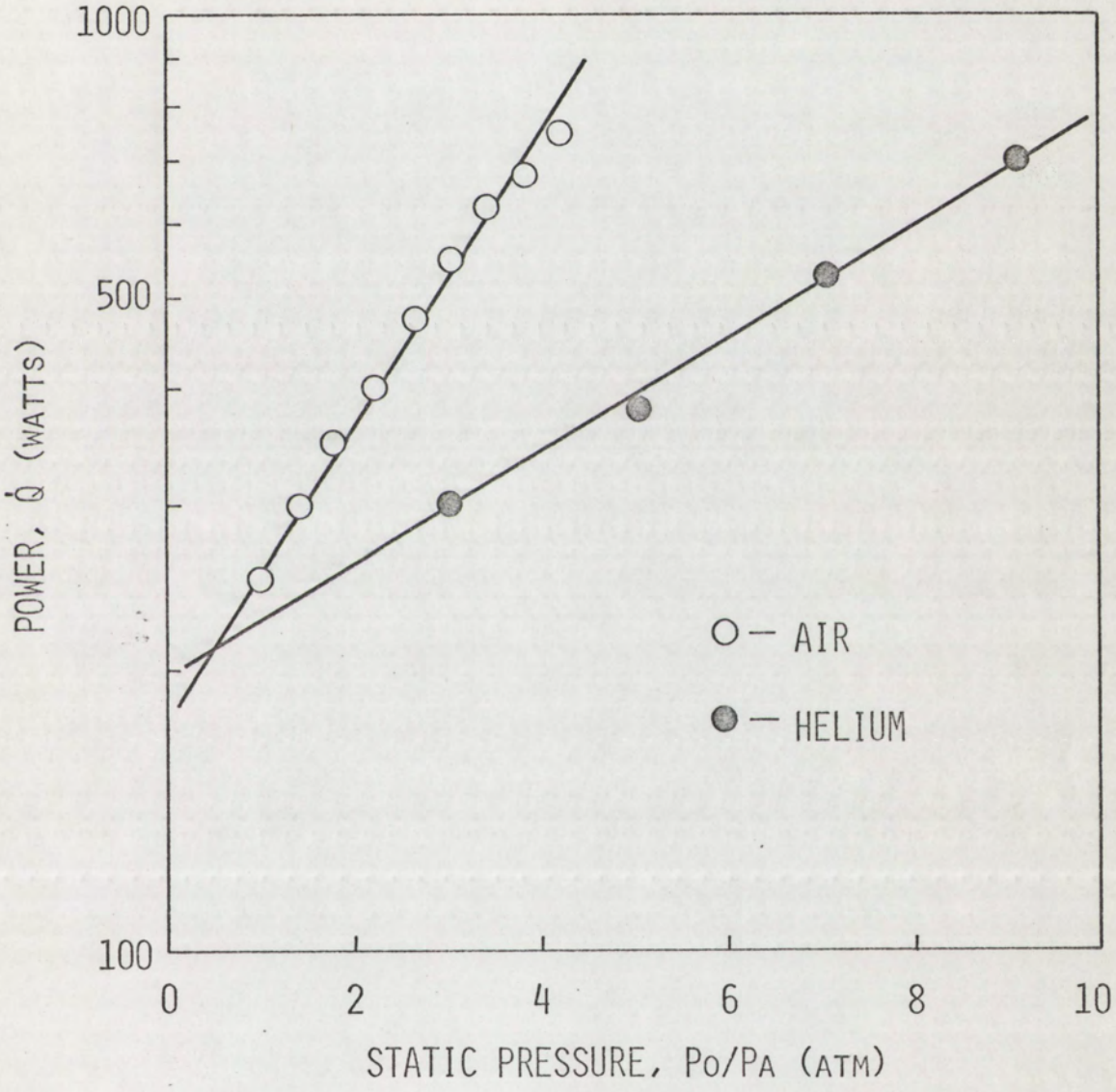

Figure 32. Required power as a function of static pressure for the inception of thermoacoustic oscillations

To be dimensionally homogeneous, the constants 175 for air and 196 for helium should have the units of watts. The accuracy of the fits was determined by a normalized correlation coefficient, r^2, defined by

$$r^2 = \frac{N \sum_{n=1}^{N} Y_{est}^2 - \left(\sum_{n=1}^{N} Y_{est} \right)^2}{N \sum_{n=1}^{N} Y^2 - \left(\sum_{n=1}^{N} Y \right)^2} , \qquad (35)$$

where N is the number of data points, Y is the dependent variable (in this case, $\dot{Q}$), and Y_{est} is the value generated by substitution of the independent variable into the equation calculated by the least squares fit.[66] If $r^2=0$, there is no correlation, and if $r^2=1$, there is perfect correlation; that is, the least squares curve fit perfectly matches every data point. From past experience, it has been determined that a correlation coefficient of $r^2=0.95$ is an acceptable fit. For Equation (33) the correlation coefficient was $r^2=0.988$ and for Equation (34) it was $r^2=0.979$.

The static mechanical efficiency $\eta_{MS}=p_o A a_o/\dot{Q}$ was also used in determining a criterion for the power required to initiate thermoacoustic oscillations for a given static pressure. The static pressure p_o was used in place of the acoustic over-pressure p to normalize the data. Figures 33 and 34

---

[66] M. R. Spiegel, Schaum's Outline of Theory and Problems of Statistics, (New York: Schaum Publishing Company, 1961), pp. 240-268.

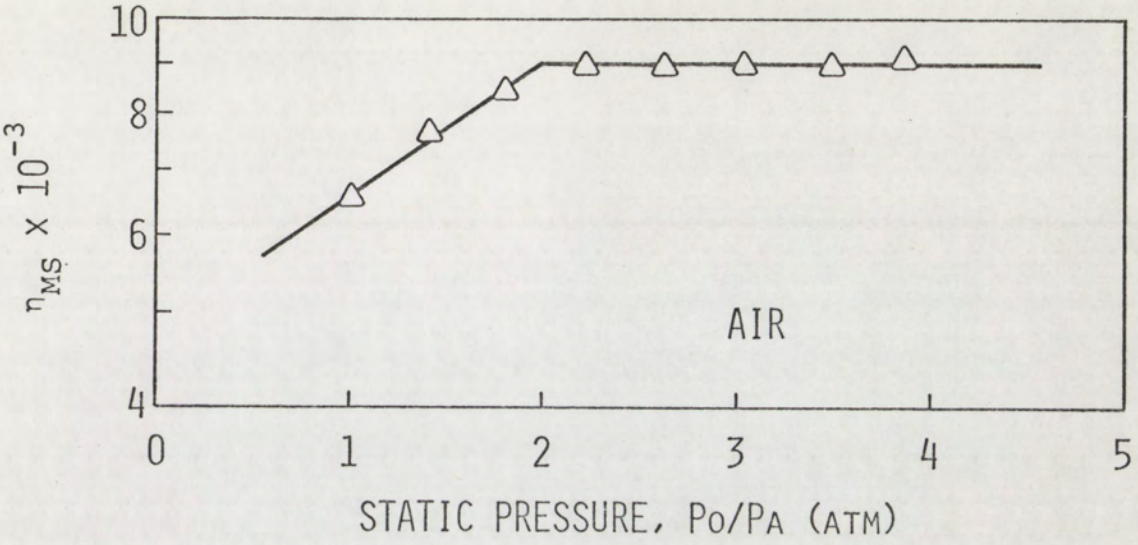

Figure 33. Static mechanical efficiency as a function of static pressure for the inception of oscillations for air

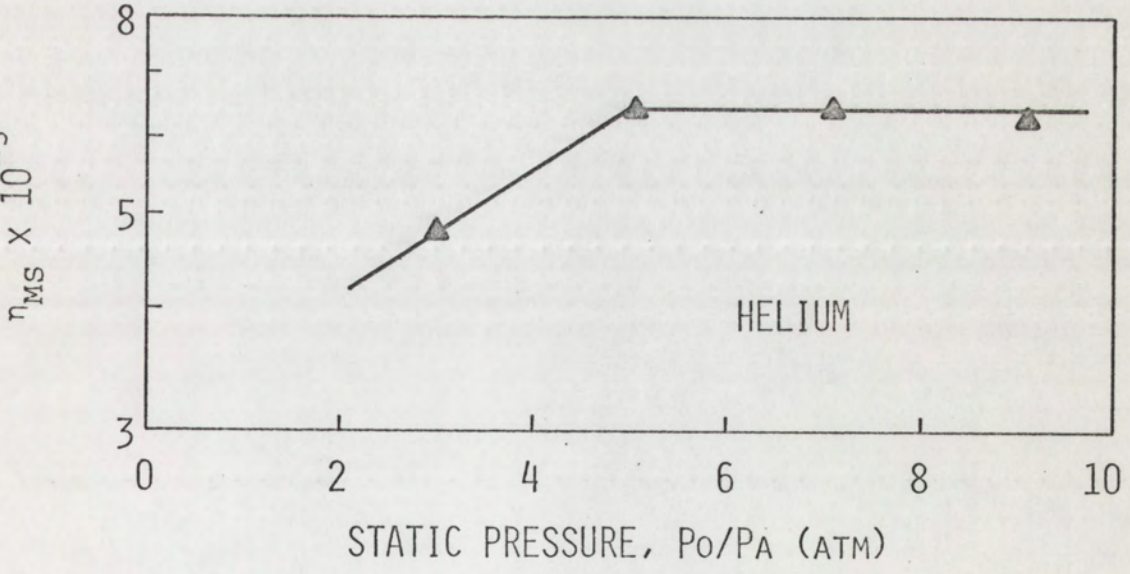

Figure 34. Static mechanical efficiency as a function of static pressure for the inception of oscillations for helium

show the static mechanical efficiency as a function of static pressure. For air (Figure 33), it can be seen that for internal oscillator pressures greater than 2 atmospheres, the static mechanical efficiency number became nearly constant, that is,

$$\eta_{MS} = 900 \quad . \tag{36}$$

For helium, the static mechanical efficiency number becomes constant for static pressures greater than 5 atmospheres. The constant for helium was given by

$$\eta_{MS} = 6500 \quad . \tag{37}$$

Therefore, the static mechanical efficiency η_{MS}=constant should be used as a design criterion for thermoacoustic oscillators operating at elevated static pressures.

Figure 35 shows the results of the analysis made to determine the critical points of the thermoacoustic system; that is, the minimum power necessary to maintain thermoacoustic oscillations for a given static pressure, once the oscillations have been initiated. The data show that the power required to sustain an oscillation at a given static pressure was somewhat less than that necessary to initiate the oscillation. It is also evident from Figure 35 that in maintaining thermoacoustic oscillations, the minimum power is very nearly a linear function of static pressure. Design equations determined from the critical point data are, for air,

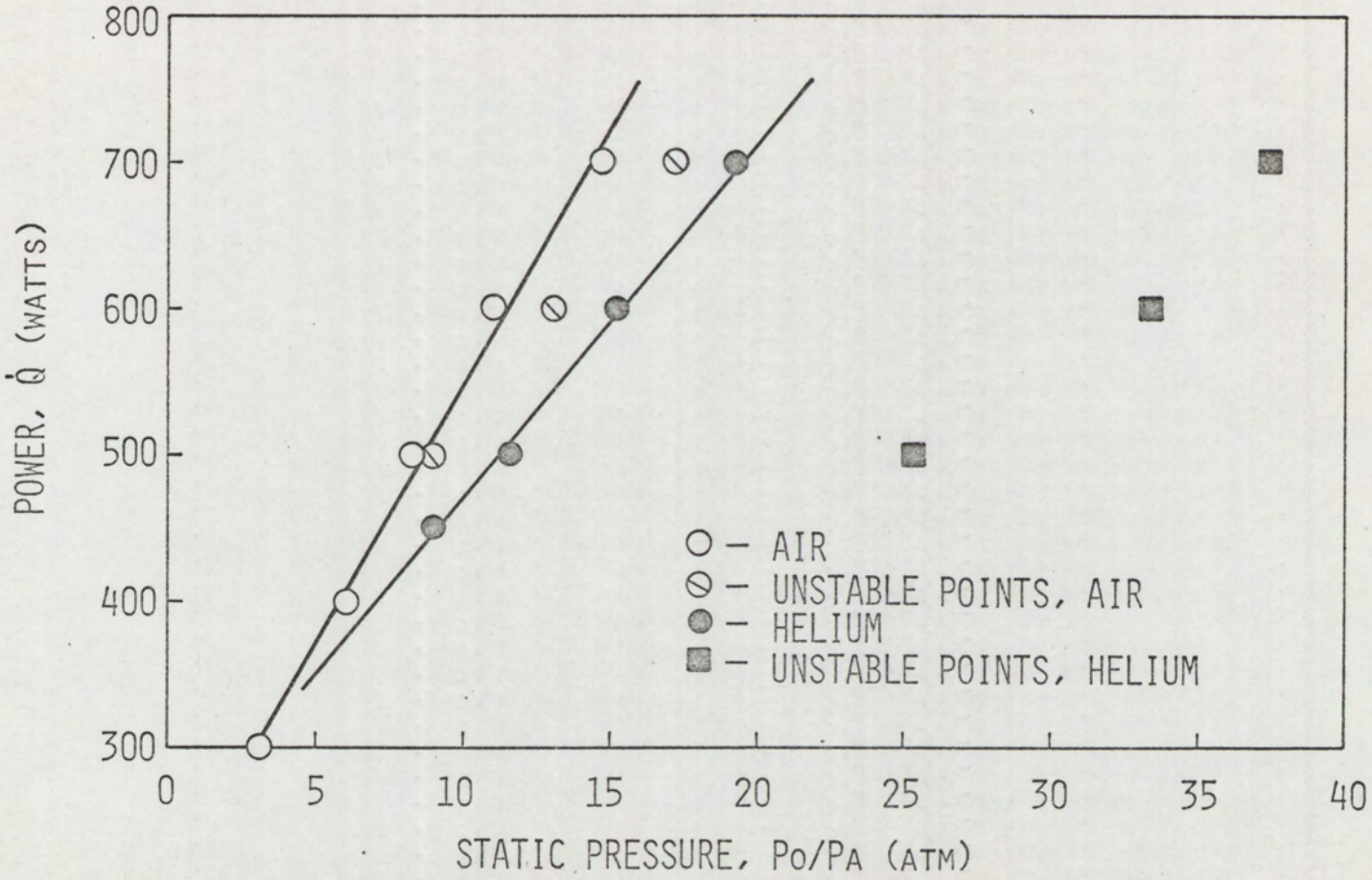

Figure 35. Power required to maintain thermoacoustic oscillations at a given static pressure

$$\dot{Q} = 35 \frac{p_o}{p_a} + 196 \text{ watts} \tag{38}$$

and, for helium,

$$\dot{Q} = 24.1 \frac{p_o}{p_a} + 230 \text{ watts} . \tag{39}$$

The points not lying on the curves are critical points determined from Figures 24-27. From the results of the maintenance analysis, it can be seen that the thermoacoustic system could not have sustained steady state oscillations at these points.

Correlation of experimental and theoretical results

In Chapter III, four equations, derived from the theory of heat release in a gas, were proposed for determining the over-pressure generated in a thermoacoustic oscillator at elevated internal pressures. These equations were

$$p = \frac{\gamma-1}{2} \frac{\dot{w}}{a_o} + \frac{QR}{V_m} \left(\frac{1}{C_a} - \frac{1}{C_b} \right) , \tag{10}$$

$$\frac{p}{p_o} = 0.325 \left(\frac{\dot{w}}{a_o p_o} \right)^{2/3} , \tag{11}$$

and

$$\frac{p}{p_o} = 0.551 \left(\frac{\dot{w}}{a_o p_o} \right)^{.586} \tag{11a}$$

for air, and

$$\frac{p}{p_o} = 0.917\left(\frac{\dot{w}}{a_o p_o}\right)^{.545} \qquad (12)$$

for helium. Equation (10) was applied only to calculations for air, since the molar specific heat of helium is invariant with temperature up to 3000°F.[67] Therefore, in Equation (10) $C_a=C_b$ for helium and the mixing term vanishes. Figures 36-41 show how theoretical Equations (10), (11), (11a), and (12) compare with the experimental results. Since there was little correlation between Equations (10) and (11) and the experimental data, these equations are plotted in Figure 36 only to show their trends. The sound-pressure levels predicted by Equation (11) were too low to even fit on the graphs shown in Figures 37 and 38. Only data for x/L=0.366 was used since this location is nearer the region of heat release.

The maximum and minimum deviations between the theoretical and experimental results are tabulated in Table 4 for the range of this analysis. The points at which the thermoacoustic system was not capable of sustaining a steady-state oscillation were not included in the error analysis. It appears that if the curves given by Equation (11a) and the air experimental data were extrapolated to higher static pressures, they would converge to a single curve.

---

[67] F. H. Crawford and W. D. Van Vorst, Thermodynamics for Engineers, (New York: Harcourt, Brace, and World, Inc., 1968), p. 152.

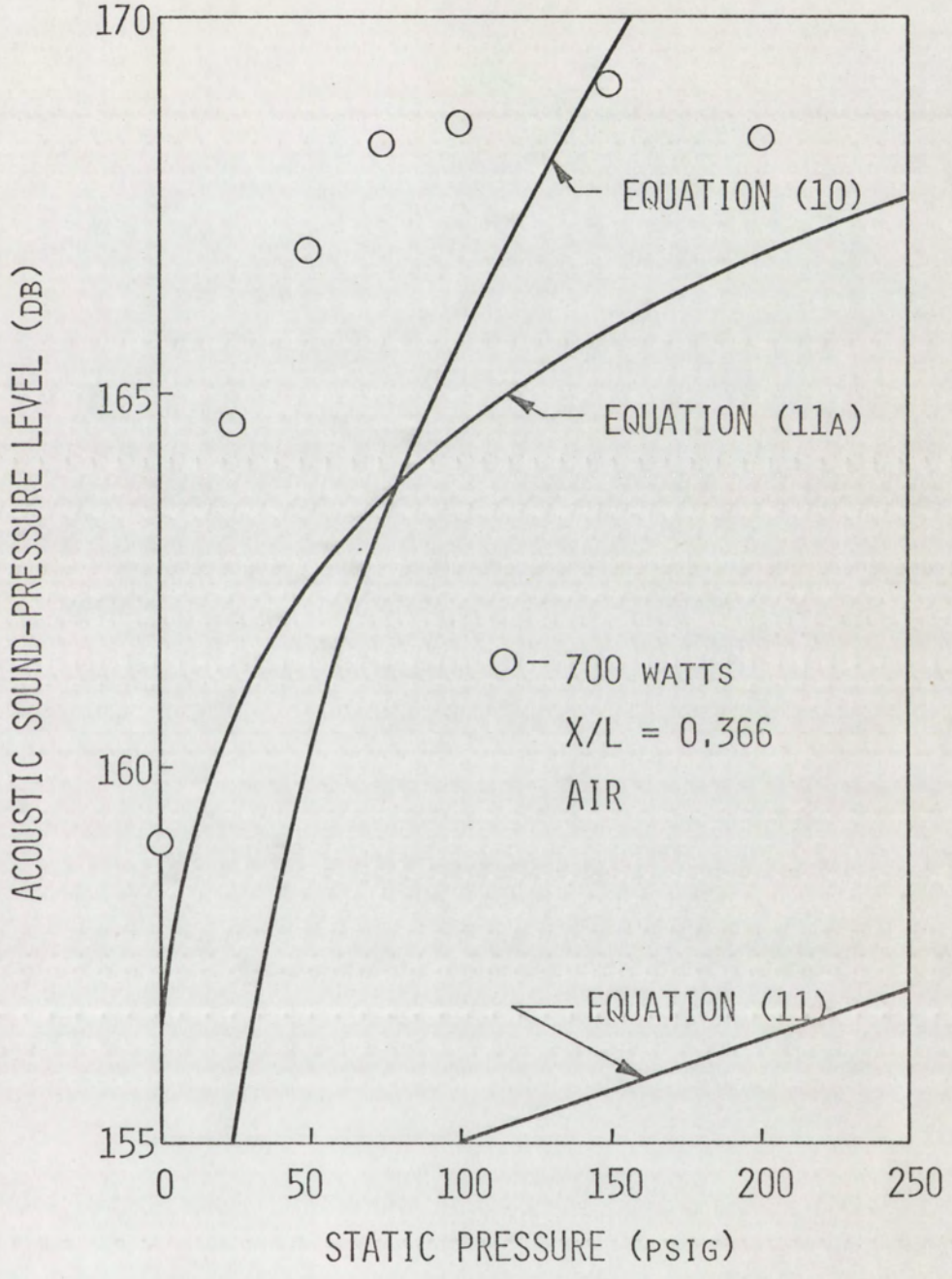

Figure 36. Correlation of experimental data with theoretical equations for air. $\dot{Q}$=700 watts

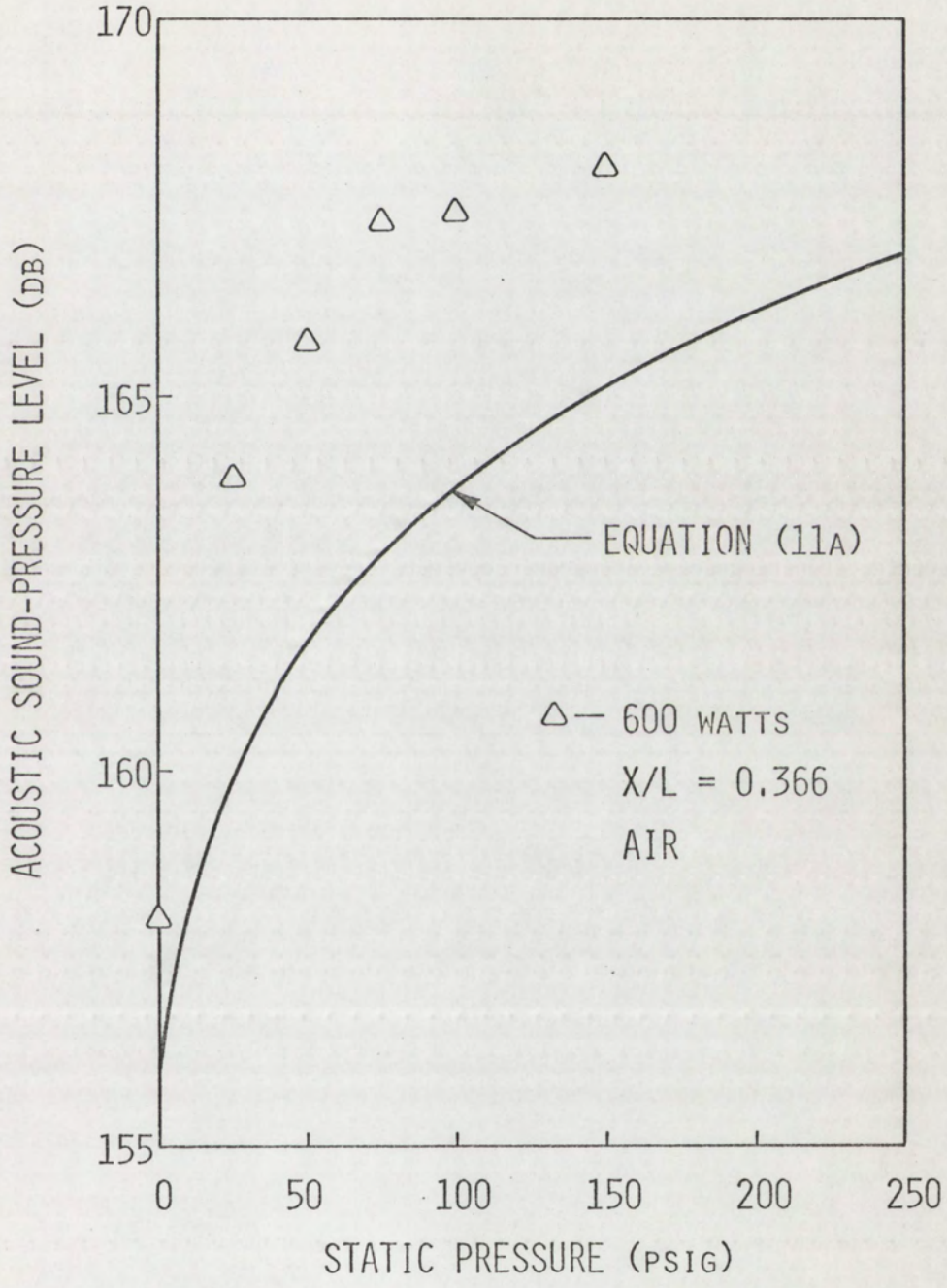

Figure 37. Correlation of experimental data with Equation (11a) for air. $\dot{Q}$=600 watts

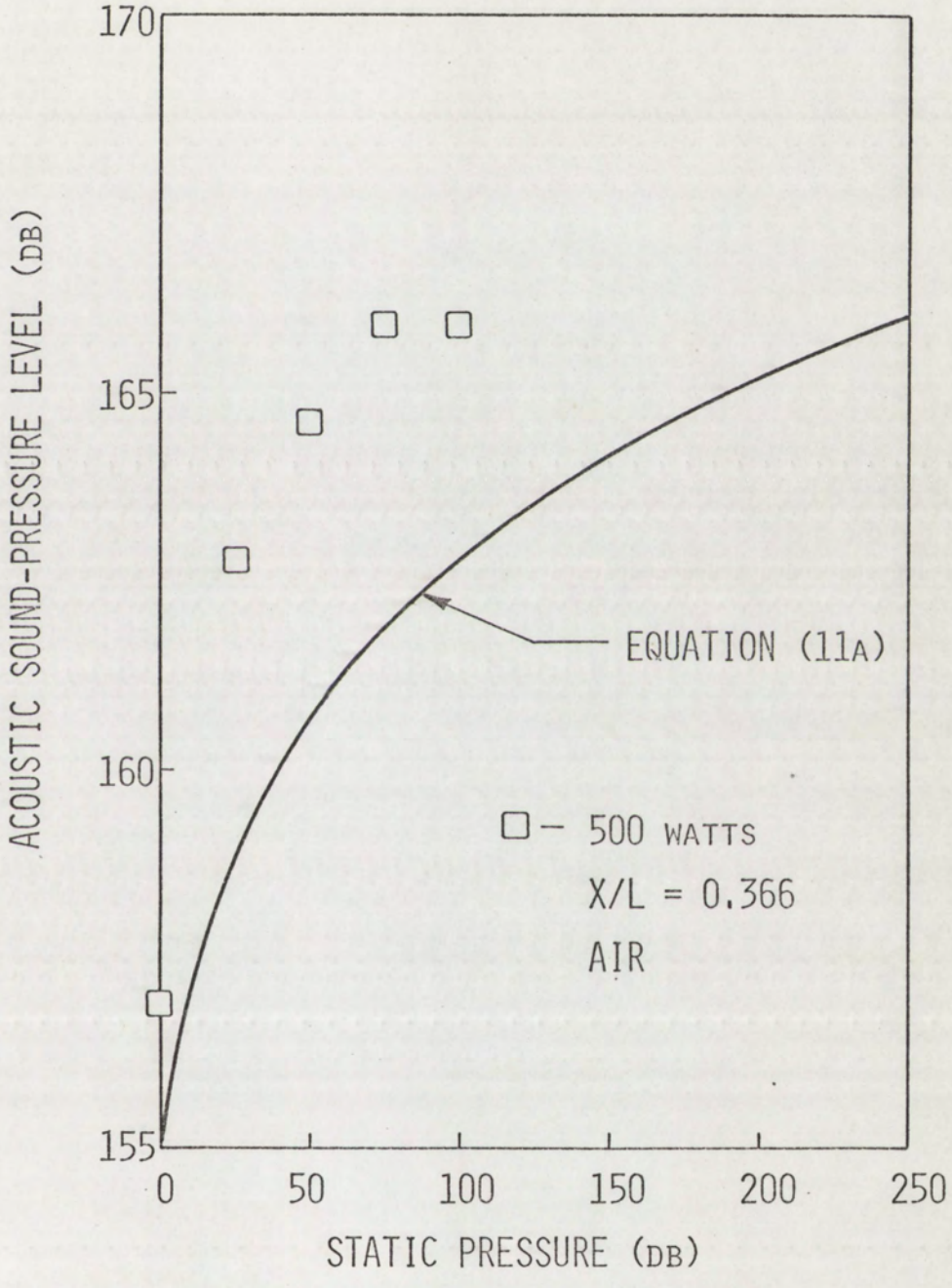

Figure 38. Correlation of experimental data with Equation (11a) for air. $\dot{Q}$=500 watts

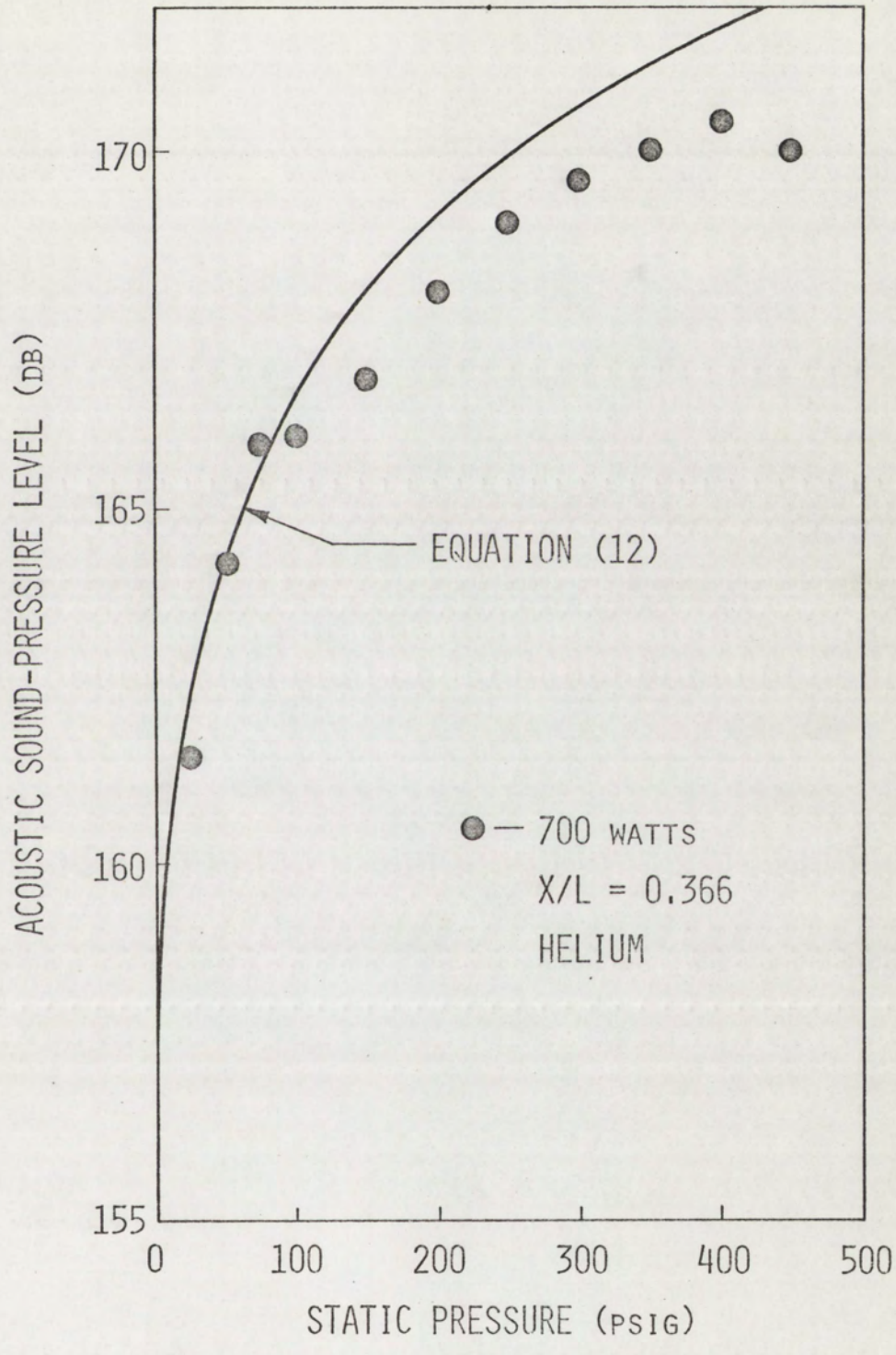

Figure 39. Correlation of experimental data with Equation (12) for helium. $\dot{Q}$=700 watts

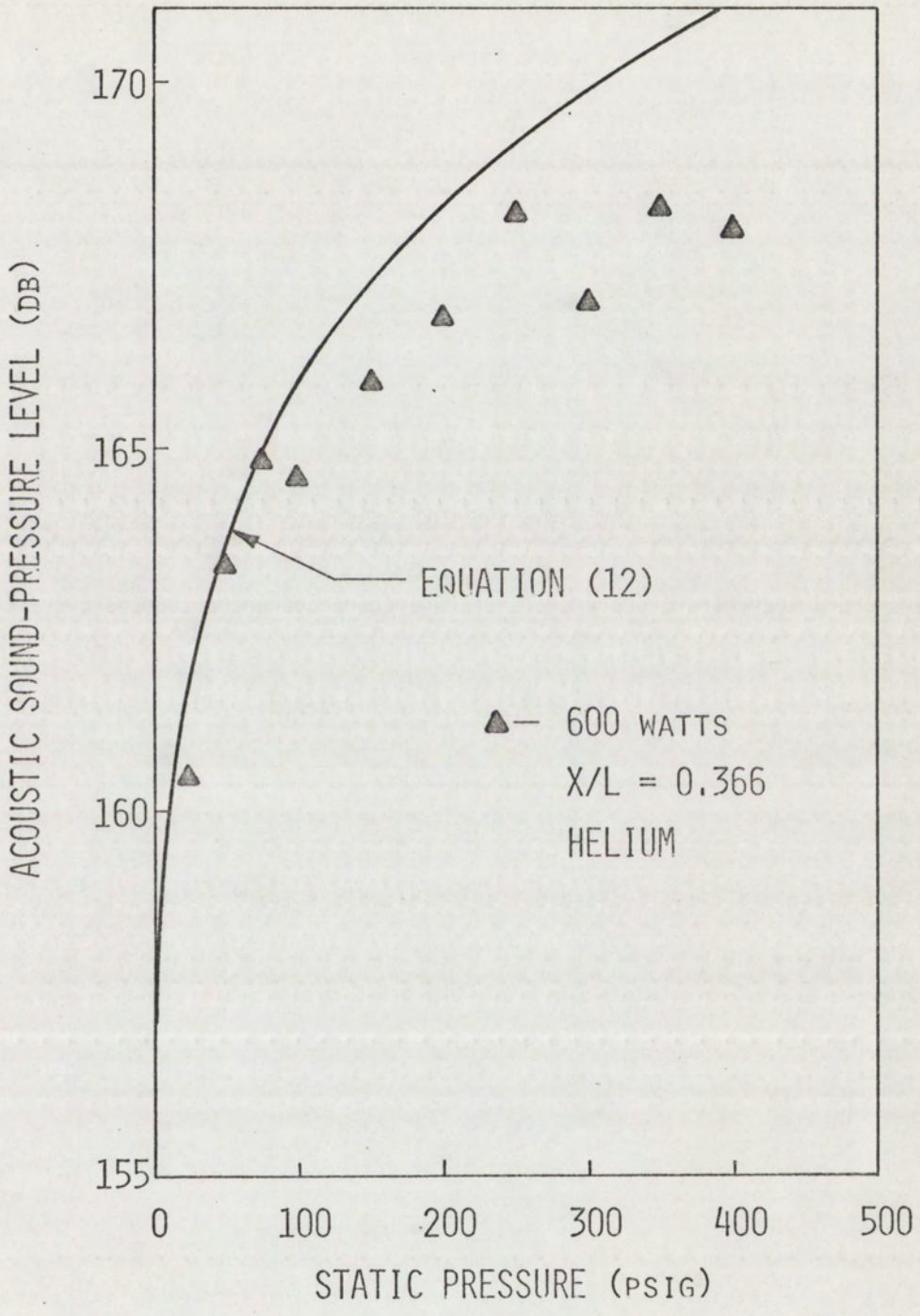

Figure 40. Correlation of experimental data with Equation (12) for helium. $\dot{Q}$=600 watts

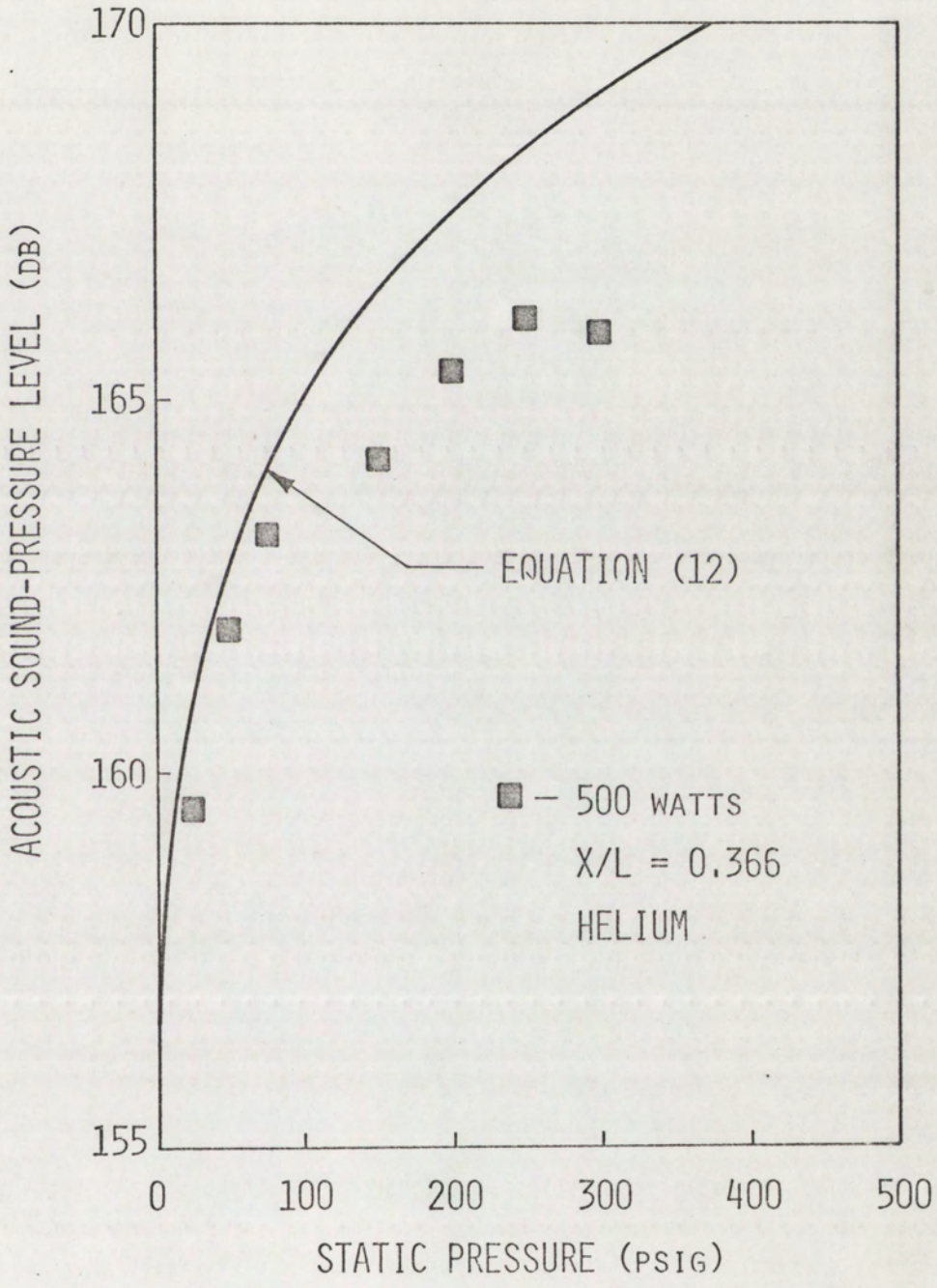

Figure 41. Correlation of experimental data with Equation (12) for helium. $\dot{Q}$=500 watts

Table 4. Maximum and minimum deviations in percent between theoretical and experimental results as shown in Figures 36 - 41

Power level	500	600	700	500	600	700
Working gas	Air	Air	Air	He	He	He
Equation no.	11a	11a	11a	12	12	12
from pressure						
Max. Dev.	43.8	37.6	28.8	23.2	28.4	14.9
Min. Dev.	13.5	22.3	24.2	8.95	7.70	0.00
from SPL						
Max. Dev.	2.40	2.50	2.79	1.38	1.71	0.82
Min. Dev.	1.15	1.39	1.51	0.49	0.12	0.00

If a single operating point of a thermoacoustic system is known, the sound-pressure level generated by the oscillator for other operating conditions can be predicted from dimensional analysis. Three equations derived from dimensional analysis were

$$p = p_r\left(\frac{\dot{Q}}{\dot{Q}_r}\right)^{2/3}\left(\frac{x_r}{x}\right)^{4/3}\left(\frac{p_o}{p_{or}}\right)^{1/3}, \tag{28}$$

$$p = p_r\left(\frac{\dot{Q}}{\dot{Q}_r}\right)^{2/3}\left(\frac{p_o}{p_{or}}\right)^{1/3}, \tag{29}$$

and

$$p = p_r\left(\frac{p_o}{p_{or}}\right)^{1/3}. \tag{30}$$

Figures 42-53 show the results of the dimensional analysis compared to the experimental data. For Equation (28), the reference values for both air and helium were chosen as $\dot{Q}_r$=700 watts, x_r=30 inches, and p_{or}=62.3 psia. The reference value for p_r was chosen separately for each gas as the actual over-pressure produced at the reference condition. In Equation (29), the reference conditions were chosen as $\dot{Q}_r$=700 watts and p_{or}=62.3 psia. Since Equation (29) is dependent upon location and the working gas, p_r had to be chosen at the reference power and static pressure for each gas and location. The reference condition for Equation (30) was chosen as p_{or}=62.3 psia. Equation (30) is dependent upon power, location, and working gas, so that a different reference over-pressure had to be chosen for each change in the dependent conditions.

In some cases, it would have been repetitious to use Equations (28) and (29) to predict sound-pressure levels at the reference conditions. For example, if the location x/L = 0.366 (x=30 inches) was under consideration, Equation (28) reduced to Equation (29). In addition, if the power level of 700 watts was also considered, Equation (29) reduced to Equation (30). Therefore, only the non-repetitive curves were plotted in Figures 42-53. When two curves were indentically predicted, this information was noted on the figure. The maximum deviation from the experimental data for each curve is tabulated in Table 5. The deviations are calculated in terms of both the actual over-pressure and the sound-pressure level.

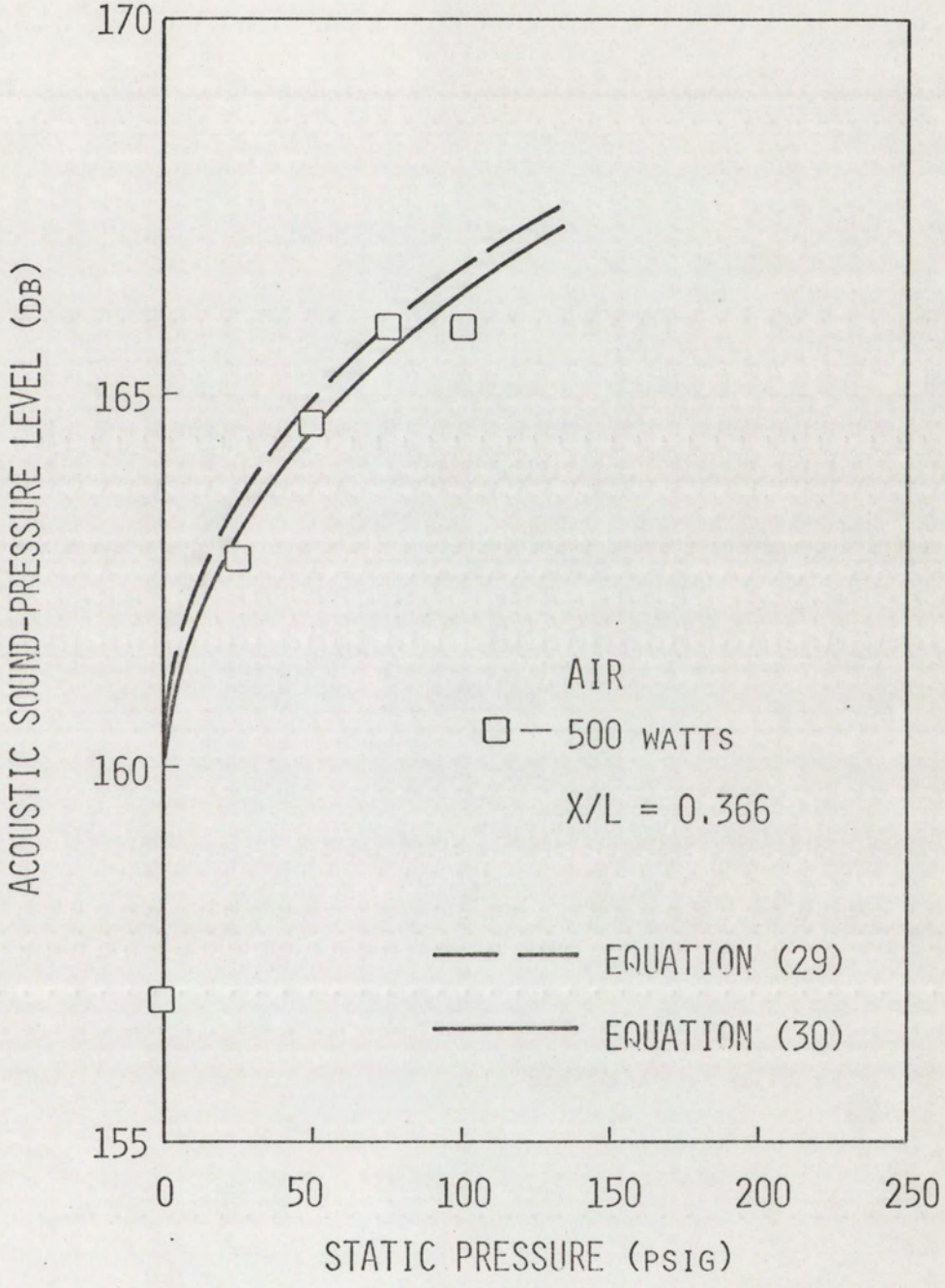

Figure 42. Comparison of experimental data to SPL predictions from dimensional analysis for air. $\dot{Q}$=500 watts, x/L=0.366

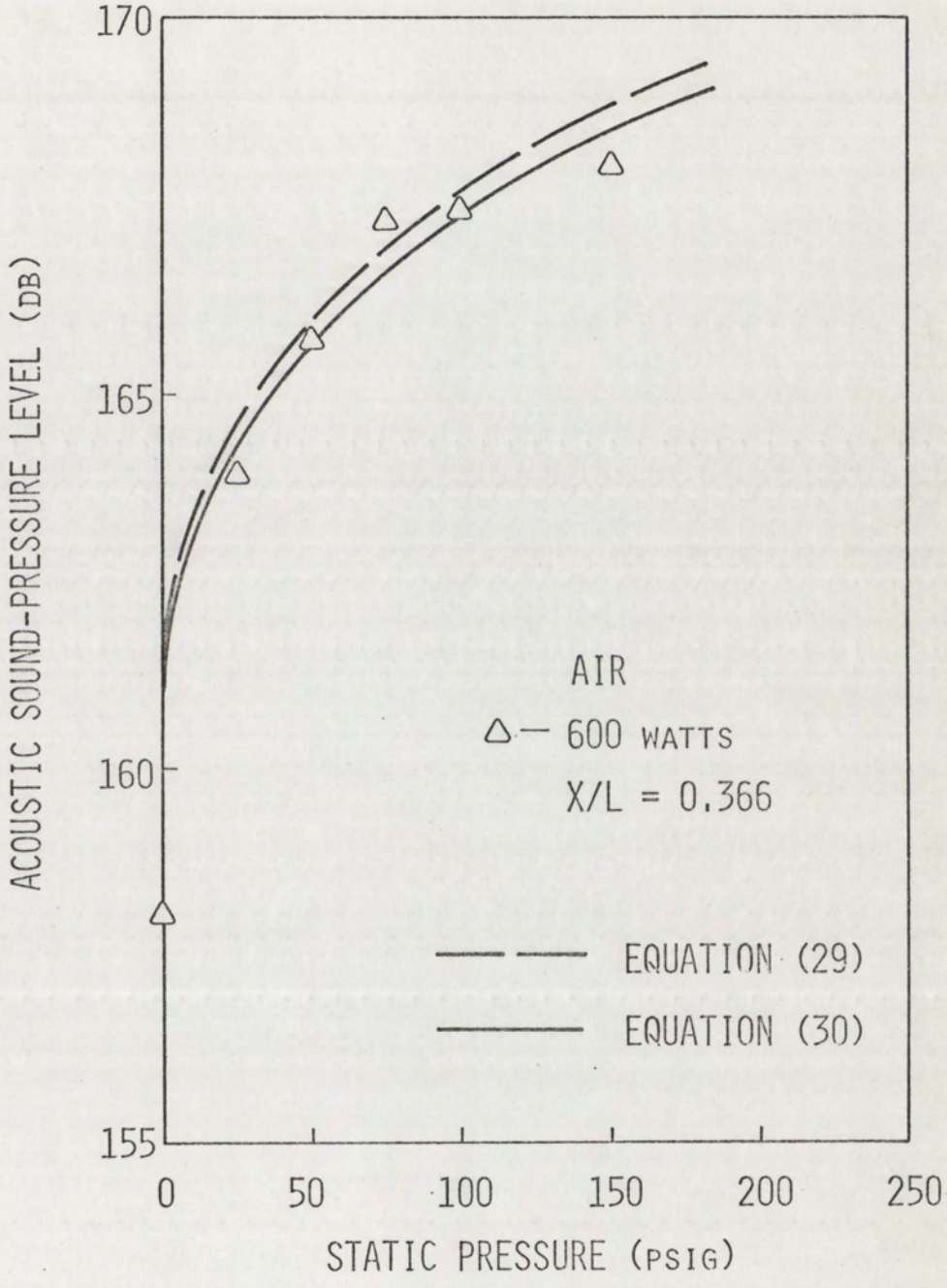

Figure 43. Comparison of experimental data to SPL predictions from dimensional analysis for air. $\dot{Q}$=600 watts, x/L=0.366

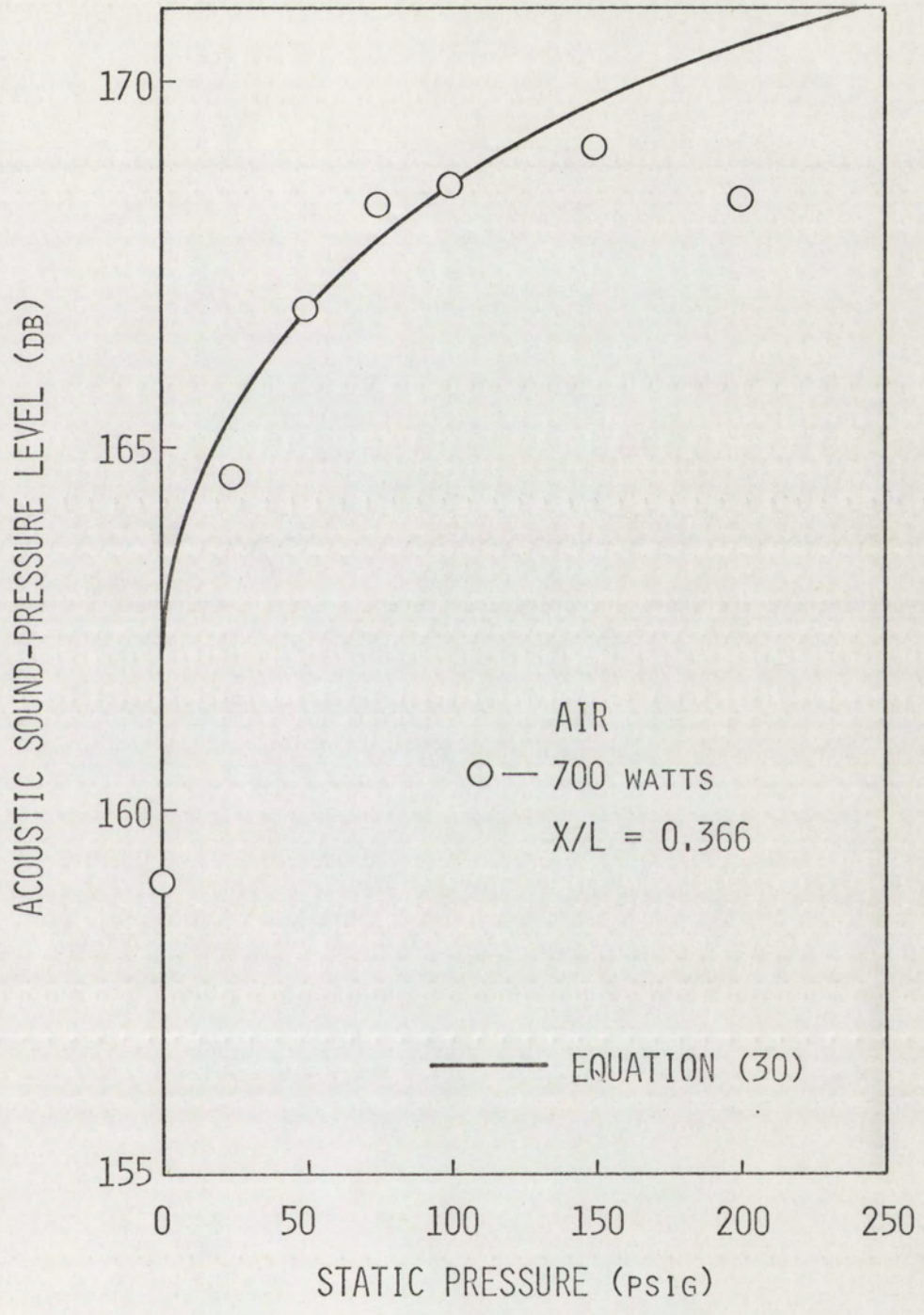

Figure 44. Comparison of experimental data to SPL predictions from dimensional analysis for air. $\dot{Q}$=700 watts, x/L-0.366

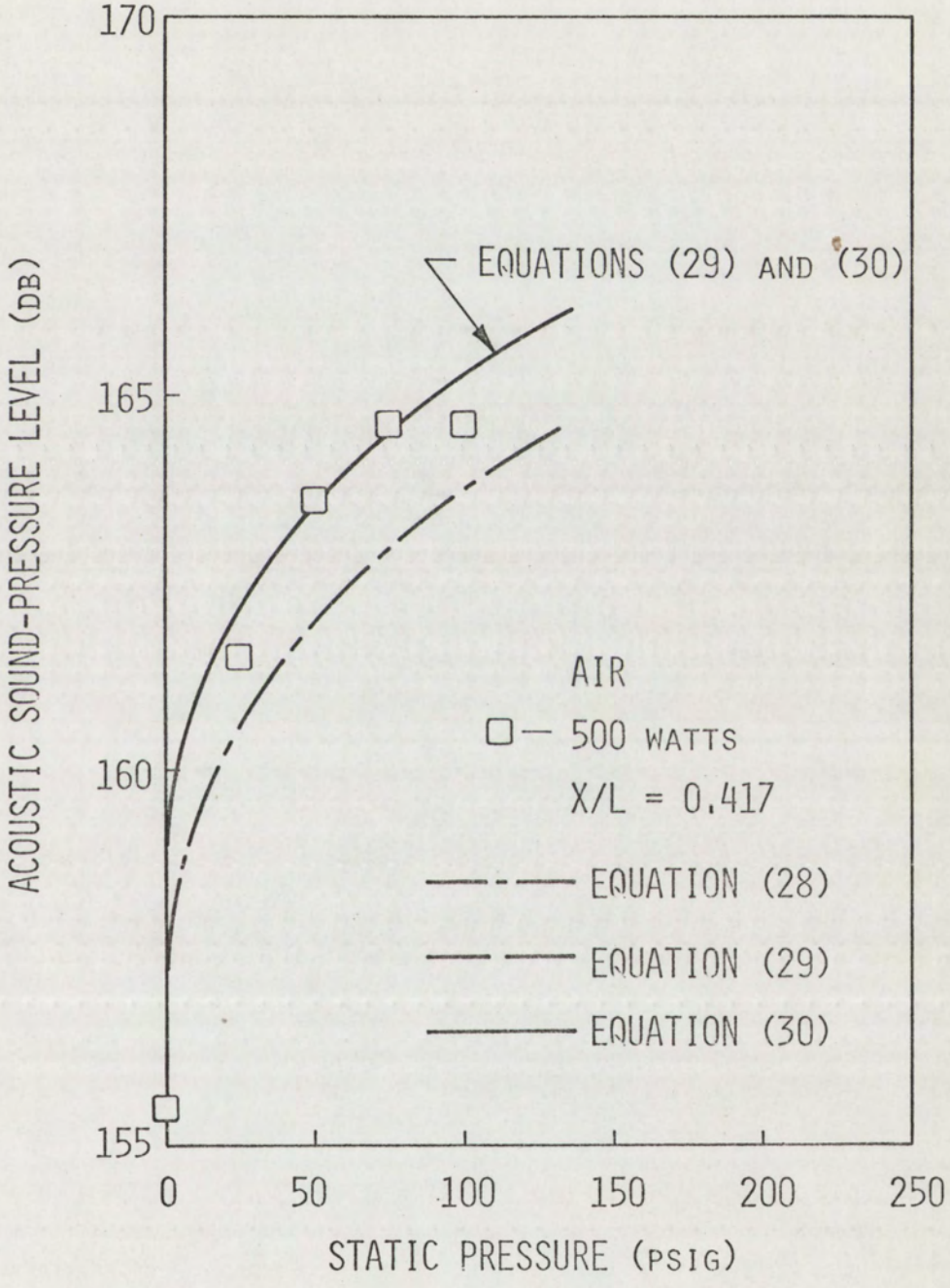

Figure 45. Comparison of experimental data to SPL predictions from dimensional analysis for air. $\dot{Q}$=500 watts, x/L=0.417

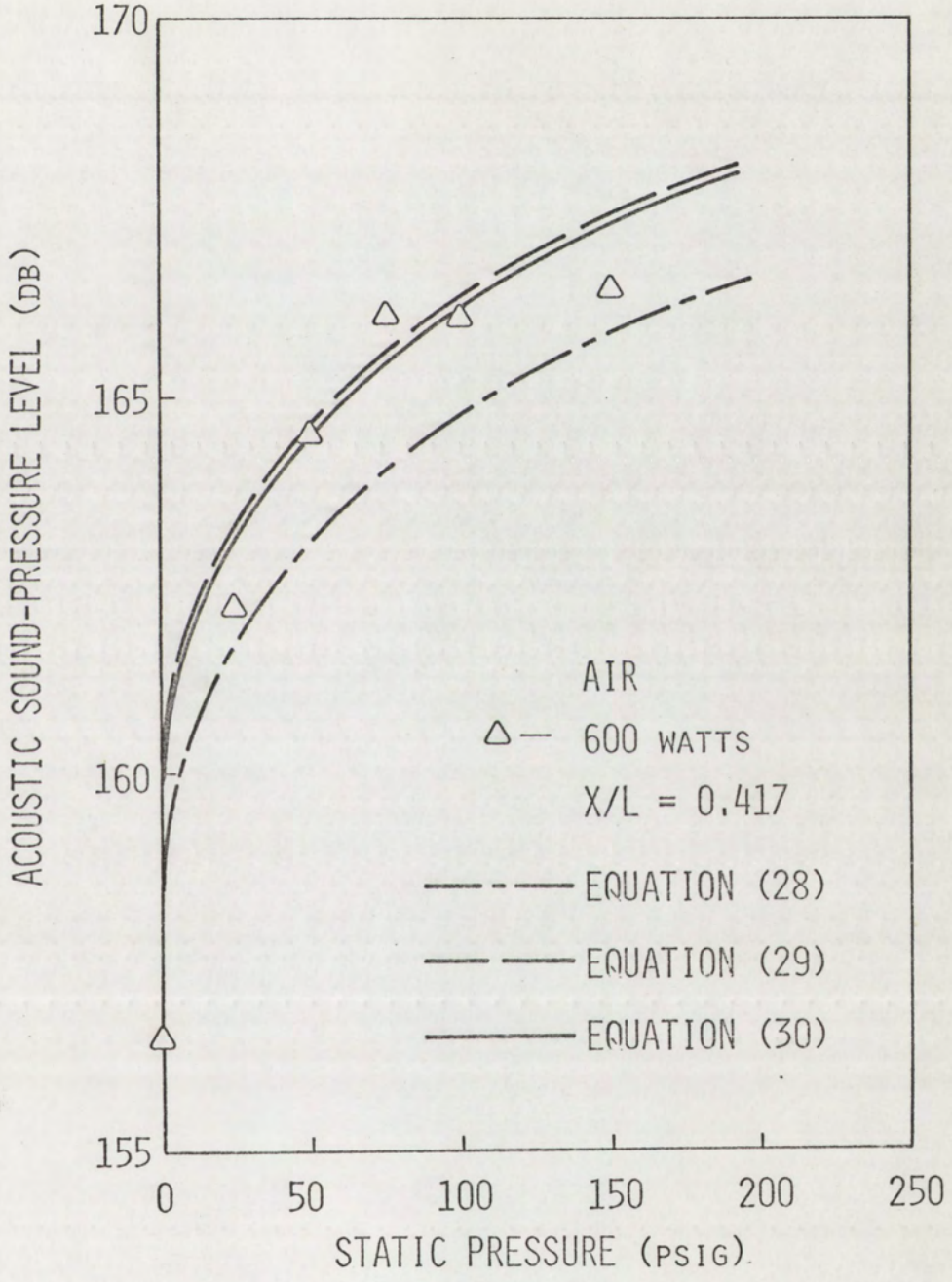

Figure 46. Comparison of experimental data to SPL predictions from dimensional analysis for air. $\dot{Q}$=600 watts, x/L=0.417

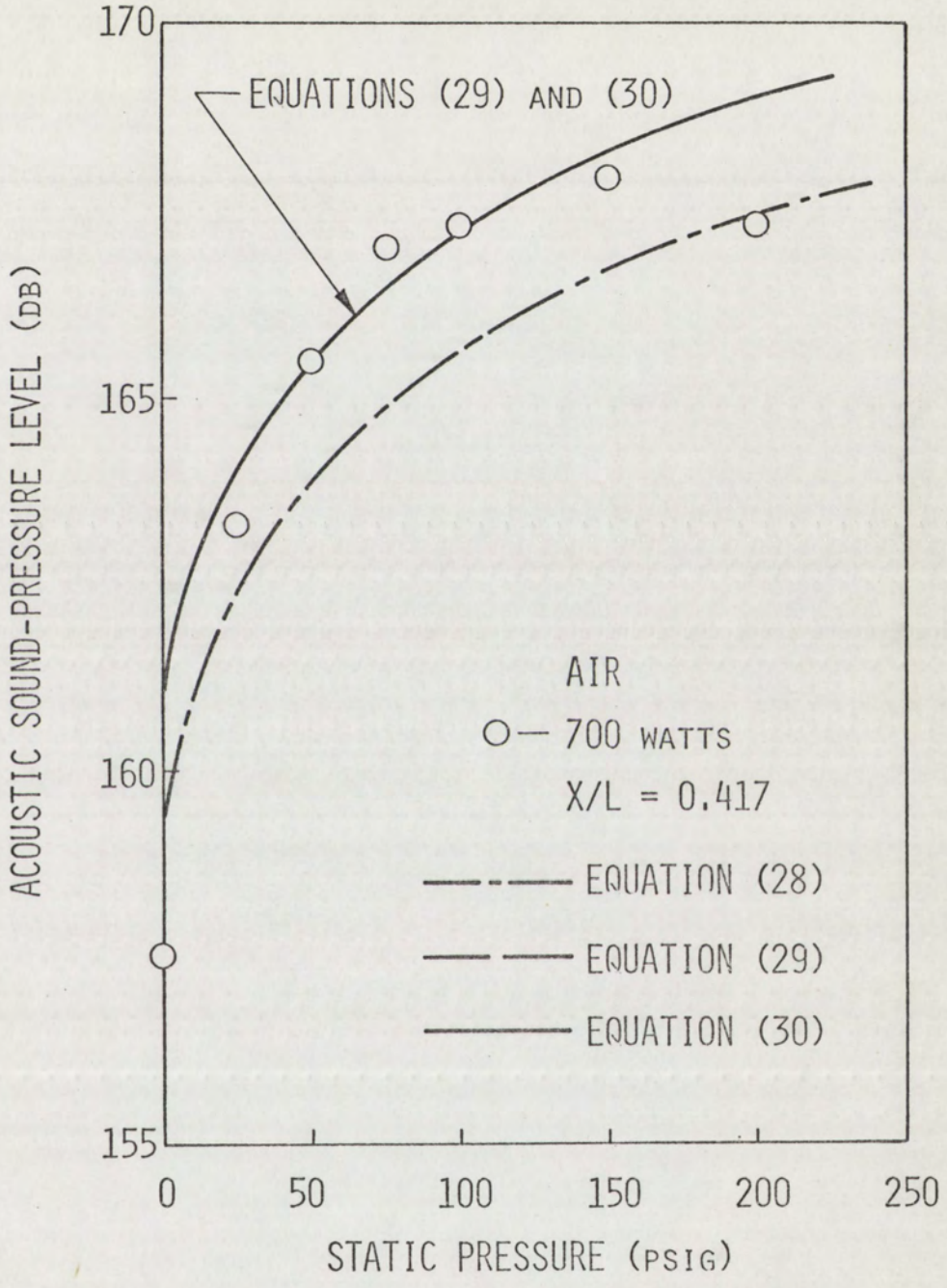

Figure 47. Comparison of experimental data to SPL predictions from dimensional analysis for air. $\dot{Q}$=700 watts, x/L=0.417

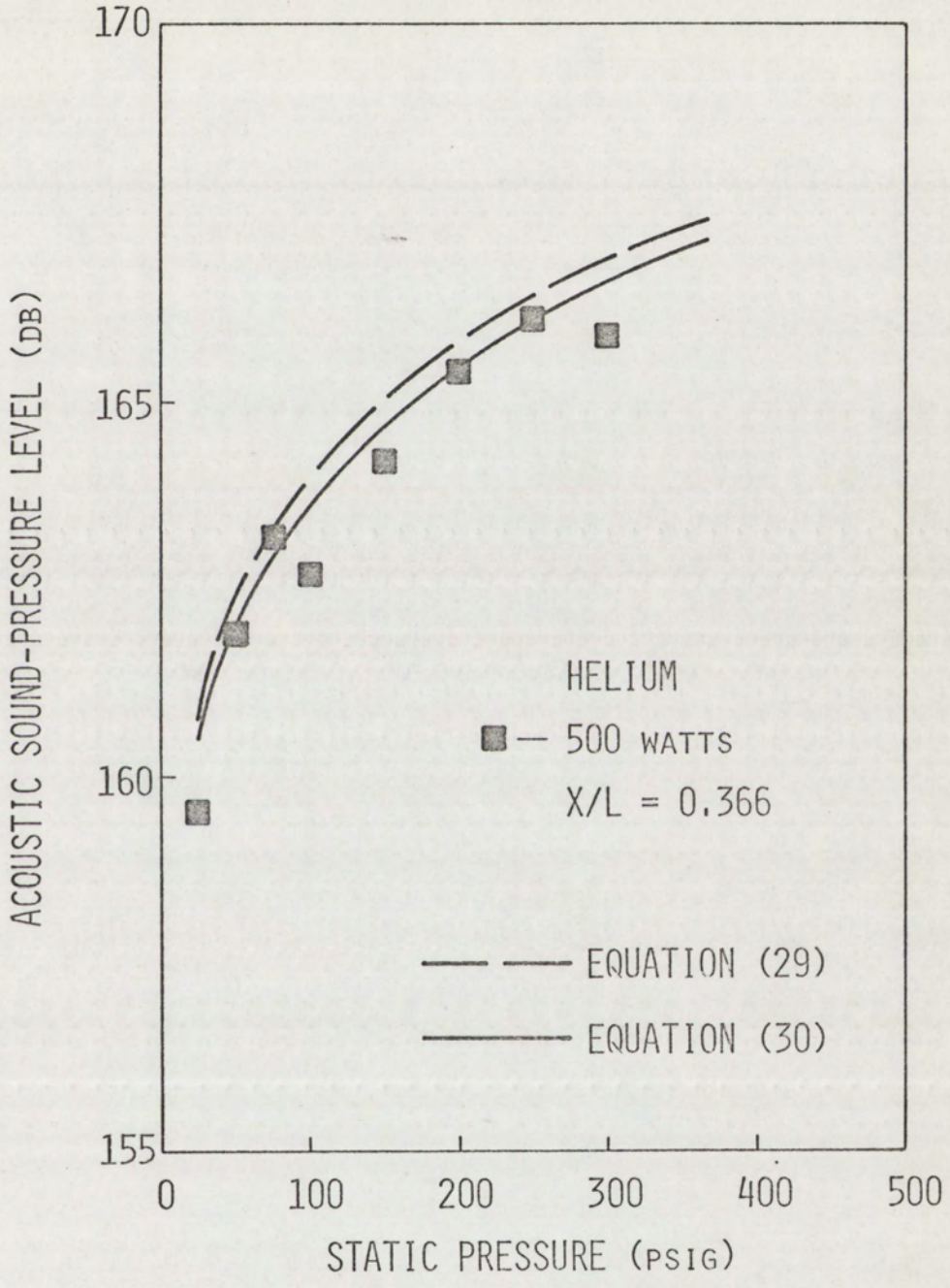

Figure 48. Comparison of experimental data to SPL predictions from dimensional analysis for helium. $\dot{Q}$=500 watts, x/L=0.366

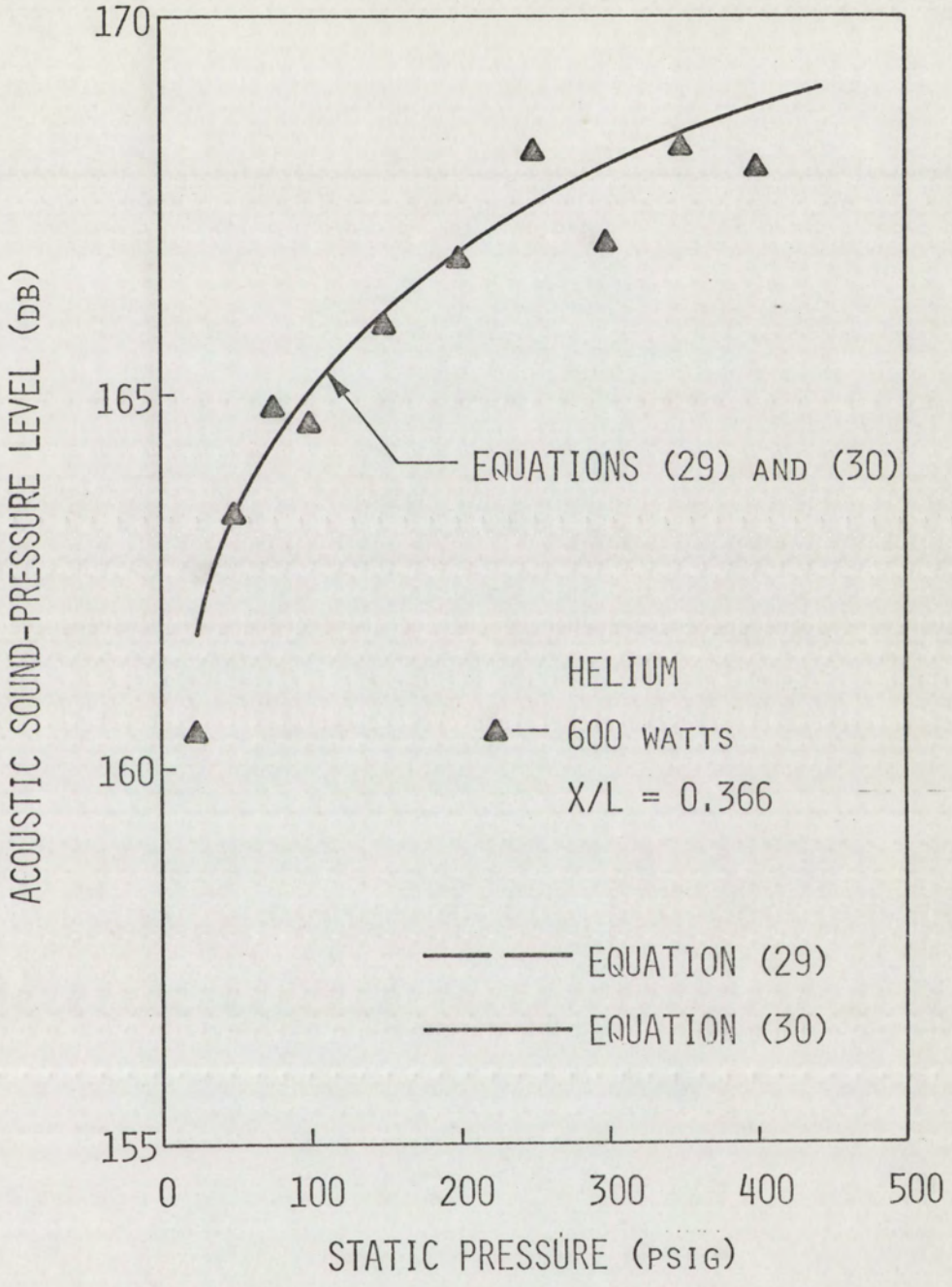

Figure 49. Comparison of experimental data to SPL predictions from dimensional analysis for helium. $\dot{Q}$=600 watts, x/L=0.366

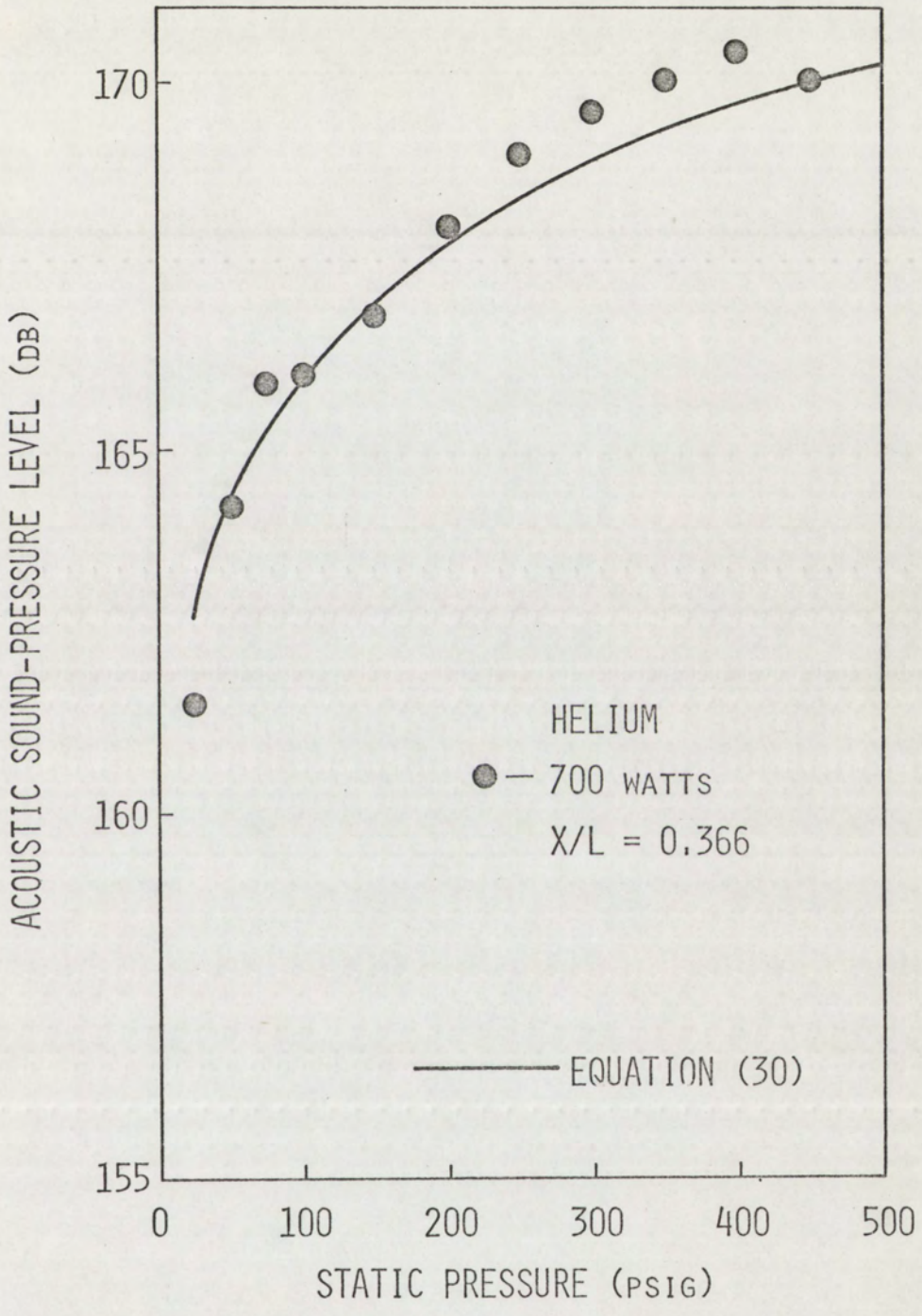

Figure 50. Comparison of experimental data to SPL predictions from dimensional analysis for helium. Q=700 watts, x/L=0.366

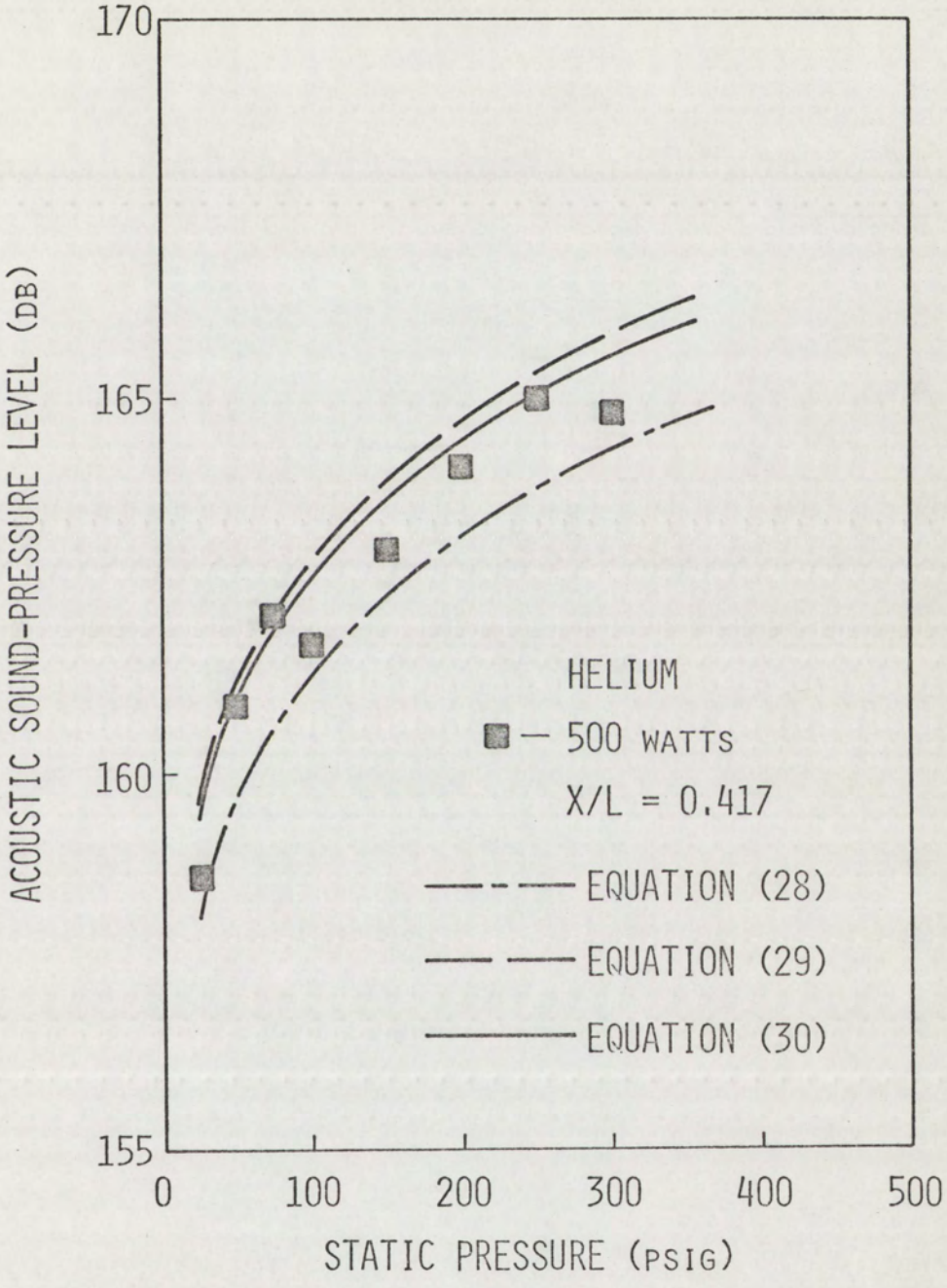

Figure 51. Comparison of experimental data to SPL predictions from dimensional analysis for helium. $\dot{Q}$=500 watts, x/L=0.417

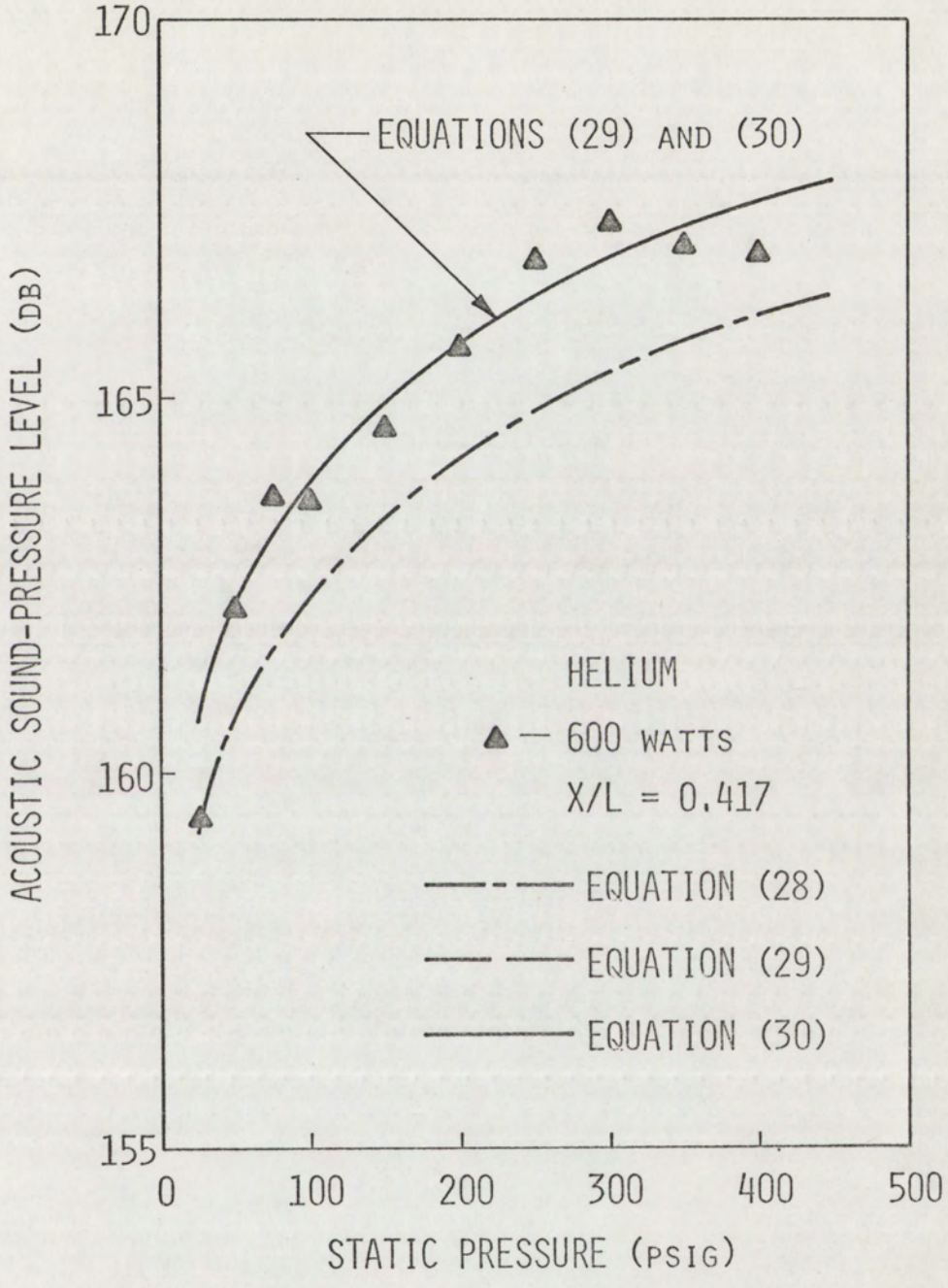

Figure 52. Comparison of experimental data to SPL predictions from dimensional analysis for helium. $\dot{Q}$=600 watts, x/L=0.417

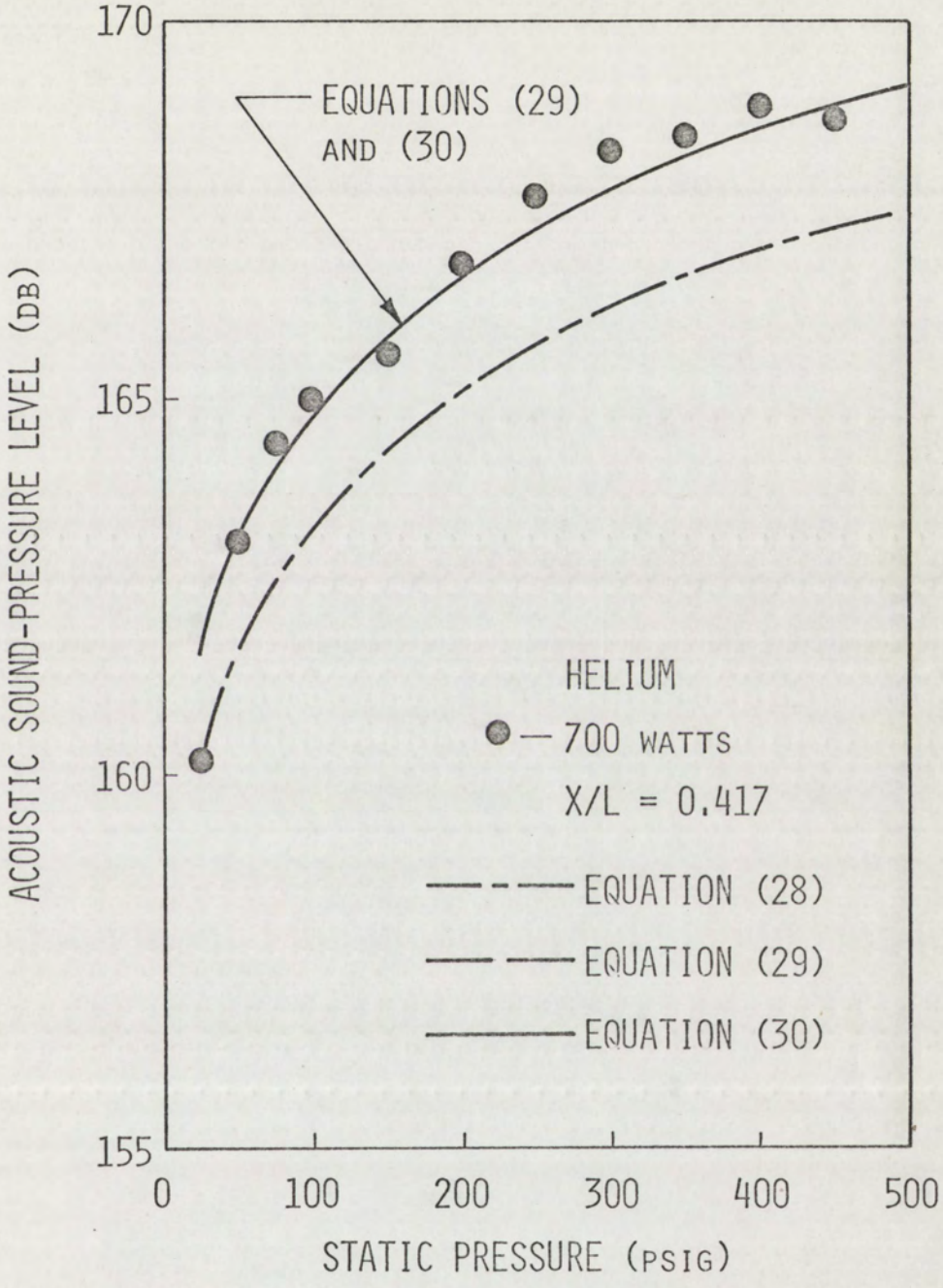

Figure 53. Comparison of experimental data to SPL predictions from dimensional analysis for helium. $\dot{Q}$=700 watts, x/L=0.417

Table 5. Maximum deviation of dimensional analysis from experimental data, in per cent

Equation No.	28		29		30	
Figure No.	Press	SPL	Press	SPL	Press	SPL
42	--*	--	48.3	2.17	43.0	1.98
43	--	--	46.4	2.08	41.2	1.90
44	--	--	--	--	44.3	2.01
45	23.3	1.16	53.9	2.12	53.9	2.12
46	24.2	1.21	4.54	2.17	3.54	2.11
47	23.0	1.14	47.3	2.09	47.3	2.09
48	--	--	16.1	0.81	12.1	0.63
49	--	--	17.4	0.87	17.4	0.87
50	--	--	--	--	14.8	0.74
51	12.9	0.73	9.53	0.63	12.3	0.50
52	20.6	1.19	16.3	0.82	16.3	0.82
53	21.4	1.25	17.5	0.87	17.5	0.87

*repetitious curves were not plotted.

Inspection of the figures and of Table 5 shows that, in general, Equation (30) is the best prediction equation, followed by Equation (29). Equation (28) is the poorest of the prediction equations. This is to be expected, since Equation (28) contains the greatest number of variables.

The restriction on Equations (28)-(30) is that at least one operating condition of the thermoacoustic system must be known. An additional restriction on Equation (28) for a double-end oscillator is that x must be within the region bounded by the tube bundle-heater element junction and the center of the pipe. Figures 45-47 and Figures 51-53 show that the prediction from x/L=0.366 to x/L=0.417 is somewhat lower than the other predictions.

By inspection of Figures 42-53, it can be concluded that if a single operating point of a thermoacoustic system is known, other conditions can be accurately predicted from dimensional analysis; that is, from Equations (28), (29), and (30).

The final correlation was made, to determine how well the experimental data compare to the relation

$$p = b_1 p_o^{b_2} \quad , \tag{40}$$

where b_1 and b_2 are constants, p is the actual over-pressure, and p_o is the absolute static pressure. An equation of the form of Equation (40) was chosen because three of the theoretical relations, namely Equations (11), (11a), and (12), are of this form. The dimensional analysis equations, Equations (28), (29), and (30), can also be reduced to this form.

Figures 54-57 show how the actual over-pressure varied with increasing absolute static pressure for the experimental data. A least squares curve fit applied to the experimental data was used to determine the constants b_1 and b_2 in Equation (40). The constants b_1 and b_2 along with the correlation coefficient r^2 are given for the experimental data in Table 6. The unstable points of the experimental data were not considered in making the least squares fits. Inspection of Figures 54-57 and of the correlation coefficients in Table 6 shows that the fits are representative of the trends of the experimental data.

Table 6. Constants from Equation (40) and correlation coefficient for experimental data

Gas	x/L	Power (watts)	b_1	b_2	r^2
Air	0.366	500	0.077	0.534	0.989
		600	0.112	0.459	0.957
		700	0.121	0.468	0.965
	0.417	500	0.065	0.543	0.991
		600	0.092	0.467	0.947
		700	0.101	0.477	0.966
Helium	0.366	500	0.111	0.358	0.954
		600	0.130	0.359	0.963
		700	0.123	0.400	0.982
	0.417	500	0.105	0.344	0.960
		600	0.097	0.398	0.969
		700	0.109	0.394	0.980

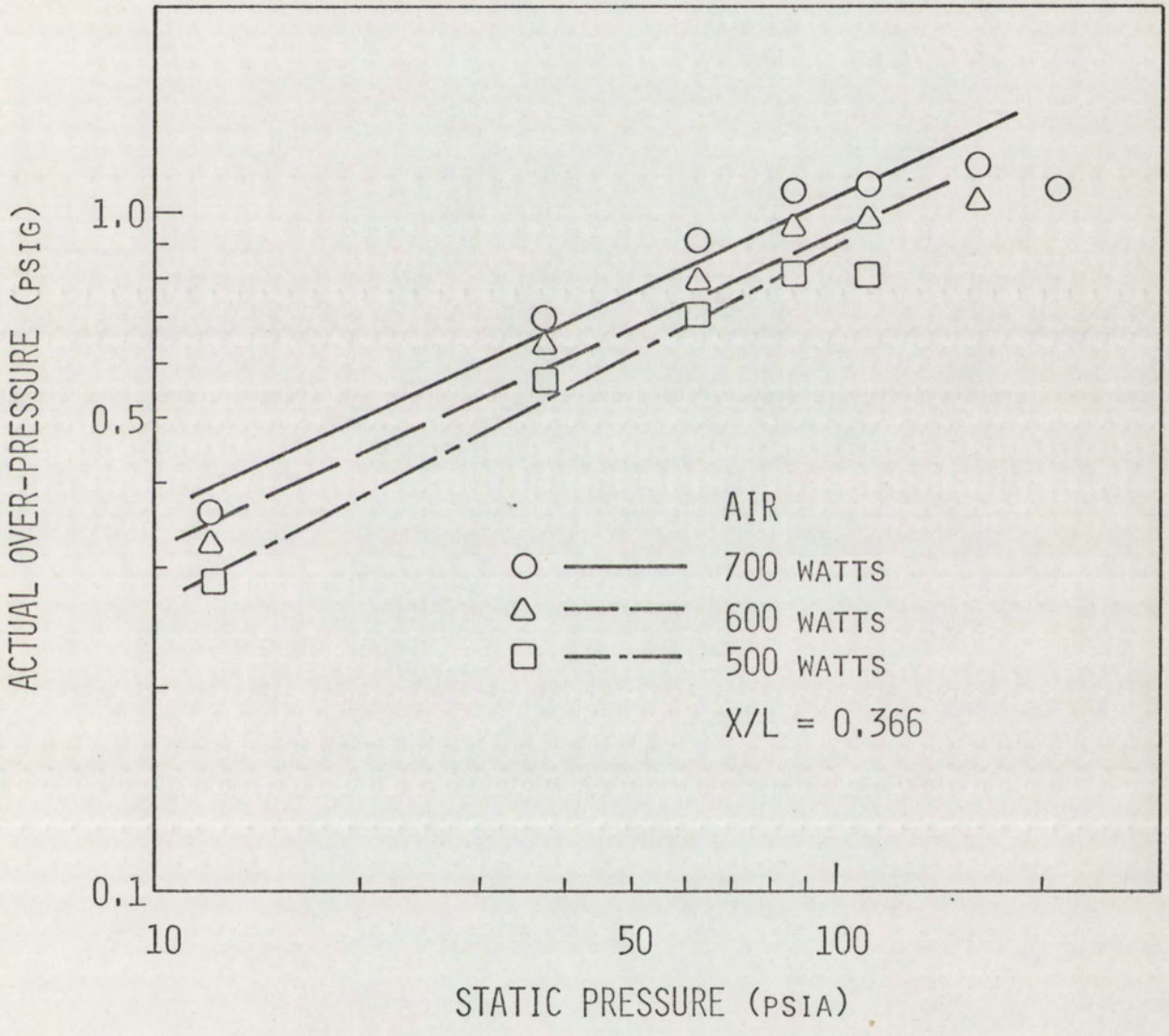

Figure 54. Actual over-pressure as a function of static pressure for air, x/L=0.366

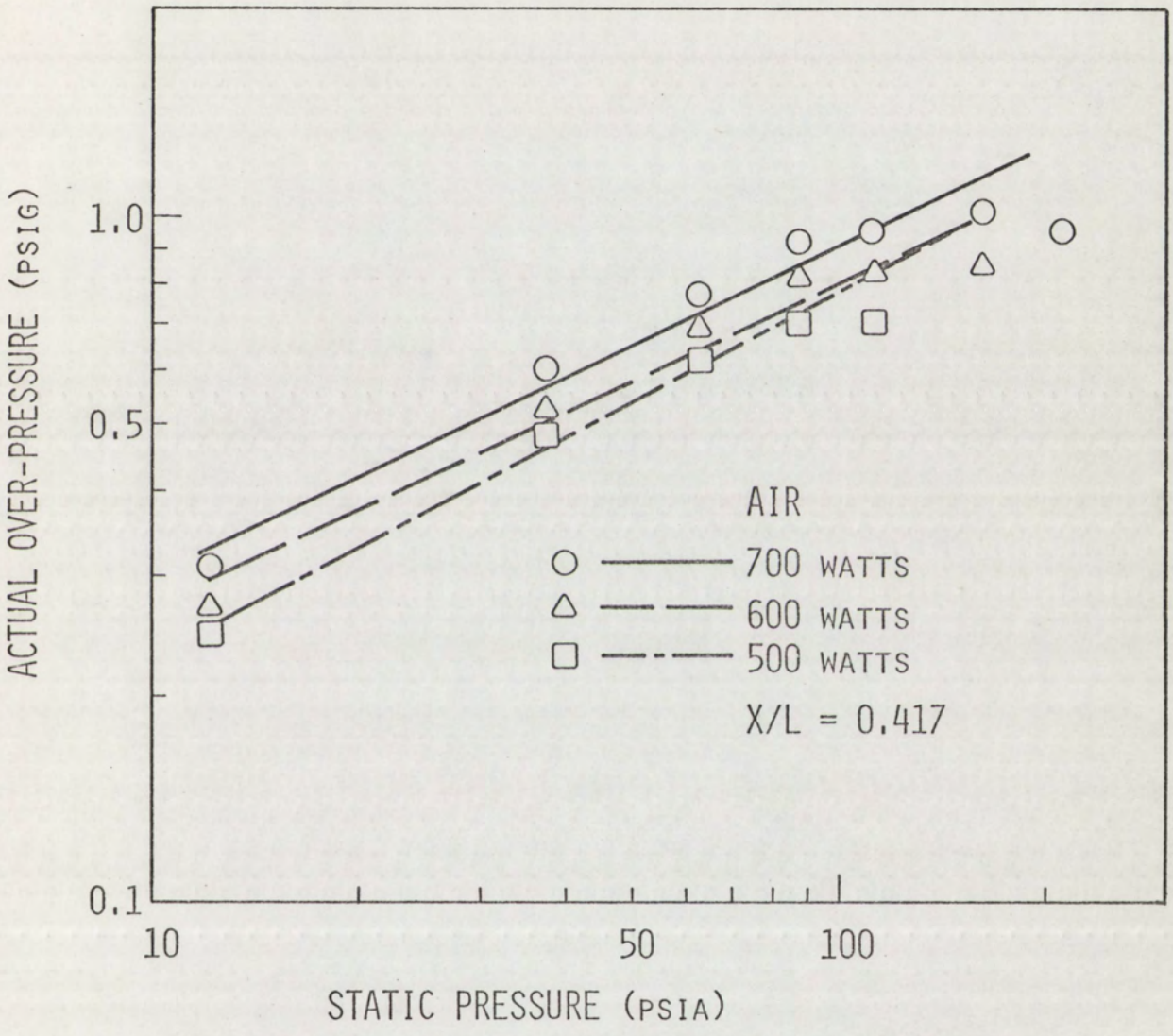

Figure 55. Actual over-pressure as a function of static pressure for air, x/L=0.417

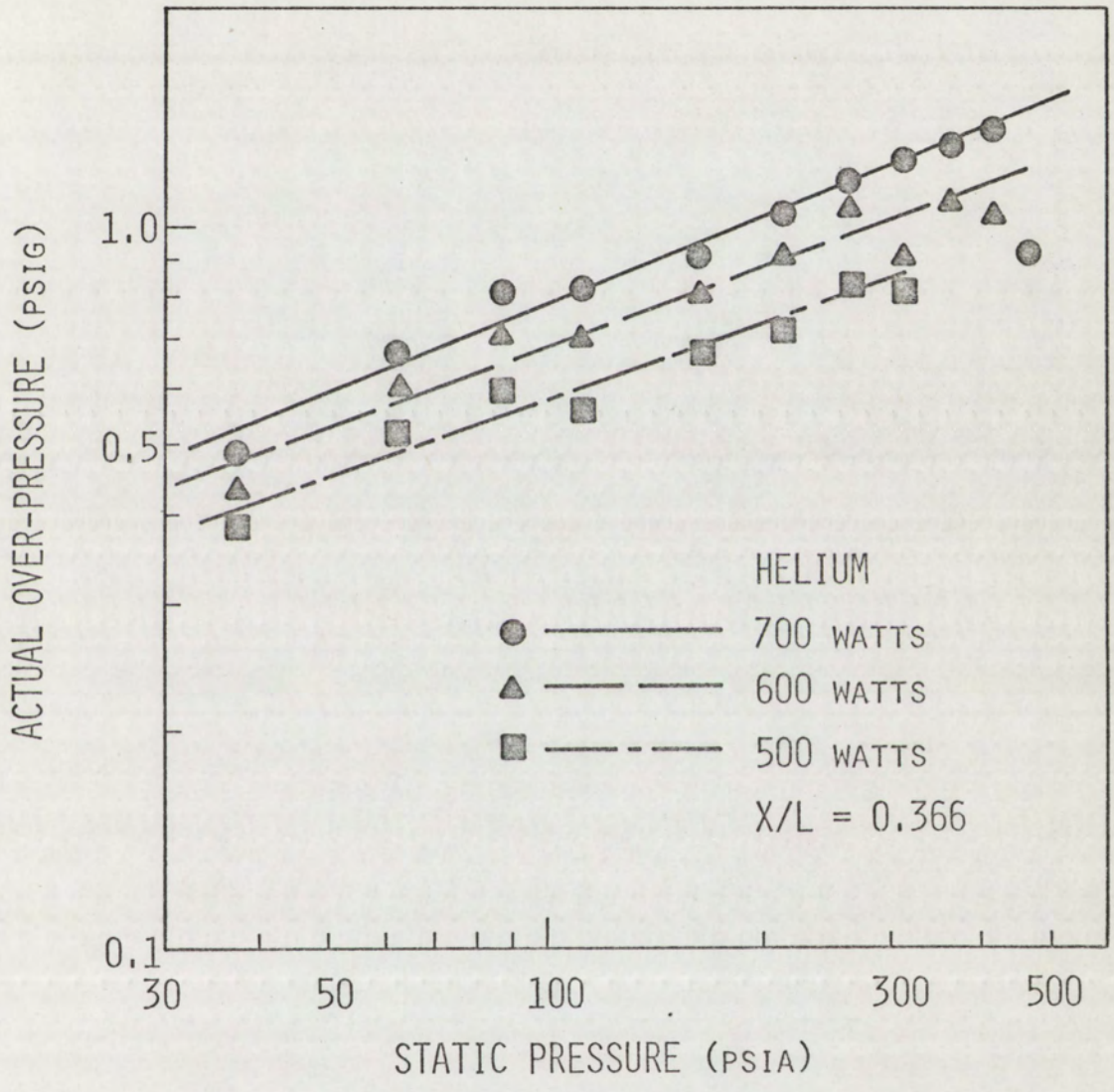

Figure 56. Actual over-pressure as a function of static pressure for helium, x/L=0.366

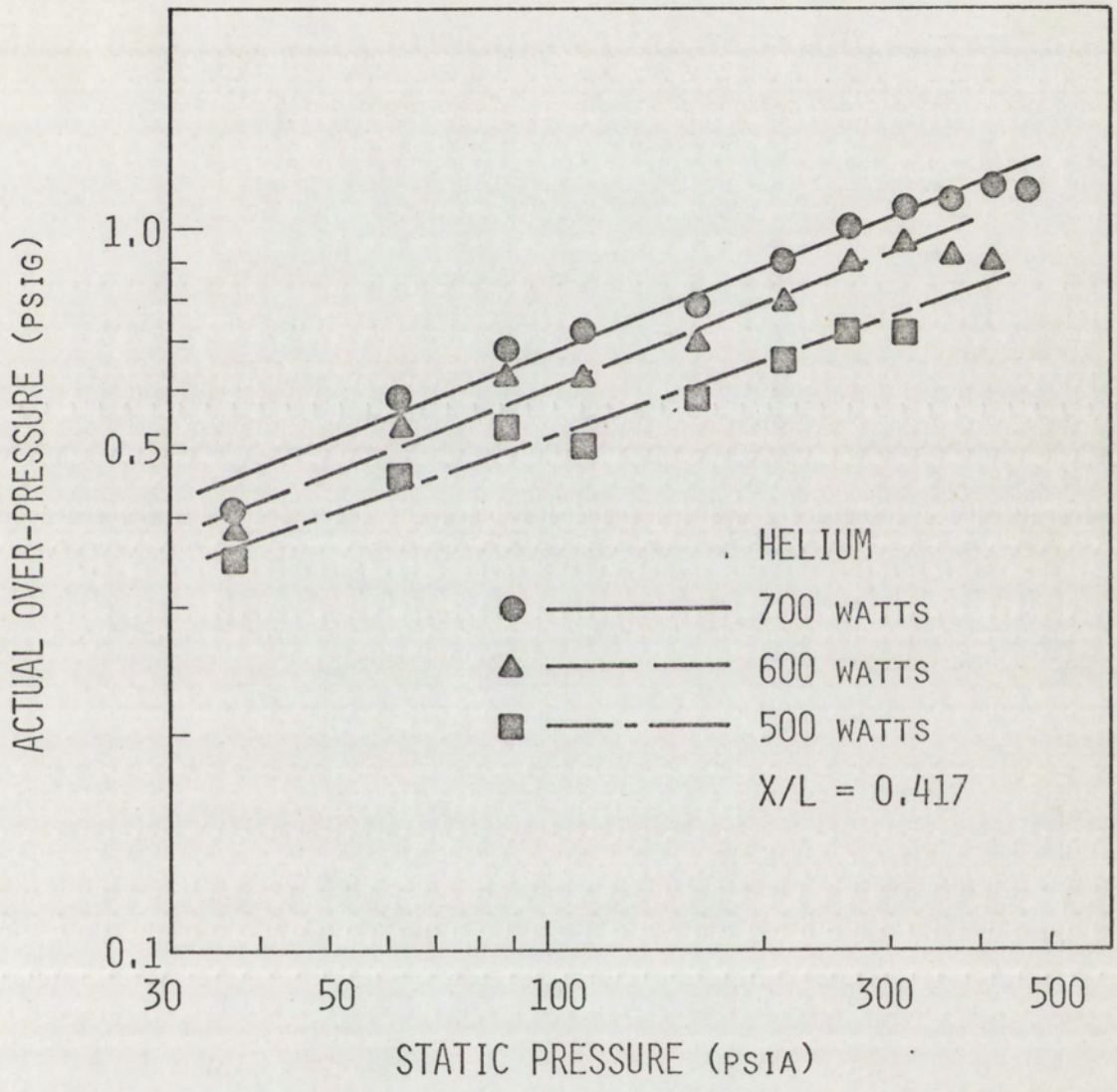

Figure 57. Actual over-pressure as a function of static pressure for helium, x/L=0.417

To complete the analysis, the theoretical Equations (11), (11a), and (12) and the dimensional analysis Equations (28)-(30) were reduced to the form of Equation (40). The only other significant theoretical equation, Equation (10), could not be reduced to the form of Equation (40). These results and the experimental results are compared in Table 7. The same reference values used in calculating the curves of Figures 42-53 were used in calculating b_1 and b_2 for Table 7. Inspection of Table 7 shows that for the same operating conditions of a thermoacoustic oscillator, in general, the range of values given by the theoretical and experimental analyses for b_1, and especially for b_2, are of the same magnitude. Therefore, in designing a thermoacoustic oscillator, Equation (40) could be used as a design equation, along with values of b_1 and b_2 from Table 7, to predict the sound-pressure levels at elevated internal pressures.

Table 7. Results of the experimental and theoretical analyses tabulated in the form of Equation (40)

Description	Gas	x/L	Power (watts)	b_1	b_2
Equation (11)	Air	--	500	0.036	0.333
Equation (11)	Air	--	600	0.041	0.333
Equation (11)	Air	--	700	0.046	0.333
Equation (11a)	Air	--	500	0.084	0.414
Equation (11a)	Air	--	600	0.090	0.414
Equation (11a)	Air	--	700	0.098	0.414
Equation (12)	Helium	--	500	0.086	0.455
Equation (12)	Helium	--	600	0.095	0.455
Equation (12)	Helium	--	700	0.103	0.455
Equation (28)	Air	0.366	500	0.197	0.333
		0.366	600	0.222	
		0.366	700	0.246	
		0.417	500	0.166	
		0.417	600	0.187	
		0.417	700	0.207	
	Helium	0.366	500	0.145	
		0.366	600	0.163	
		0.366	700	0.181	
		0.417	500	0.122	
		0.417	600	0.137	
		0.417	700	0.152	
Equation (29)	Air	0.366	500	0.197	
		0.366	600	0.222	
		0.366	700	0.246	
		0.417	500	0.168	
		0.417	600	0.190	
		0.417	700	0.210	
	Helium	0.366	500	0.145	
		0.366	600	0.163	
		0.366	700	0.181	
		0.417	500	0.127	
		0.417	600	0.143	
		0.417	700	0.159	
Equation (30)	Air	0.366	500	0.190	
		0.366	600	0.215	
		0.366	700	0.246	
		0.417	500	0.168	
		0.417	600	0.188	
		0.417	700	0.210	
	Helium	0.366	500	0.139	
		0.366	600	0.164	
		0.366	700	0.181	
		0.417	500	0.123	
		0.417	600	0.143	
		0.417	700	0.159	

Table 7 continued

Description	Gas	x/L	Power (watts)	b_1	b_2
Experimental	Air	0.366	500	0.077	0.534
		0.366	600	0.112	0.459
		0.366	700	0.121	0.468
		0.417	500	0.065	0.543
		0.417	600	0.092	0.467
		0.417	700	0.101	0.477
	Helium	0.366	500	0.111	0.358
		0.366	600	0.130	0.359
		0.366	700	0.123	0.400
		0.417	500	0.105	0.344
		0.417	600	0.097	0.398
		0.417	700	0.109	0.394

CHAPTER VI

CONCLUSIONS AND RECOMMENDATIONS FOR FURTHER STUDY

Conclusions

The most important conclusion of this study is that as long as a system is capable of maintaining thermoacoustic oscillations, the acoustic sound-pressure level increases with an increase in static pressure. This fact was substantiated by both the experimental and the theoretical investigations. The mechanical efficiency increased with static pressure as long as the thermoacoustic system was stable. The thermoacoustic efficiency abruptly increased with static pressure up to 6 atmospheres and then gradually decreased with increasing static pressure.

Design criteria for thermoacoustic oscillators was developed. In general, equations of the form

$$p = b_1 p_o^{b_2} \tag{40}$$

were found to predict sound-pressure levels within 3 percent (based on SPL) for systems operating at elevated static pressures. The pertinent equations of this form were

$$\frac{p}{p_o} = 0.551\left(\frac{\dot{w}}{a_o p_o}\right)^{.586} \quad \text{for air,} \tag{11a}$$

and

$$\frac{p}{p_o} = 0.917\left(\frac{\dot{w}}{a_o p_o}\right)^{.545} \quad \text{for helium.} \tag{12}$$

The dimensional analysis equations were also shown to be of the form of Equation (40). These equations were

$$p = p_r\left(\frac{\dot{Q}}{\dot{Q}_r}\right)^{2/3}\left(\frac{x_r}{x}\right)^{4/3}\left(\frac{p_o}{p_{or}}\right)^{1/3}, \tag{28}$$

$$p = p_r\left(\frac{\dot{Q}}{\dot{Q}_r}\right)^{2/3}\left(\frac{p_o}{p_{or}}\right)^{1/3}, \tag{29}$$

and

$$p = p_r\left(\frac{p_o}{p_{or}}\right)^{1/3}. \tag{30}$$

The above Equations ((28)-(30)) are subject to the restrictions previously mentioned.

It was concluded that the efficiency of a thermoacoustic oscillator was dependent upon the capability of the cooling system. Therefore, design data presented in Chapter V is limited to oscillators with similar heat removal systems.

Recommendations for further study

Based upon the results of this investigation, the following topics are recommended for further study:

1) a study of the beating phenomenon, to investigate the possibility of designing a steady-state beating oscillator,
2) a study to design more efficient cooling systems.

Some research has already been done on optimizing the cooling system. It was found that a tube-heat exchanger design was the most efficient cooling system.[68] However, since the removal of heat from a thermoacoustic system is one of the main limitations on achieving higher power and pressure levels, it is recommended that further study be made of cooling devices, possibly utilizing liquid gases as the refrigerant.

---

[68] Feldman, "The Mechanism Causing Heat Driven Pressure Oscillations in a Gas-Thermoacoustic Generator Design," op. cit., p. 29.

APPENDIX

TABLE 8. PRESSURE (PSI) AS A FUNCTION OF SOUND PRESSURE LEVEL,SPL(DB)
SPL REFERENCED TO 0.0002 MICROBAR

SPL	0.0	0.1	0.2	0.3	0.4	0.5	0.6	0.7	0.8	0.9
150.	0.0917	0.0928	0.0938	0.0949	0.0960	0.0971	0.0983	0.0994	0.1006	0.1017
151.	0.1029	0.1041	0.1053	0.1065	0.1077	0.1090	0.1103	0.1115	0.1128	0.1141
152.	0.1154	0.1168	0.1181	0.1195	0.1209	0.1223	0.1237	0.1251	0.1266	0.1281
153.	0.1295	0.1310	0.1325	0.1341	0.1356	0.1372	0.1388	0.1404	0.1420	0.1437
154.	0.1453	0.1470	0.1487	0.1504	0.1522	0.1539	0.1557	0.1575	0.1594	0.1612
155.	0.1631	0.1650	0.1669	0.1688	0.1708	0.1727	0.1747	0.1768	0.1788	0.1809
156.	0.1830	0.1851	0.1872	0.1894	0.1916	0.1938	0.1960	0.1983	0.2006	0.2029
157.	0.2053	0.2077	0.2101	0.2125	0.2150	0.2174	0.2200	0.2225	0.2251	0.2277
158.	0.2303	0.2330	0.2357	0.2384	0.2412	0.2440	0.2468	0.2497	0.2526	0.2555
159.	0.2584	0.2614	0.2645	0.2675	0.2706	0.2737	0.2769	0.2801	0.2834	0.2866
160.	0.2900	0.2933	0.2967	0.3002	0.3036	0.3071	0.3107	0.3143	0.3179	0.3216
161.	0.3253	0.3291	0.3329	0.3368	0.3407	0.3446	0.3486	0.3526	0.3567	0.3609
162.	0.3650	0.3693	0.3735	0.3779	0.3822	0.3867	0.3911	0.3957	0.4002	0.4049
163.	0.4096	0.4143	0.4191	0.4240	0.4289	0.4338	0.4389	0.4439	0.4491	0.4543
164.	0.4595	0.4649	0.4703	0.4757	0.4812	0.4868	0.4924	0.4981	0.5039	0.5097
165.	0.5156	0.5216	0.5276	0.5337	0.5399	0.5462	0.5525	0.5589	0.5654	0.5719
166.	0.5785	0.5852	0.5920	0.5989	0.6058	0.6128	0.6199	0.6271	0.6343	0.6417
167.	0.6491	0.6566	0.6642	0.6719	0.6797	0.6876	0.6955	0.7036	0.7117	0.7200
168.	0.7283	0.7367	0.7453	0.7539	0.7626	0.7715	0.7804	0.7894	0.7986	0.8078
169.	0.8172	0.8266	0.8362	0.8459	0.8557	0.8656	0.8756	0.8857	0.8960	0.9064
170.	0.9169	0.9275	0.9382	0.9491	0.9601	0.9712	0.9824	0.9938	1.0053	1.0169
171.	1.0287	1.0406	1.0527	1.0649	1.0772	1.0897	1.1023	1.1151	1.1280	1.1410
172.	1.1542	1.1676	1.1811	1.1948	1.2086	1.2226	1.2368	1.2511	1.2656	1.2802
173.	1.2951	1.3100	1.3252	1.3406	1.3561	1.3718	1.3877	1.4037	1.4200	1.4364
174.	1.4531	1.4699	1.4869	1.5041	1.5215	1.5391	1.5570	1.5750	1.5932	1.6117
175.	1.6303	1.6492	1.6683	1.6876	1.7072	1.7269	1.7469	1.7671	1.7876	1.8083
176.	1.8293	1.8504	1.8719	1.8935	1.9154	1.9376	1.9601	1.9828	2.0057	2.0289
177.	2.0524	2.0762	2.1002	2.1246	2.1492	2.1740	2.1992	2.2247	2.2504	2.2765
178.	2.3029	2.3295	2.3565	2.3838	2.4113	2.4393	2.4675	2.4961	2.5250	2.5542
179.	2.5838	2.6137	2.6440	2.6746	2.7056	2.7369	2.7686	2.8006	2.8331	2.8659

Table 9. Significant constants for air and helium[69]

Description	Air	Helium
Molecular weight (gm/mole)	28.95	4.002
Gas constant, R, ($ft\text{-}lb_f\text{-}°R$)*	53.35	386.2
Specific heat at constant pressure, c_p, ($ft\text{-}lb_f/lb_m\text{-}°R$)*	0.238	1.25
Specific heat at constant volume, c_v, ($ft\text{-}lb_f/lb_m\text{-}°R$)*	0.170	0.755
Specific heat ratio, γ*	1.40	1.66
Density, ρ_o, (lb_m/ft^3)*	0.77	0.00975
Acoustic velocity, a_o, (ft-sec)*	1136	3334
Characteristics	Corrosive	Inert

*properties calculated at 14.7 psia and 77°F

---

[69] F. Krieth, Principles of Heat Transfer, 2nd ed., (Scranton: International Textbook Company, 1966), pp. 595-596.

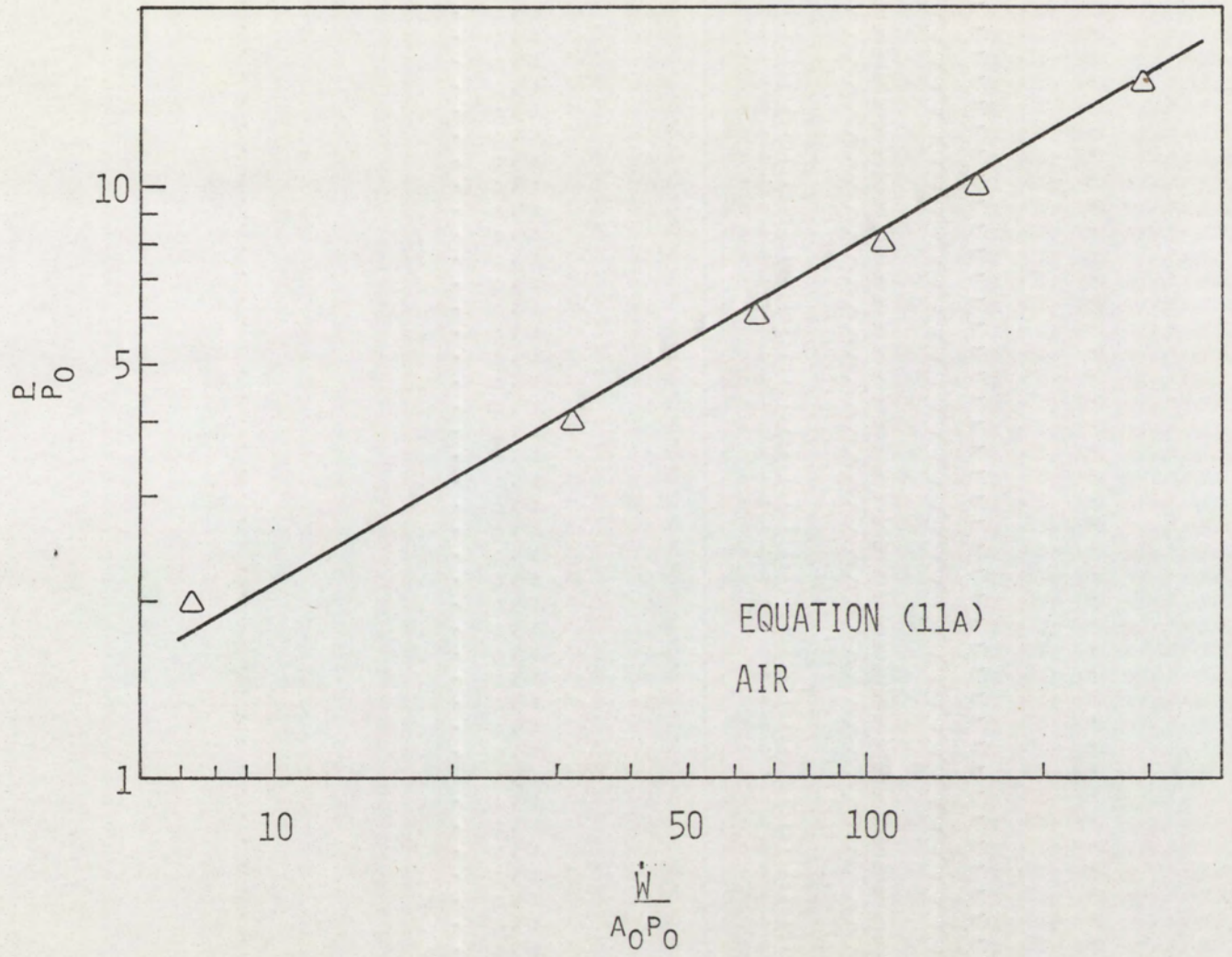

Figure 58. Plot of data used in least squares fit to determine Equation (11a) from Equation (5)

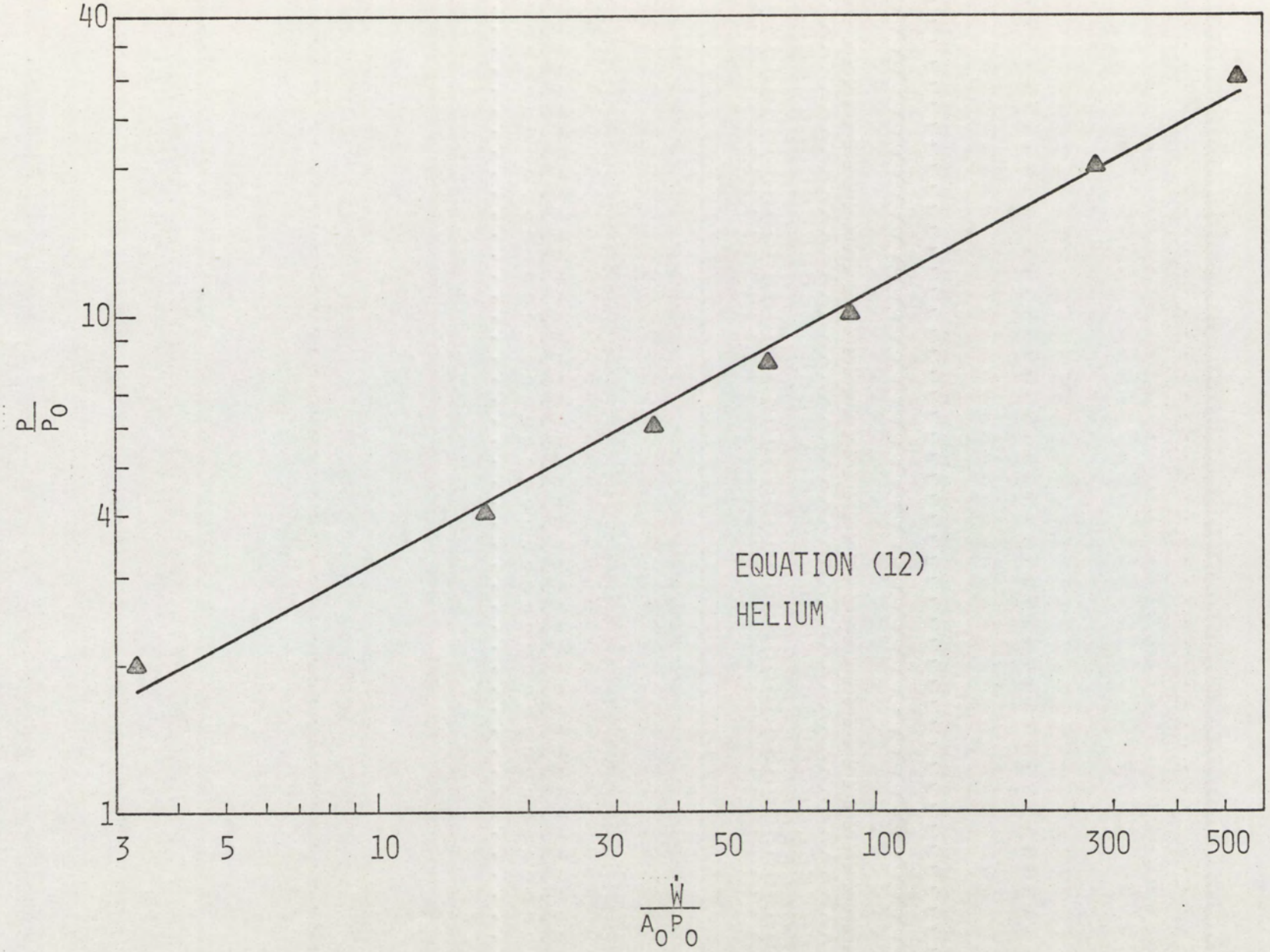

Figure 59. Plot of data used in least squares fit to determine Equation (12) from Equation (5)

BIBLIOGRAPHY

1. Baumeister, T., ed., Mark's Standard Handbook for Mechanical Engineers, 7th ed., New York: McGraw-Hill Book Company, Inc., 1967.

2. Beckwith, T. G. and Buck, N. L., Mechanical Measurements, Reading, Mass.: Addison-Wesley Publishing Company, Inc., 1964.

3. Beranek, L. L., Acoustics, New York: McGraw-Hill Book Company, Inc., 1954.

4. Brombacher, W. G., "40 Years of Precise Pressure Measurement," Instruments and Control Systems, Vol. 40, September 1967, pp. 87-92.

5. Carter, R. L, and Feldman, K. T., Jr., "An Acoustically Resonant Stirling Engine," (Associated Midwest Universities-Argonne National Laboratory Conference on Direct Energy Conversion, Argonne, Illinois), November 4-5, 1963, ANL-6802, pp. 166-169.

6. Carter, R. L., Feldman, K. T., Jr., and McKinnon, C. N., Jr., "Applicability of Thermoacoustic Phenomena to Magnetohydrodynamic Conversion Systems," Engineering Experiment Station Reprint No. 64, The University of Missouri, Columbia, Missouri, July 1964, p. 11.

7. Carter, R. L., White, M., and Steele, (Atomics International Division of North American Aviation, Inc.), private communication to K. T. Feldman, Jr., September 24, 1962.

8. Chu, B. T., "Analysis of a Self-Sustained Thermally Driven Nonlinear Vibration," The Physics of Fluids, 6:1638-1644, November 1963.

9. Chu, B. T., "Pressure Waves Generated by Addition of Heat in a Gaseous Medium," National Advisory Committee for Aeronautics, Technical Note 3411, June 1955.

10. Chu, B. T., "Stability of Systems Containing a Heat Source - The Rayleigh Criterion," National Advisory Committee for Aeronautics, Research Memorandum 56D27, June 1956.

11. Chu, B. T. and Ying, S. J., "Thermally Driven Nonlinear Oscilations in a Pipe with Traveling Shock Waves," The Physics of Fluids, 6:1625-1637, November 1963.

12. Clement, J. R. and Gaffney, J., "Thermal Oscillations in Low-Temperature Apparatus," Advances in Cryogenic Engineering, Vol. 1 (Proceedings of 1954 Cryogenic Engineering Conference, Boulder, Colorado, September 1954, Paper H-7), pp. 302-306.

13. Crawford, F. H. and Van Vorst, W. D., Thermodynamics for Engineers, New York: Harcourt, Brace, and World, Inc., 1968.

14. Doebelin, E. O, Measurement Systems: Application and Design, New York: McGraw-Hill Book Company, Inc., 1966.

15. Eshbach, O. W., Handbook of Engineering Fundamentals, 2nd ed., New York: John Wiley and Sons, Inc., 1966.

16. Fand, R. M., "Evaluation of Richardson's Correlation of the Influence of Sound on Heat Transfer as Measured by Fand and Kaye," Journal of Heat Transfer, May 1966, pp. 247-248.

17. Fand, R. M., "Mechanism of Interaction between Vibrations and Heat Transfer," The Journal of the Acoustical Society of America, Vol. 34, No. 12, December 1962, pp. 1887-1893.

18. Fand, R. M. and Kaye, J., "Acoustic Streaming near a Heated Cylinder," The Journal of the Acoustical Society of America, Vol. 32, No. 5, May 1960, pp. 579-584.

19. Fand, R. M. and Kaye, J., "The Influence of Sound of Free Convection from a Horizontal Cylinder," Journal of Heat Transfer, May 1961, pp. 133-148.

20. Feingold, A., "Mixing of Gases at the Same Original Pressure but Different Original Temperatures," paper presented at the Missouri Academy of Sciences, University of Missouri, Columbia, Missouri, April 18, 1964.

21. Feldman, K. T., Jr., Application to the Office of Naval Research for Funds to Support research Entitled, "Investigation of a Thermoacoustic Oscillator as an Underwater Sound Source," Mechanical Engineering Department, University of New Mexico, February 1967 (in the files of the department).

22. Feldman, K. T., Jr., "The Mechanism Causing Heat Driven Pressure Oscillations in a Gas - Thermoacoustic Generator Design," Technical Report ME-29, Bureau of Engineering Research, University of New Mexico, September 1967.

23. Feldman, K. T., Jr., "A Study of Heat Generated Pressure Oscillations in a Closed End Pipe," Ph.D. dissertation, University of Missouri, also available as Report ME-18, Bureau of Engineering Research, University of New Mexico, November 1965.

24. Feldman, K. T., Jr., "Review of the Literature on Rijke Thermoacoustic Phenomena," Journal of Sound and Vibration, Vol. VII(1), 1968, pp. 83-89.

25. Feldman, K. T., Jr., "Review of the Literature on Sondhauss Thermoacoustic Phenomena," Journal of Sound and Vibration, Vol. VII(1), 1968, pp. 71-82.

26. Feldman, K. T., Jr., and Hirsch, H., "Final Report on the Mechanism Causing Heat Driven Pressure Oscillations in a Gas," Technical Report ME-22, Bureau of Engineering Research, University of New Mexico, June 1966.

27. Gould, R. K., "Heat Transfer across a Solid-Liquid Interface in the Presence of Acoustic Streaming," The Journal of the Acoustical Society of America, Vol. 40, No. 1, 1966, pp. 219-225.

28. Hartz, R. A., "Temperature Transducers: A Guide for Selection," Machine Design, September 15, 1966, pp. 188-192.

29. Henderson, R. L., (Environmental Test Group, Sandia Corporation, Albuquerque, New Mexico), private communication to K. T. Feldman, Jr., June 1965.

30. Jones, J. B. and Hawkins, G. A., Engineering Thermodynamics, New York: John Wiley and Sons, Inc., 1963.

31. Kaufman, E. N., "Charge Amplifier Versus Source Follower," Instruments and Control Systems, Vol. 39, April 1966, pp. 129-130.

32. Kirk, W. H., "Thermocouple Primer," Instruments and Control Systems, Vol. 41, March 1968, pp. 77-82.

33. Kinsler, L. E. and Frey, A. R., Fundamentals of Acoustics, 2nd ed., New York: John Wiley and Sons, Inc., 1962.

34. Kistler Instrument Corporation, "Operating and Service Instructions for Kistler Model 556 Charge Amplifier," Clarence, New York.

35. Kistler Instrument Corporation, "Operating and Service Instructions for Kistler Quartz Transducers," Clarence, New York.

36. Kramers, H. A., "Vibrations of a Gas Column," Physica, 15: 971-983, December 1949.

37. Krieth, F., Principles of Heat Transfer, 2nd ed., Scranton: International Textbook Company, 1966.

38. Kubanskii, P. N., "The Effect of Acoustic Streaming on Convective Heat Exchange," Zhur. Tekh. Fiz., Vol. 22, 1952, pp. 585-591; Translation USSR Academy of Science, Vol. 82, 1958, pp. 49-54.

39. Lederer, P. S., "Performance-Testing Pressure Transducers," Instruments and Control Systems, Vol. 40, September 1967, pp. 93-99.

40. Loeffler, R. F., "Thermocouples, Resistance Temperature Detectors, Thermistors - Which?", Instruments and Control Systems, Vol. 40, May 1967, pp. 89-93.

41. Loesecke, P. V., "Reducing Noise with Intelligent Cabling," Instruments and Control Systems, Vol. 40, August 1967, pp. 106-109.

42. Muth, S., Jr., "Reference Junctions," Instruments and Control Systems, Vol. 40, May 1967, pp. 133-134.

43. Owczarek, J. A., Fundamentals of Gas Dynamics, Scranton: International Textbook Company, 1964.

44. Peterson, A. P. G. and Gross, E. E., Jr., Handbook of Noise Measurement, 5th ed., West Concord, Mass.: General Radio Company, 1963.

45. Qvale, E. B. and Smith, J. L., Jr., "A Mathematical Model for Steady Operation of Stirling-Type Engines," Paper No. 67-Wa/Ener-1, American Society of Mechanical Engineers, Transactions of ASME, 1967.

46. Raushenbakh, B. V., Vibrational Combustion, Wright-Patterson Air Force Base, Ohio: Foreign Technology Division, Defense Documentation Center, 1963.

47. Lord Rayleigh, "The Explanation of Certain Acoustical Phenomena," Nature, 18:319, July 1878.

48. Lord Rayleigh, Theory of Sound, Vol. II, New York: Dover Publications, 1945.

49. Shames, I. H., Mechanics of Fluids, New York: McGraw-Hill Book Company, Inc., 1962.

50. Skoglund, V. J., Similitude Applications and Theory, Scranton: International Textbook Company, 1967.

51. Smith, P., "Selecting a Charge Amplifier," Instruments and Control Systems, Vol. 40, April 1967, pp. 117-122.

52. Sondhauss, C., "Uber die Schallschwingungun der Luft in erhitzten Glasröhren und in gedeckten Pfeifen von ungleicher Weite," Poggendorff Annalen der Physik and Chemie, 79:1-34, February 1850.

53. Spiegel, M. R., Schaum's Outline of Theory and Problems of Statistics, New York: Schaum Publishing Company, 1961.

54. Taconis, K. W., et al., "Vapor-Liquid Equilibrium of Solutions of He^3 in He^4," Physica, 15:738, September 1949.

55. Temkin, S., "Nonlinear Gas Oscillations in a Resonant Tube," The Physics of Fluids, Vol. 11, No. 5, May 1968, pp. 960-963.

56. Thurston, R. S., "Thermal-Acoustic Oscillations Induced by Forced Convection Heating of Dense Hydrogen," Ph. D. dissertation, University of New Mexico, also available as LA-3543, Los Alamos Scientific Laboratory of the University of California, Los Alamos, New Mexico, August 26, 1966.

57. Thurston, R. S. and Rogers, J. D., "The Avoidance of Thermal-Acoustic Oscillations Induced by Forced-Convection Film Boiling in Tubes," American Society of Mechanical Engineers, paper 67-Vibr-53, 1967.

58. Thurston, R. S., Rogers, J. D., and Skoglund, V. J., "Pressure Oscillations Induced by Forced Convection Heating of Dense Hydrogen," Proceedings of Cryogenic Engineering Conference, Paper H-4, 1966.

59. Trilling, L., "On Thermally Induced Sound Fields," The Journal of the Acoustical Society of America, 27:425-231, May 1955.

60. Wang, T. P., "Temperature Sensors," Instruments and Control Systems, Vol. 40, May 1967, pp. 103-107.

61. Weiner, S., "Standing Sound Waves of Finite Amplitude," The Journal of the Acoustical Society of America, Vol. 40, No. 1, 1966, pp. 240-243.